Journal of the
OPTICAL SOCIETY
of AMERICA

VOLUME 37, NUMBER 9 SEPTEMBER, 1947

Interferometer Studies of Telescopic Systems*

HOWARD S. COLEMAN, DAVID G. CLARK, AND MADELINE F. COLEMAN
The Optical Inspection Laboratory, The Pennsylvania State College, State College, Pennsylvania

(Received May 19, 1947)

The usefulness of the interferometer in controlling the quality of telescopic systems has been studied. The study consisted of collecting interferograms for individual and mixtures of the common aberrations under a variety of focal adjustments of the telescopic system under consideration. These interferograms were compared with predicted patterns computed from a knowledge of the aberrations and from an "optical-path-difference equation." Experimental and computed patterns were found to be in excellent agreement, thus constituting a check on the optical-path-difference equation used. The experimental and computed interferometer patterns were used to form a basis for determining the usefulness of the interferometer. Two distinct uses appeared evident from the point of view of quality control. The first of these is to acquaint an inspector with design limitations of optical systems under consideration. This may be done from a knowledge of the form of patterns that should be produced if the design were properly executed. The second use of the interferometer is in connection with a routine procedure for evaluating the quality of an optical system under test. In this connection it was found impractical to attempt to analyze the interference pattern for individual component aberrations on the basis of the shape and number of interference fringes even in the case of a simple mixture of aberrations. Therefore a method was developed which does not depend particularly on the number of fringes present nor the shape of the interference pattern. This method is based on a study of interferometer patterns of telescopic systems focused visually on large numerals placed optically at a great distance. For such a focal adjustment, the interferometer pattern is found to have the largest possible diameter covered by a light or dark interference area, the size of which depends upon the magnitude and types of aberrations present. A measure of the quality is related to the largest circle that can be inscribed in this area. When the diameter of the inscribed circle is expressed as a percentage of the diameter of the axial entrance pupil, the quantity obtained is referred to as the "Interferometer Quality." This quantity is found to be in agreement with quality evaluations based on resolving power measurements. The Interferometer Quality may be determined for telescopic systems at various field angles and is likely the most accurate and rapid procedure available at the present time for evaluating the optical quality of telescopic systems.

INTRODUCTION

DURING World War II, a study was started of the permissible tolerances of optical aberrations in telescopic systems and their component parts. In this study considerable difficulty was encountered in the making of quantitative impersonal measurements of the aberrations generally encountered in high grade telescopic systems. Among other procedures, consideration was given to the interferometer developed by Twyman.[1] It was understood that the interferometer was in common use in England but, at the time the study was started, there was less than a dozen in use in the optical industries

* This work was performed, in part, under terms of OSRD Contract OEMsr 1197 at The Pennsylvania State College.

[1] F. Twyman, "Interferometers for the experimental study of optical systems from the point of view of the wave theory," Phil. Mag. (S. 6) **35**, 49 (1918).

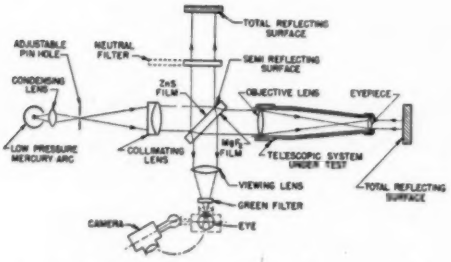

FIG. 1. Schematic diagram of interferometer used to test telescopic systems.

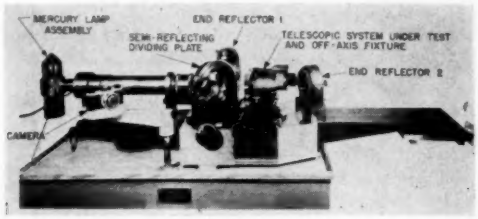

FIG. 2. Interferometer used to test telescopic systems.

and educational institutions in this country. The lack of such devices in the United States may be attributed to the existence of British patents covering such equipment and the misconception in this country that interferometers were extremely difficult to produce and required extraordinary training to use. It was also understood that the British were using interferometers for custom-made optics and, hence, some doubt was cast as to the possibility of such equipment fitting into our mass production programs here. After a survey of the existing literature and a study of interferometers in this country indicated no real reason to expect that the interferometer could not be produced in sufficient quantities to be effective, the Optical Inspection Laboratory was requested to develop an interferometer adaptable to our own production system. It was specified that this interferometer was to be "versatile enough to permit the testing of lenses, prisms, and telescopic systems and to be geared to our mass production operations under way." This task was completed and a number of units designed, constructed, and furnished to the Army, Navy, and the NDRC. In a research program at the Optical Inspection Laboratory, a number of military telescopic systems were studied by means of the interferometers. In this program, thousands of photographs were taken of typical interferometer patterns. It is the purpose of this paper to describe some of the results based on a study of these patterns and to present a simple method for evaluating the quality of telescopic systems by means of an interferometer. This method is applicable to optical parts as well as complete instruments and appears to be the most precise and rapid method for evaluation of quality available at the present time.

THE APPARATUS

The apparatus used in studying telescopic systems by means of the interferometer consisted of the interferometer itself and five telescopic systems referred to as "aberration modifiers." The interferometer differs only mechanically with those described by Twyman and is therefore not described in detail here. One of the designs developed is shown in schematic and photographic form in Figs. 1 and 2. The aberration modifiers are simple telescopic systems in which the aberrations can be varied continuously. These modifiers make it possible to catalog the interferometer patterns associated with the individual aberrations and known mixtures of aberrations. The modifiers were designed to have the same general characteristics as a $5\times35\times12°$ telescopic system being mass produced during the War.

THE ASTIGMATISM MODIFIER

The method of varying astigmatism in the modifier is shown schematically in Fig. 3. The astigmatism is varied by rotating a coma-free astigmatic telescopic objective about its nodal point as indicated. The modifier has a clear

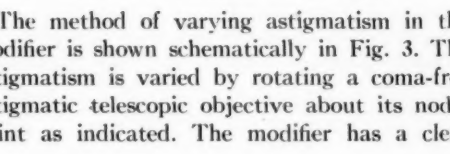

FIG. 3. Schematic diagram of the astigmatism modifier.

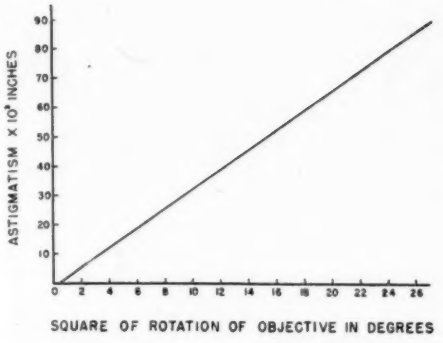

FIG. 4. Calibration of astigmatism modifier No. 1. Entrance pupil = 1.40 inches; E.F.L. Objective = 11.40 inches; E.F.L. Eyepiece = 1.90 inches.

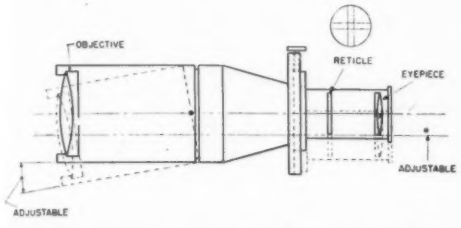

FIG. 5. Schematic diagram of the coma modifier.

aperture of 1.40 inches, an effective focal length of 11.5 inches for the objective, and a magnification of 6×. The calibration curve for this modifier is shown in Fig. 4.

THE COMA MODIFIER

The method used to vary the coma in the modifier is shown schematically in Fig. 5. The method uses a cemented doublet objective two inches in diameter which has considerable spherical aberration at full aperture. The spherical aberration is removed by reducing the effective aperture to 1.40 inches by an internal stop about which the objective may be rotated. By selecting the position of the stop properly, it is possible to limit the off-axis aberrations to practically pure primary tangential coma. Because the objective rotates about an axis through the stop and not its nodal point, it is necessary to provide the eyepiece of the modifier with a lateral adjustment to insure that the eyepiece can be used on axis. The calibration of the coma in terms of the rotation of the objective about its aperture stop is shown in Fig. 6.

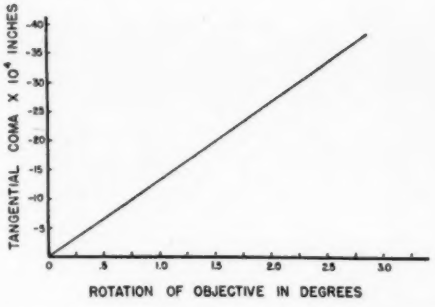

FIG. 6. Calibration of coma modifier. Entrance pupil = 1.40 inches; E.F.L. Objective = 6.03 inches; E.F.L. Objective = 1.28 inches.

THE SPHERICAL ABERRATION MODIFIERS

Two different methods were used to vary the spherical aberration. These are shown schematically in Figs. 7 and 8. In spherical aberration modifier No. 1, the aperture of the modifier is constant, and the aberration is varied by changing the position of a meniscus along the optical axis between the objective and eyepiece in an otherwise high grade telescopic system. In spherical aberration modifier No. 2, the aberration is introduced by reversing the objective of a telescopic objective and varying the spherical aberration by means of a set of aperture stops. The calibration of the spherical aberration modifiers is shown in Figs. 9 and 10.

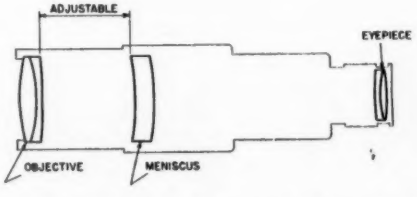

FIG. 7. Schematic diagram of spherical aberration modifier No. 1.

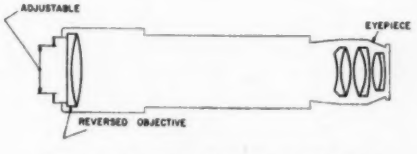

FIG. 8. Schematic diagram of spherical aberration modifier No. 2.

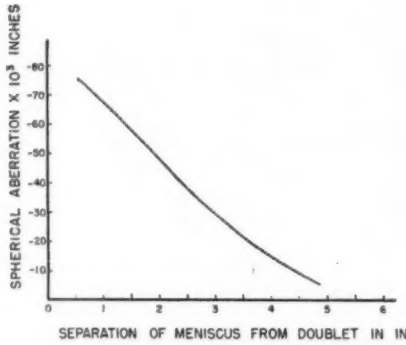

FIG. 9. Calibration of spherical aberration modifier No. 1. Entrance pupil = 1.40 inches; E.F.L. Objective = 6.34 inches; E.F.L. Eyepiece = 1.28 inches.

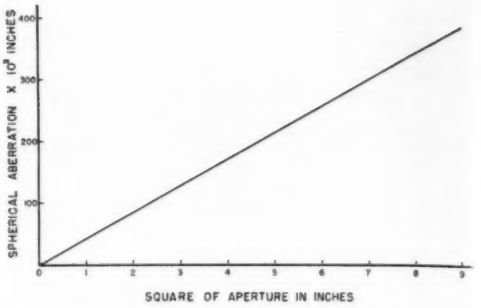

FIG. 10. Calibration of spherical aberration modifier No. 2. E.F.L. Objective = 15.84 inches; E.F.L. Eyepiece = 1.625 inches.

THE 6×25×4° *f*:11.5 ABERRATION MODIFIER

In addition to the modifiers producing essentially pure aberrations, a modifier was developed which produced a mixture of aberrations. This modifier is shown schematically in Fig. 11. This modifier is the same instrument as the astigmatism modifier No. 1 except that the objective has been reversed, and an aperture stop of 25 mm is used to limit the spherical aberration to a reasonable amount. The aberrations are varied by rotating the objective about its nodal point as indicated. The calibration of the aberrations in terms of the rotation of the objective is shown in Fig. 12.

THE PROCEDURE AND DATA

The procedure followed in determining the usefulness of an interferometer in evaluating the quality of telescopic systems was divided into two parts. The first of these was to study the types of patterns obtained for the individual aberrations, under a variety of possible focal adjustments. This study was made in order to select any particular focal adjustment which might make it possible to evaluate the optical quality with exceptional ease and to check the theoretical calibration of the aberration modifiers. In this part of the study, methods were developed for analyzing the interferometer patterns for the magnitude of single aberrations for each of the focal adjustments. In addition, this part of the procedure resulted in establishing a catalog of patterns for known values of single and mixed aberrations. The second part of the procedure consisted of the development of a method for assigning a numerical rating of quality, by means of an interferometer, to a telescopic system having any combination of aberrations. Finally, the quality was evaluated for a number of military telescopic systems and the aberration modifiers.

PART ONE OF THE PROCEDURE AND DATA

In this part of the procedure, each of the aberration modifiers was studied by means of the interferometer for lateral and longitudinal focal adjustments. The procedure described by Twyman for testing lenses may be applied if the plane end reflector No. 2, shown in Fig. 2, and the eyepiece of the optical system under test are regarded as equivalent to a spherical end reflector used in lens testing. This has been tested experimentally and found to hold. The fact that this may be done simplifies the problem of testing telescopic systems, since a great deal has been published concerning the testing of lenses by means of the interferometer. For example, the

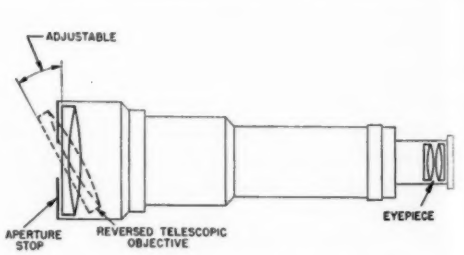

FIG. 11. Schematic diagram of 6×25×4° f:11.5 aberration modifier.

work of Kingslake[2] could be used as a means of checking the calibrations of the modifiers and serves as a guide in deciding which focal adjustments might yield useful results. Further, since the comparisons made by Kingslake of computed and experimental patterns were only qualitative, it was considered worth while to make a quantitative check of the "optical-path-difference equation" he describes. This equation was checked thoroughly and apart from a missing factor of $\frac{1}{3}$ in the coma term, the agreement between the computed and experimental patterns was found to be remarkably close. Figures 13 to 30, inclusive, show a comparison of computed and experimental interferometer patterns for the aberration modifiers under different conditions of adjustment. It is seen from these figures that the eyepieces of the modifiers do not contribute appreciably to the magnitude of the aberrations. This suggests a possible method of making routine interferometer inspections of objectives. The objectives could be combined with an eyepiece and tested as a telescope. This would require a less complex interferometer since only one plane end reflector would be needed. It is much less difficult to test a telescope than a lens because the alignment is much less complex.

The experimental patterns in the preceding figures were examined to see whether any particular focal adjustment yielded great accuracy or proved especially simple in measuring the magnitudes of the aberrations. A method was developed for determining the magnitude of the

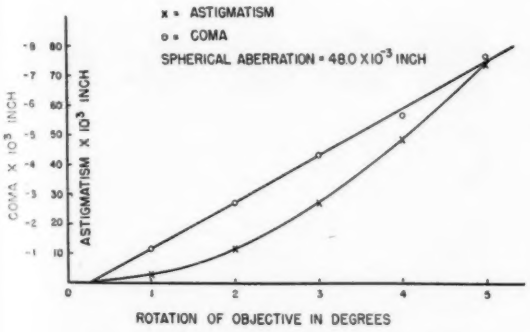
x = ASTIGMATISM
o = COMA
SPHERICAL ABERRATION = 48.0 X10⁻³ INCH
COMA X 10³ INCH
ASTIGMATISM X 10³ INCH
ROTATION OF OBJECTIVE IN DEGREES

FIG. 12. Calibration of 6×25×4° f:11.5 aberration modifier.

[2] R. Kingslake, "Interferometer patterns due to primary aberrations," Trans. Opt. Soc. **27**, 94 (1926).

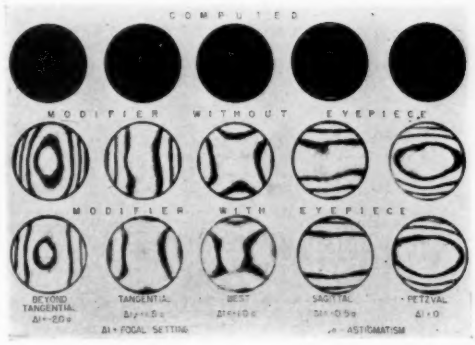

FIG. 13. A comparison of computed and experimental interferometer patterns for astigmatism modifier No. 1 at 2° for various focal surfaces. (Astigmatism = 11.8×10^{-3} inch; Aperture = 1.40 inches.)

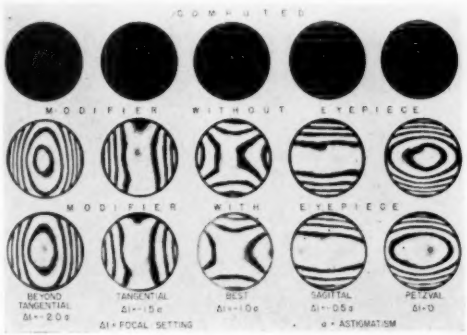

FIG. 14. A comparison of computed and experimental interferometer patterns for astigmatism modifier No. 1 at 2.5° for various focal surfaces. (Astigmatism = 19.7×10^{-3} inch; Aperture = 1.4 inches.)

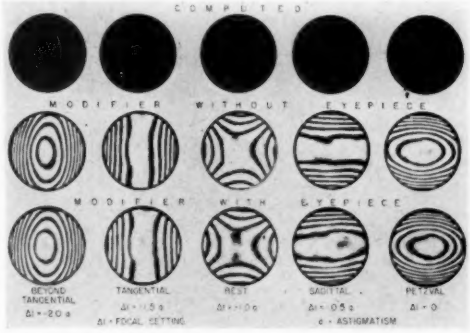

FIG. 15. A comparison of computed and experimental interferometer patterns for astigmatism modifier No. 1 at 3° for various focal surfaces. (Astigmatism = 28.3×10^{-3} inch; Aperture = 1.4 inches.)

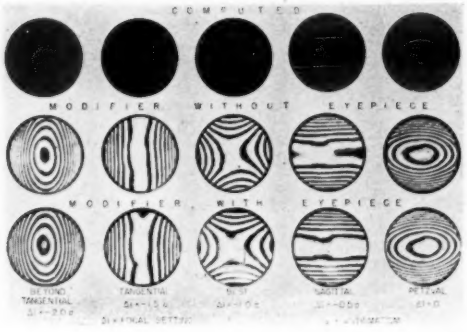

FIG. 16. A comparison of computed and experimental interferometer patterns for astigmatism modifier No. 1 at 3.5° for various focal surfaces. (Astigmatism = 39.4×10^{-3} inch; Aperture = 1.4 inches.)

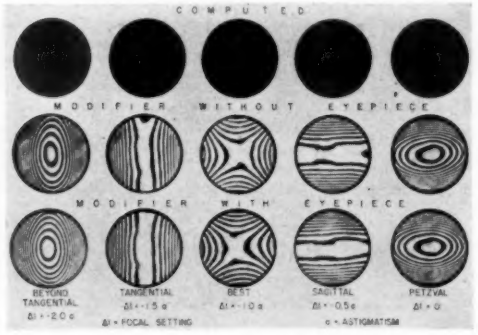

FIG. 17. A comparison of computed and experimental interferometer patterns for astigmatism modifier No. 1 at 4° for various focal surfaces. (Astigmatism = 52.0×10^{-3} inch; Aperture = 1.4 inches.)

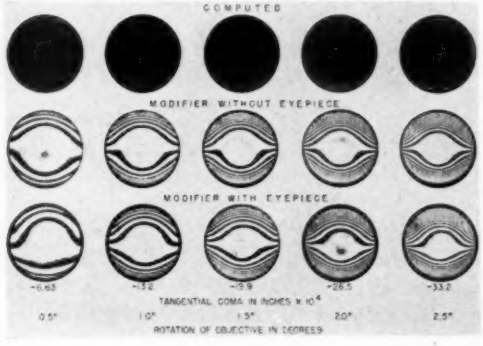

FIG. 18. A comparison of computed and experimental interferometer patterns for coma modifier. (Adjusted for paraxial focus.)

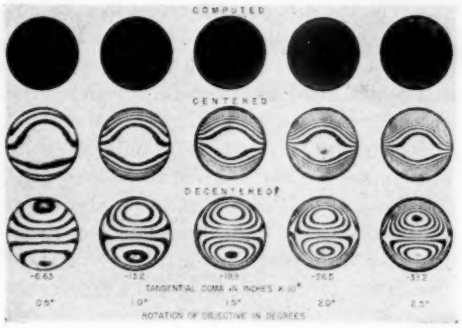

FIG. 19. A comparison of computed and experimental interferometer patterns for coma modifier. (Adjusted for paraxial focus.)

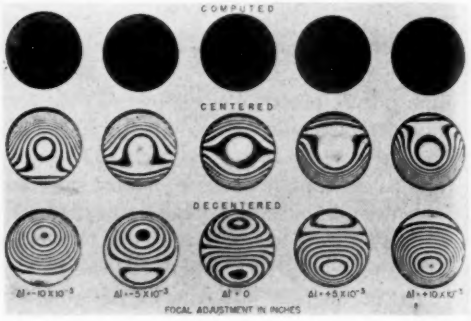

FIG. 20. A comparison of computed and experimental interferometer patterns for tangential coma for various longitudinal focal adjustments of the interferometer. ((−) Tangential coma = 13.2×10^{-4} inch; Rotation of Objective = 1°.)

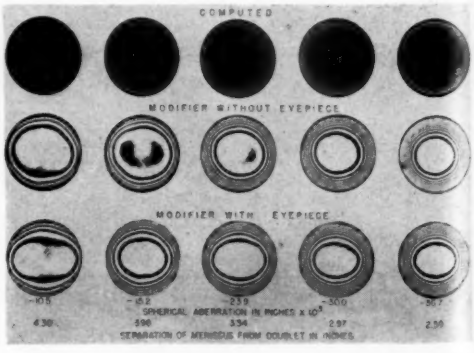

FIG. 21. A comparison of computed and experimental interferometer patterns for spherical aberration modifier No. 1. (Adjusted for paraxial focus.)

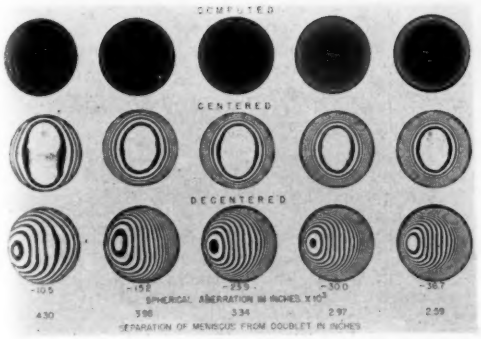

FIG. 22. A comparison of computed and experimental interferometer patterns for spherical aberration modifier No. 1. (Adjusted for paraxial focus.)

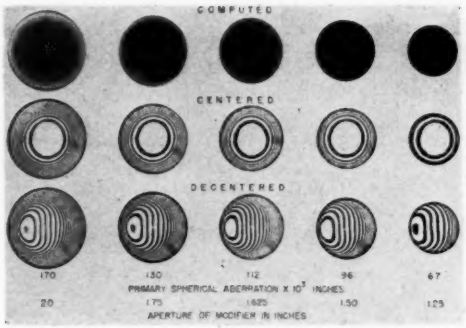

FIG. 24. A comparison of computed and experimental interferometer patterns for spherical aberration modifier No. 2. (Adjusted for paraxial focus.)

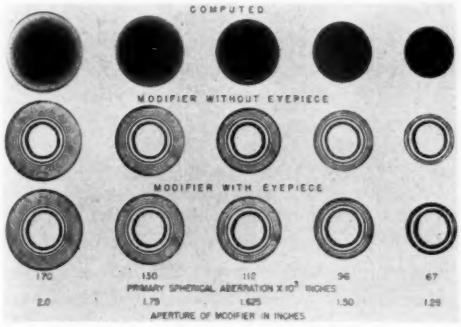

FIG. 23. A comparison of computed and experimental interferometer patterns for spherical aberration modifier No. 2. (Adjusted for paraxial focus.)

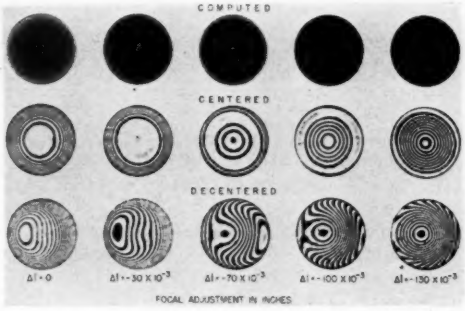

FIG. 25. A comparison of computed and experimental interferometer patterns for primary spherical aberration for different longitudinal focal adjustments of the interferometer. (Spherical aberration modifier No. 2. Spherical aberration = 130×10^{-3} inch; Aperture = 1.75 inches.)

aberrations present. This method is based on certain expressions derived from Kingslake's optical-path-difference equation. The method requires a knowledge of a total number of fringes, N, to be counted in a specified fashion, the wave-length of light, λ, used in the interferometer, the semi-aperture, (S), of the objective of the telescopic system under consideration, and the effective focal length, f, of the objective of the optical system under test. From a knowledge of these quantities, and by means of the following expressions, interferometer patterns produced by pure primary aberrations may be analyzed for the magnitude of the aberration for the focal adjustment indicated:

(1) Astigmatism $= \Delta N[\lambda/(S^2/f^2)]$ for any longitudinal focal adjustment when ΔN = the difference between the

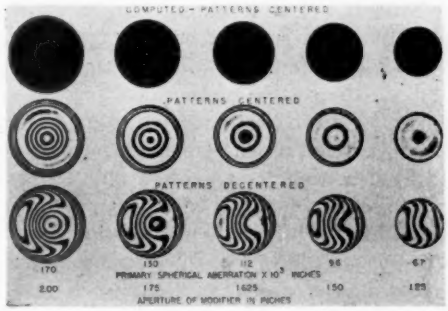

FIG. 26. A comparison of computed and experimental interferometer patterns for pure primary spherical aberration. [Interferometer adjusted for zonal focus—$\Delta l = (LA'/2)$. Spherical aberration modifier No. 2.]

TABLE I. A comparison of lens bench and interferometer determinations of astigmatism for modifier No. 1 at various focal surfaces.*

Rotation of objective	Interferometer measurements $\times 10^3$ inches					
	Lens bench	Petzval focus	Sagittal focus	Best focus	Tangential focus	Beyond tangential focus
2.0°	11.8	11.4	11.4	11.4	9.6	11.4
2.5°	19.7	17.1	17.1	17.1	17.1	17.1
3.0°	28.3	27.1	27.1	25.6	25.6	27.1
3.5°	39.4	34.2	35.1	34.2	34.2	35.6
4.0°	52.0	48.5	48.5	47.0	48.5	49.8

TABLE II. A comparison of computed, lens bench, and interferometer determinations of tangential coma for coma modifier adjusted for paraxial focus.

Rotation of objective	Tangential coma $\times 10^4$ inches		
	Computed	Lens bench	Interferometer
0		0	
0.5	− 6.95	− 6.63	− 6.0
1.0	−13.9	−13.2	−12.5
1.5	−20.8	−19.9	−20.8
2.0	−27.8	−26.5	−29.2
2.5	−34.7	−33.2	−36.5

maximum and minimum number of fringes obtained counting from the center out to the edge of the pattern.

(2) Spherical aberration $= 2\lambda/(S^2/f^2)$ for paraxial and marginal foci.

(3) Spherical aberration $= N[4\lambda/(S^2/f^2)]$ for zonal focus.

(4) Tangential coma $= N(3/4)[\lambda/(S/f)]$ for any longitudinal focus when N = maximum number of fringes across a diameter of the pattern.

It might be noted that in the case of spherical aberration, the number of fringes produced for zonal focus is just half the number produced for paraxial and marginal focus. Also, it is seen that the zonal focus may be identified as that longitudinal focal adjustment which produces an equal number of fringes inside and outside the zone. It can be shown from the optical-path-difference equation that this adjustment corresponds to the setting of the focal plane of the eyepiece of the telescopic system under test, halfway between the marginal and paraxial foci. This focal setting is at a point on the optical axis intersected by rays that pass through a zone at a height of 0.707, the semi-aperture.

The magnitude of the aberrations indicated by the interferometer patterns presented in Figs. 13 to 26 are presented in Tables I to VII inclusive. For comparison purposes, computed and lens bench values of the aberrations are included in the tables.

TABLE III. Interferometer determinations of tangential coma for modifier set for 1° and for different longitudinal focal adjustments.

Distance from paraxial focus $\times 10^3$ inches	Tangential coma $\times 10^4$ inches
+10	−12.4
+ 5	−13.8
0	−13.8
− 5	−16.6
−10	−14.5

TABLE IV. A comparison of computed, lens bench, and interferometer determinations of spherical aberration for modifier No. 1 adjusted for paraxial focus.

Setting of meniscus (inches)	Spherical aberration $\times 10^3$ inches		
	Lens bench	Computed	Interferometer
0.73	−72.6	−72.6	−76.7
1.10	−66.0	−66.0	−69.4
1.47	−58.4	−59.1	−58.4
1.84	−51.5	−51.5	−51.2
2.22	−45.2	−43.8	−45.6
2.59	−38.7	−36.7	−35.0
2.97	−32.8	−30.0	−27.0
3.34	−27.7	−23.9	−20.0
3.98	−19.0	−15.2	−14.6
4.83	−10.2	− 6.6	− 5.5
4.30	− 7.8	− 5.7	− 7.3

Special consideration was given to the interferometer patterns, showing the mixture of aberrations, presented in Figs. 29 and 30. It was concluded that while the computed and experimental patterns were in excellent agreement, an analysis of the mixture of aberrations into the individual components was found to require more time than could be used in practical situations. On the basis of this conclusion, a new approach was considered. This is described in the next section.

PART TWO OF THE PROCEDURE AND DATA

Because of the difficulty in analyzing the interferometer patterns produced by complex mixture

TABLE V. A comparison of computed, lens bench, and interferometer determinations of spherical aberration for modifier No. 2 adjusted for paraxial focus.

Modifier aperture (inches)	Spherical aberration $\times 10^3$ inches		
	Computed	Lens bench	Interferometer
2.000	160.0	170.0	150.0
1.875	141.0	151.0	142.0
1.750	122.0	130.0	115.0
1.625	106.0	112.0	100.0
1.500	91.0	96.0	80.0
1.250	63.0	67.0	55.2
1.000	40.8	43.0	43.2

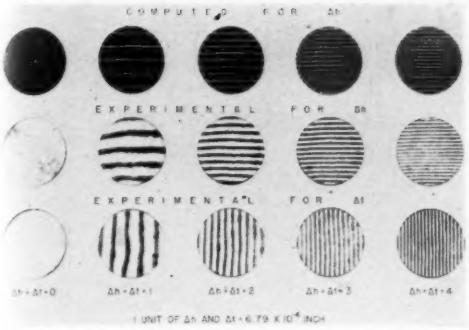

FIG. 27. A comparison of computed and experimental interferometer patterns for lateral adjustments of the spherical end mirror of the interferometer. (Telescope objective free from spherical aberration at an aperture of 1.25 inches.)

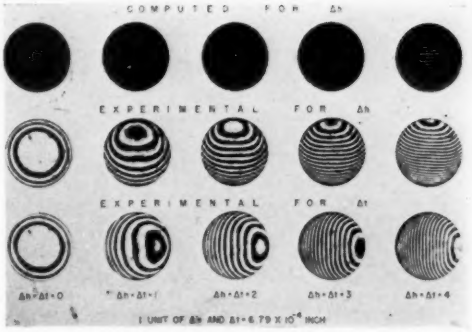

FIG. 28. A comparison of computed and experimental interferometer patterns for lateral adjustments of the spherical end mirror of the interferometer. (Telescope objective with 67×10^{-3} inch spherical aberration at an aperture of 1.25 inches.)

of aberrations, consideration was given to the possibility of evaluating the quality of the telescopic system on a basis that did not require the specification of the magnitudes of the specific

TABLE VI. A comparison of interferometer determinations for spherical aberration modifier No. 2 adjusted for paraxial and zonal focus.

Modifier aperture (inches)	Spherical aberration $\times10^3$ inches	
	Paraxial focus	Zonal focus
2.000	150.0	146.0
1.875	142.0	135.0
1.750	115.0	130.0
1.625	100.0	105.0
1.500	80.0	76.8
1.250	55.2	55.2
1.000	43.2	43.2

TABLE VII. Interferometer determinations of spherical aberration of modifier No. 2 at an aperture of 1.75 inches for different longitudinal focal adjustments.

Distance from paraxial focus $\times10^3$ inches	Spherical aberration $\times10^3$ inches
+ 10	128
0	129
− 10	134
− 20	136
− 30	138
− 40	136
− 50	120
− 60	128
− 70	139
− 80	130
− 90	128
−100	129
−110	128
−120	134
−130	126
−140	132

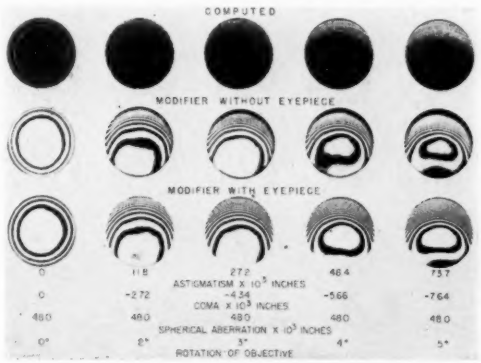

FIG. 29. A comparison of computed and experimental interferometer patterns for an optical system containing a mixture of aberrations. (Aperture = 1.00 inch; E.F.L. = 11.5 inches; Adjusted for paraxial focus.)

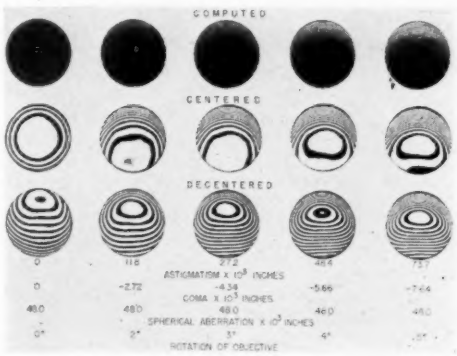

FIG. 30. A comparison of computed and experimental interferometer patterns for $6\times25\times4°$ f:11.5 aberration modifier.

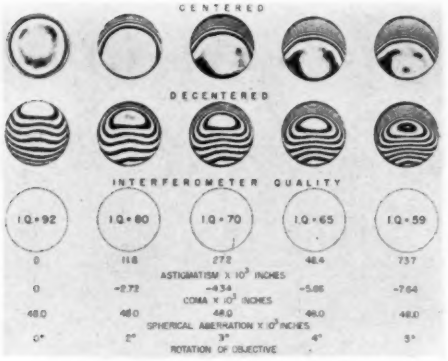

FIG. 31. Interferometer quality of 6×25×4° *f*:11.5 aberration modifier. (Adjusted for best focus.)

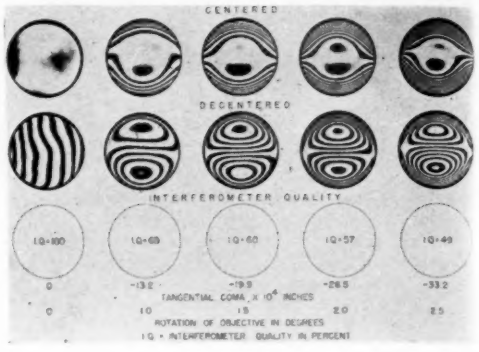

FIG. 34. Interferometer quality of coma modifier. (Adjusted for best focus.)

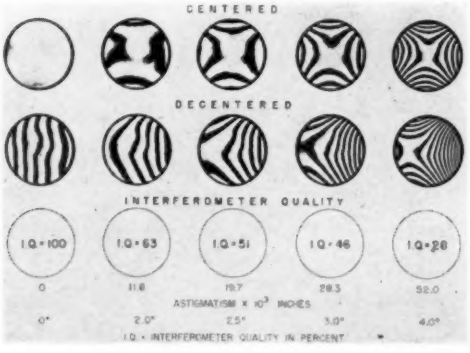

FIG. 32. Interferometer quality of astigmatism modifier No. 1. (Adjusted for best focus.)

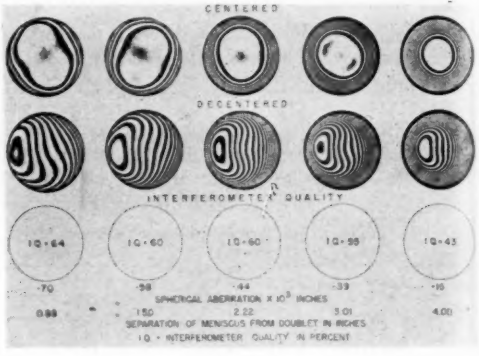

FIG. 35. Interferometer quality of spherical aberration modifier No. 1. (Adjusted for best focus.)

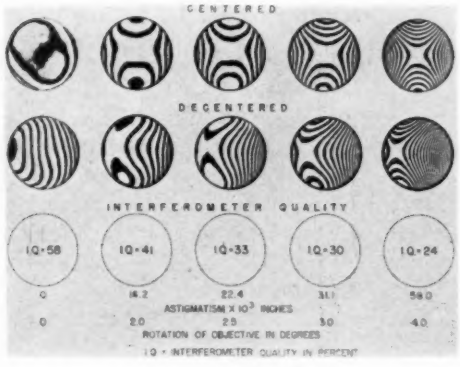

FIG. 33. Interferometer quality of astigmatism modifier No. 2. (Adjusted for best focus.)

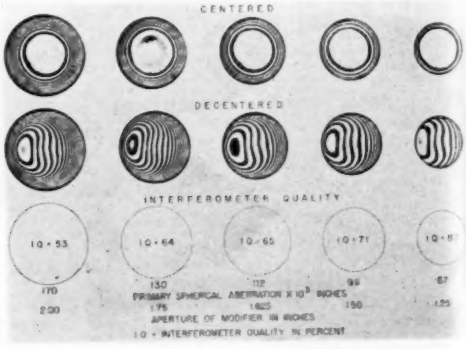

FIG. 36. Interferometer quality of spherical aberration modifier No. 2. (Adjusted for best focus.)

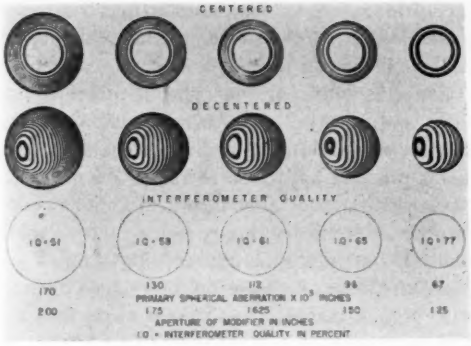

FIG. 37. Interferometer quality of spherical aberration modifier No. 2. (Adjusted for best visual focus.)

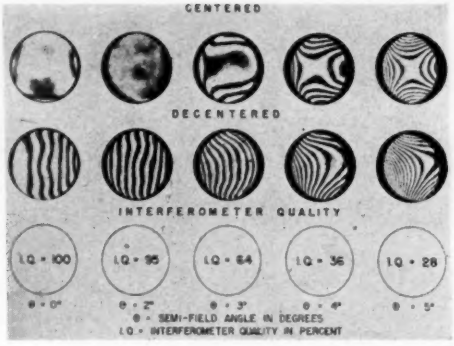

FIG. 40. The interferometer quality of a 3×21×23° lens erecting telescope. (Adjusted for best focus. Design No. 3.)

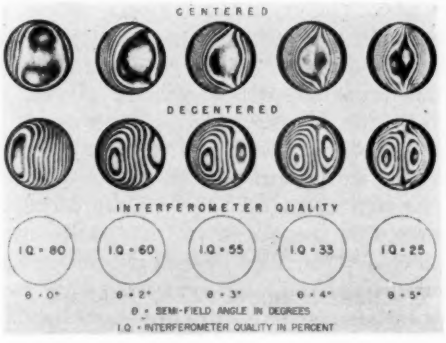

FIG. 38. The interferometer quality of a 3×21×23° lens erecting telescope. (Adjusted for best focus. Design No. 1.)

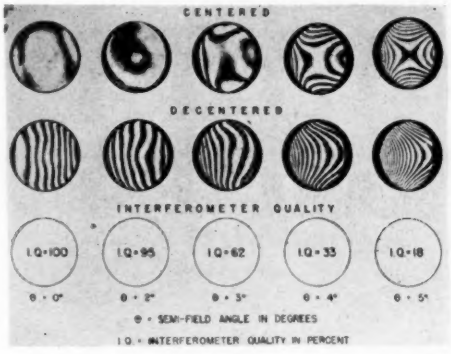

FIG. 41. The interferometer quality of a 3×21×23° lens erecting telescope. (Adjusted for best visual focus. Design No. 3.)

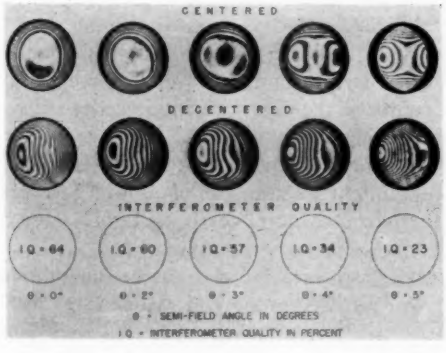

FIG. 39. The interferometer quality of a 3×21×23° lens erecting telescope. (Adjusted for best focus. Design No. 2.)

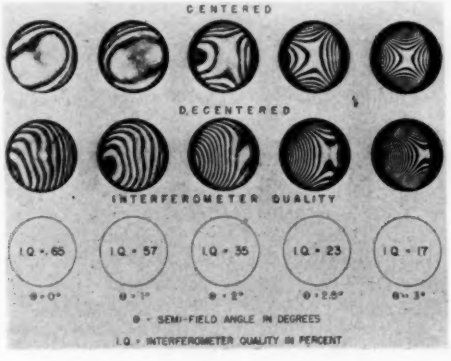

FIG. 42. The interferometer quality of a 6×30×9° prism erecting telescope at various field angles. (Adjusted for best focus.)

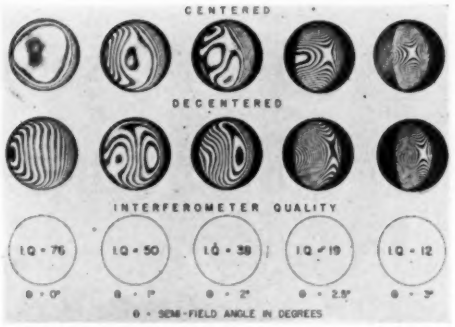

FIG. 43. The interferometer quality of a 7×50×7° prism erecting telescope at various field angles. (Adjusted for best focus.)

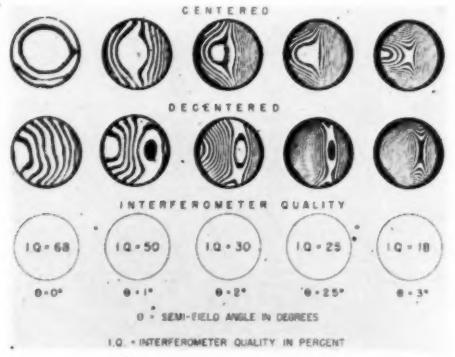

FIG. 44. The interferometer quality of a 7×50×10° prism erecting telescope at various field angles. (Adjusted for best focus.)

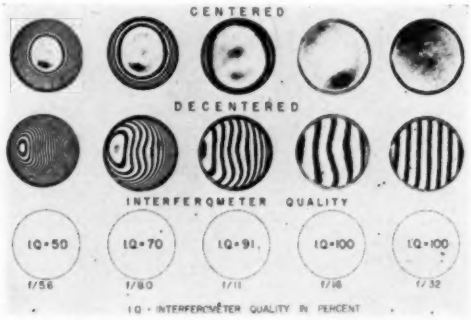

FIG. 45. Axial interferometer quality of an Ic Tessar photographic objective at various relative apertures. (Adjusted for best focus. Effective focal length = 11.75 inches.)

aberrations. Since the main objective of this research program was to evaluate the optical quality of visual telescopic systems, an investigation was made of the type of interferometer patterns produced by telescopic systems focused visually in hopes that such patterns might suggest a possible approach to the problem. In this investigation the aberration modifiers and a number of military instruments were visually focused on numerals subtending angles well above the limit of resolution and placed optically at a great distance. The investigation indicated that the best visual focus was found to give rise to interferometer patterns having one part covered by a single interference area. Slight displacements from the best visual focus were found to result in a decrease in the diameter of this area. This region corresponds to the area over which the optical-path-difference does not exceed one-quarter of a wave-length (taking into account the double passage of the light through the telescopic system under test). The diameter of the largest circle that could be inscribed in this area was taken to be a measure of the optical quality. When this diameter is expressed as the percent of the axial entrance pupil of the system under test, the percentage is referred to as the interferometer quality (hereafter interferometer quality may be abbreviated to I.Q.).

The diameter of the inscribed circle is referred to as the I.Q. circle and is defined in terms of the area over which the optical-path-difference, introduced by a system under test, does not exceed one-quarter of a wave-length. Since the interferometer and the system under test are usually adjusted to produce a light rather than a dark area, the diameter would be measured to the center of the first dark interference fringe on the basis of this definition.

For practical purposes, the interferometer quality might be thought of as the percentage of the entrance pupil of the system under test that is free from aberrations.

The I.Q. values for the aberration modifiers and the number of optical systems of current interest are presented together with their corresponding interferometer patterns in Figs. 31 to 47 inclusive. In this connection it might be mentioned that the instruments studied represent

the simplest telescopic systems to complex systems containing 20 elements and as many as 26 air-glass surfaces.

Figures 36, 37, 40, and 41 are presented to show typical comparison of interferometer patterns for instruments focused visually and focused by means of the interferometer.

In order to be able to compare the interferometer quality of current telescopic systems with current photographic objectives, the I.Q. of an Ic Tessar objective was measured. This objective was tested at various relative apertures and semi-field angles. The results are shown in Figs. 45, 46, and 47. The resolving power of this same lens has been reported previously.[1] There is close agreement between the I.Q. and K.D.C. efficiency values.

It might be noted that a photographic procedure was followed in recording the above I.Q. data. While this is not particularly time consuming, I.Q. values can be obtained more rapidly by measuring the I.Q. circle by means of a finely graduated reticle placed slightly in front of the eye and near the focal plane of the viewing lens of the interferometer.

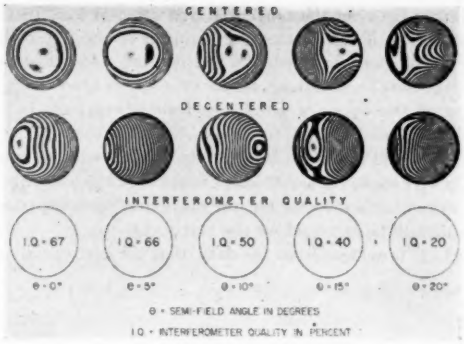

FIG. 46. Interferometer quality of an f:8 Ic Tessar photographic objective at various semi-field angles. (Adjusted for best focus. Effective focal length = 11.75 inches.)

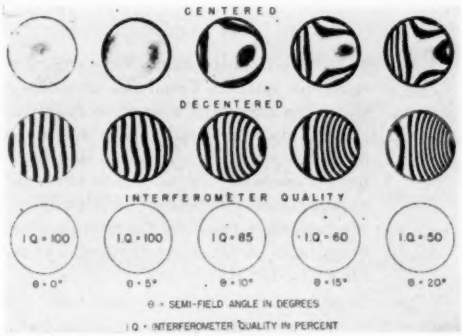

FIG. 47. Interferometer quality of an f:16 Ic Tessar photographic objective at various semi-field angles. (Adjusted for best focus. Effective focal length = 11.75 inches.)

DISCUSSION AND CONCLUSIONS

The discussion and conclusions of this interferometer study of telescopic systems are stated in the following paragraphs:

1. A satisfactory method has been developed for evaluating the quality of telescopic systems by means of the interferometer. This method is referred to as the Interferometer Quality (I.Q.) method.

2. The I.Q. method makes it possible to assign numerical values describing the quality of an optical system. The I.Q. method is simple, rapid, and probably the most accurate procedure available at present for determining the quality of telescopic systems.

3. The I.Q. method may be applied to evaluating the quality of lenses and prisms as well as telescopic systems.

4. Numerical values of the interferometer quality are in close agreement with measurements of resolving power.

5. The form of interferometer patterns for a known mixture of aberrations can be predicted by computation and may be used to check conformance with a given design. The analysis, however, into individual components of even a simple mixture of aberrations is difficult and too time consuming to be of practical interest in mass production.

6. The interferometer may be used for routine testing of telescopic systems at various field angles.

7. The I.Q. method of using the interferometer to evaluate the quality of telescopic systems has face value on the basis that the telescopic system under test is focused exactly the same as it would be for visual use.

8. The best focal plane has been found to be very close to the paraxial focus for telescopic systems afflicted with primary spherical aberration for magnitudes of the aberrations greater than one-quarter of a wave-length. Geometrical optics and wave theory would place the best focal plane three-quarters and one-half the distance from the paraxial to the marginal foci, respectively.

9. It is evident from the preceding data that the eye selects as the best focal plane the focus that produces the largest possible I.Q. circle. This indicates that the eye focuses on the image formed by the rays passing through an area of the entrance pupil over which the optical paths do not vary by more than a quarter of a wave-length. The rays outside of this area are out of focus and simply reduce the apparent image contrast.

10. It is evident from the above data that the best visual and best interferometer focus for primary astigmatism is

halfway between the tangential and saggital foci. In this connection, it is seen that the diameter of the I.Q. circles for the tangential and saggital foci are always less than that for the best focal setting. However, there is often a larger area of the entrance pupil free from aberrations in the tangential and saggital foci than in the best focus pattern, which would indicate that if a rectangular entrance pupil stop were used, a brighter image could be obtained for these foci than for best focus, but the maximum resolving power would still be obtained for the best focus.

11. It is evident from the data, that the best visual and the best interferometer focus for coma is very close to the paraxial focus.

ACKNOWLEDGMENT

The optical design for the Coma Modifier and Spherical Aberration Modifier No. 1 mentioned in this paper were developed by Drs. J. L. Greenstein and L. G. Henyey of the Yerkes Observatory under terms of OSRD Contract OEMsr-1078.

JOURNAL OF THE OPTICAL SOCIETY OF AMERICA VOLUME 37, NUMBER 9 SEPTEMBER, 1947

The Reduction in Image Contrast Caused by the Aberrations in Telescopic Systems

HOWARD S. COLEMAN
The Optical Inspection Laboratory, The Pennsylvania State College, State College, Pennsylvania
(Received May 16, 1947)

A study has been made of the reduction in image contrast caused by optical aberrations in telescopic systems. Visual measurements were made of the resolution of telescopic systems, in which the amount of aberration could be varied continuously, and in a number of telescopic systems of current design. The resolution measurements were made using Foucault test objects of high contrast. The contrast of the image of the test object on the retina was determined at the limit of resolution for the various telescopic systems. This contrast was found to have a value of approximately four percent for telescopic systems free from all aberrations. From a knowledge of the contrast required by the retina for resolution and the loss in resolution caused by different magnitudes of the aberrations, it was possible to compute the reduction in image contrast caused by the aberrations.

INTRODUCTION

THE ill effects caused by aberrations in visual telescopic systems are under consideration. The purpose of this consideration is to establish allowable tolerances in optical designs based on actual performance. One ill effect caused by an optical aberration is to reduce the contrast of the images of objects in the case of recognition observations. This reduction in contrast has been measured for a number of telescopic systems afflicted with the common primary aberrations and for mixtures of aberrations found in current designs. It is the purpose of this paper to describe the methods used in these measurements and to present the values obtained.

TABLE I.

K.D.C. efficiency in percent	Specific coefficient of—resolution in mm —radians $\times 10^3$	Apparent contrast in percent
100	55.4	100.0
90	61.5	21.6
80	69.3	10.4
70	79.2	6.8
60	92.3	5.2
50	110.8	4.4

THE APPARATUS AND PROCEDURE

The resolution measurements were determined by means of the K.D.C. apparatus,[1] and by a number of telescopic systems in which the magnitude of the primary aberrations can be varied continuously.

The procedure consisted of measuring the

TABLE II.

Astigmatism $\times 10^3$ inches	Reduction in contrast
0.0	0.0%
8.1	78.4
14.5	89.6
20.0	93.2
24.8	94.8
34.0	95.6

[1] H. S. Coleman and S. W. Harding, J. Opt. Soc. Am. **37**, 263 (1947).

TABLE III.

Coma $\times 10^4$ inches	Reduction in contrast
0.0	0.0%
−11.6	78.4
−21.0	89.6
−28.2	93.2
−34.0	94.8
−38.0	95.6

TABLE IV.

Spherical aberration $\times 10^3$ inches	Reduction in contrast
0.0	0.0%
−11.5	78.4
−24.5	89.6
−38.0	93.2
−51.0	94.8
−64.0	95.6

specific coefficient of resolution (defined to be the product of the aperture in millimeters and the minimum resolvable angle in radians) for various amounts of primary astigmatism, tangential coma, and spherical aberration. In addition, the specific coefficient of resolution was determined for eight different specimens of a current design of prism-erecting telescopes. A high contrast Foucault test object was used in these measurements. Since the contrast required by the retina for resolution[1] (four percent contrast for the test objects used) is independent of the aberrations in the telescopic systems, any reduction in resolution caused by the aberrations can be related to the contrast of the image presented to the eye by means of the theoretical curves described in an earlier paper.[2]

THE DATA

The data are presented in tabular form. Table I shows the theoretical data referred to in reference 2. This table shows the relation among the K.D.C. efficiency, specific coefficient of resolution, and the apparent contrast of the image of the test object formed by an optical system under consideration for conditions in which the retina requires a contrast of four percent for resolution.

Table II shows the reduction in contrast caused by various amounts of primary astigmatism for a telescopic system having an entrance pupil of 1.40 inches, a magnification of 60×, and an objective having an effective focal length of 11.5 inches.

Table III shows the reduction in contrast caused by various amounts of over-corrected tangential coma for a telescopic system having an entrance pupil of 1.40 inches, a magnification of 50×, and an objective having an effective focal length of 6.03 inches.

Table IV shows the reduction in contrast caused by over-corrected spherical aberration in a telescopic system having an entrance pupil of 1.40 inches, a magnification of 50×, and an objective having an effective focal length of 6.34 inches.

Table V shows the reduction in contrast caused by various amounts of under-corrected spherical aberration for a telescopic system having an effective focal length of 15.75 inches, a magnification of 80×, and apertures ranging from 0.00 to 2.00 inches.

Table VI shows the reduction in contrast caused by a mixture of unidentified aberrations found on the optical axis of eight 7×50×7° prism-erecting telescopic systems of the same design.

DISCUSSIONS AND CONCLUSIONS

The conclusions reached as to the reduction in image contrast caused by aberrations in telescopic systems are summarized as follows:

TABLE V.

Aperture in inches	Spherical aberration $\times 10^3$ inches	Reduction in contrast
0.00	0.0	0.0%
1.25	68.0	78.4
1.38	81.0	89.6
1.50	98.0	93.2
1.75	132.0	94.8
2.00	175.0	95.6

TABLE VI.

Specimen number	Specific coefficient of—resolution in mm —radians $\times 10^3$	Reduction in contrast
1	60	73.4%
2	65	85.5
3	70	90.0
4	74	91.7
5	80	93.3
6	85	94.1
7	94	94.9
8	126	95.8

[2] H. S. Coleman and M. F. Coleman, "Theoretical resolution angles for point and line test objects in the presence of a luminous background," J. Opt. Soc. Am. **37**, 572 (1947).

(1) The reduction in image contrast produced by the common aberrations is great. This suggests that the ill effects of optical aberrations of the type mentioned in this paper may be described in terms of the reduction in image contrast. Thus the reduction in contrast could be used as a general basis for discussing such imperfections. When this reduction is expressed on a percentage basis, the ill effects of the aberration may be treated in the same fashion as stray light[3] in the case of targets subtending angles well above the limit of resolution. By means of such a treatment the reduction in contrast can be computed for targets of any inherent contrast from a knowledge of the contrast reduction produced for a target of high contrast. Since high contrast targets can be used, the resolution measurements can be made with considerable precision.[1]

(2) The contrast reduction caused by a mixture of unknown aberrations can be determined just as easily as the case of single identifiable aberrations. This reduction may, therefore, be used as a general measure of the imperfection in optical quality for any optical system without a knowledge of the specific aberrations present.

[3] H. S. Coleman, "Stray light in optical systems," J. Opt. Soc. Am. **37**, 434 (1947).

JOURNAL OF THE OPTICAL SOCIETY OF AMERICA VOLUME 37, NUMBER 9 SEPTEMBER, 1947

Neutral Density Filters of Chromel A[1]

MARY BANNING
Institute of Optics, University of Rochester, Rochester, New York

(Received February 3, 1947)

A short review of the available neutral density filters is given, with emphasis placed on the evaporation of Chromel A to form a film of any practical density that has neutral transmission throughout the visible and into the infra-red and ultraviolet regions. These films are simple to make and have proved to have good durability, resisting corrosion and rough handling.

A SEARCH has been conducted to find a good neutral density filter that stands up under extreme heat and weather conditions, exhibits very little light scatter, and is simple and

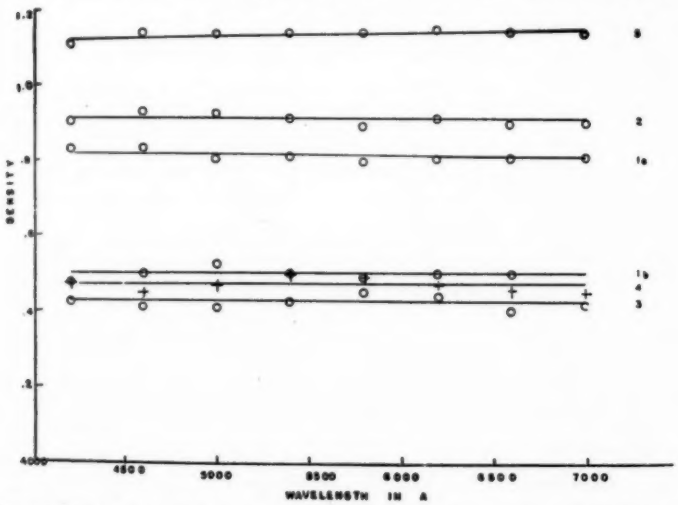

FIG. 1. Neutral density filters: (1*a*) photographic density, specular; (1*b*) photographic density, diffuse; (2) palladium; (3) tungsten; (4) Duolux; (5) Chromel A.

[1] The work described here was carried out in whole or in part under contract with Division 16 of the Office of Scientific Research and Development, at the University of Rochester.

inexpensive to produce. Photographic neutrals, as shown in curves 1*a* and 1*b* of Fig. 1, show good neutrality over the visible spectrum, but very high diffusion. It was hoped that some non-diffusing evaporated metallic film would be found that was as neutral as the photographic films.* Tests were made on over twenty-five metals and alloys, with the best results shown in curves 2 to 5 in Fig. 1.

Tungsten and palladium films, although good neutrals, are difficult to make and control because of the high evaporating temperatures of the materials. Duolux[2] is a commercial film which is of interest for comparison. Best results were obtained by the evaporation of Chromel A, a standard resistance wire. Chromel A is an alloy composed of 80 percent nickel and 20 percent chromium. When evaporated properly it gives a film of quite neutral density from 2400A to 15,000A, with a maximum density variation over this range of 12 percent. Films have been made with good neutrality of densities ranging from 0.1 to 2.0.

The alloy is evaporated in the same manner as aluminum from an open tungsten wire. Like aluminum, it melts before evaporating. Because molten nickel attacks tungsten very quickly, it is necessary to use a thick tungsten filament and a small amount of Chromel A; 50-mil tungsten rod and 18-gauge Chromel A are used here. The melting point of Chromel A lies between the evaporation temperatures of chromium and nickel, i.e., the temperatures at which their vapor pressures equal 10^{-2} mm Hg.[3] Thus if the evaporation takes place at approximately the melting point of Chromel and at 10^{-2} mm Hg pressure (or somewhat less), only chromium will deposit. If, however, the vapor pressures are such that the melting temperature of Chromel A is sufficient to evaporate both materials at 10^{-4} mm Hg, a combination film will be deposited.

Curve 1 in Fig. 2 shows the density variation of pure evaporated chromium. Curve 2 is a sample of Chromel A evaporated at 10^{-3} mm Hg;

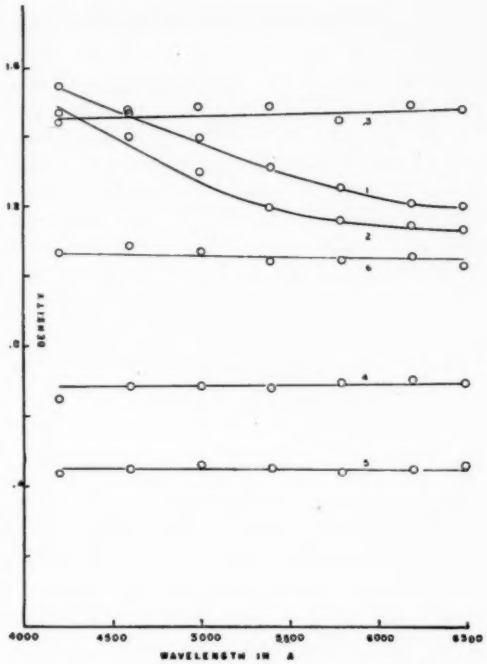

FIG. 2. Density of chromium and Chromel A. (1) chromium; (2) Chromel A, evaporated at 10^{-3} mm Hg; (3)–(6) Chromel A evaporated at 10^{-4} mm Hg.

chemical analysis of this sample showed chromium but no trace of nickel. As the pressure in the evaporating chamber is reduced to 10^{-4} mm Hg or lower, a good deal of nickel also comes off, and gives a density variation as shown in curve 3; this sample showed a large proportion of nickel present. Curves 4–6 are other neutral samples of Chromel A.

If densities greater than 2 are desired, it is better to combine two filters rather than to attempt further evaporation on one. Films that are too thick show a reddish transmission, because of the evaporation of too much chromium.

These neutral films are about as hard as pure chromium and withstand a great deal of punishment, especially if heated to approximately 200°C after evaporation. An opaque Chromel A film can be used in most cases as a substitute for chromium, as for a mirror or a backing for aluminum. This is often desirable because Chromel A evaporates from tungsten more simply and more quickly than pure chromium.

* Previous studies of combination aluminum and chromium films by R. E. Hopkins, at the University of Rochester (1939), showed that evaporated neutral films held great promise.

[2] Duolux is made by the Evaporated Metal Films Corporation, Ithaca, New York.

[3] J. Strong, *Procedures in Experimental Physics* (Prentice-Hall, Inc., New York, 1938), p. 169.

Partially Reflecting Mirrors of High Efficiency and Durability[1]

MARY BANNING
Institute of Optics, University of Rochester, Rochester, New York

(Received February 3, 1947)

A simple laboratory method for making partially reflecting mirrors of high efficiency is provided by fuming titanium tetrachloride onto glass. The reaction of the tetrachloride with atmospheric water vapor allows a thin coating of titanium dioxide to deposit on hot glass.

$$TiCl_4+2H_2O\rightarrow TiO_2+4HCl.$$

This coating is extremely durable and can be washed frequently without producing pinholes. The critical thickness for maximum reflectivity is regulated by watching the color of the reflected light. A single coating reflects 30 and transmits 70 percent of incident light.

Alternate layers of fumed titanium dioxide and evaporated magnesium fluoride afford reflectivities over the visible range of from 30 to over 60 percent, depending on the number of layers.

A SIMPLE and effective method of fuming titanium dioxide films onto glass to form a partially reflecting mirror of high efficiency has been developed following the general method first proposed by Cartwright and Turner in 1939,[2] and further developed by J. A. Sanderson at the Naval Research Laboratories.

Liquid titanium tetrachloride is poured into a 10-inch evaporating dish and brought to a temperature of approximately 60°C. An air jet, formed by passing a stream of ordinary compressed air through a funnel of 3-inch diameter, is then played on the surface of the liquid. This contains enough water vapor to react with the tetrachloride and form a cloud of swirling dense white smoke over the dish. If a hot piece of glass is held in this cloud, titanium dioxide will condense upon it in a hard, tenacious film.

The index and hardness of films deposited in this way varies with the temperature of the glass and the tetrachloride. Indices range from 2.2 on warm glass to 2.9 when the glass is heated to 200°C and coated immediately. A soft foggy film deposits if the glass is at room temperature, increasing in hardness as the temperature is raised. Best results are obtained with glass at 200°C and tetrachloride at 60°C. In order to obtain maximum reflection for visible light, the dioxide film is made $\frac{1}{4}$-wave-length thick for green light, so that the reflections from the glass-film and air-film surfaces are in phase. This is the case when the film reflects a bright white color; too thick a film reflects yellow or magenta in the same manner as zinc sulfide.[3] Very little practice is needed to stop the deposition at the proper point.

Constant motion of the plate in and out of the cloud is necessary to insure a uniform surface. If the same part of the glass always cuts into the cloud first, there is a greater deposit on this part of the plate, so it is rotated several times during deposition. A film quickly deposited, in approximately half a minute, is always more uniform than one deposited slowly as uneven cooling will result in uneven thickness.

All parts of the glass that are to be kept clear are either covered or coated with a high melting point stopcock grease that can later be cleaned off. If the glass is of odd shape and grease is not desired, a paper housing may be made for it; Scotch Tape, when subjected to such a high temperature tends to melt and is very difficult to remove later. The air stream is adjusted to give a good white cloud, but not allowed to become so strong as to spatter liquid or particles up onto the plate. All work is done under a hood with a strong air intake, to remove the hydrochloric acid fumes that are formed with the titanium dioxide.

For best results, the glass is first boiled in nitric acid and then cleaned as carefully as for

[1] The work described here was carried out in whole or in part under contract with Division 16 of the Office of Scientific Research and Development, at the University of Rochester.

[2] C. H. Cartwright and A. F. Turner, Phys. Rev. **55**, 1128A (1939).

[3] A. H. Pfund, J. Opt. Soc. Am. **24**, 99 (1934).

evaporation. Such a film will withstand moderate rubbing with Bon Ami without producing pinholes. All films withstand any mild cleaning agent and are completely removed from the glass only by boiling in concentrated nitric acid or by repolishing the surface. In such cleaning, care must be taken to keep acid away from extra dense flints, and especially barium glasses, as the glass is easily etched.

Films have been made by this method on plates of glass four inches square with good uniformity. Reflections of 30 percent over the visible region are easily obtained if one side of a plate is coated, and 43 percent if both sides are coated, the rest of the light being transmitted. A "sandwich" built up of two titanium dioxide layers, with a $\frac{1}{4}$-wave-length magenta layer of evaporated magnesium fluoride in between, reflects 53 percent of incident visible light at 45 degrees incidence.

Beam-splitting devices, using both reflected and transmitted light without absorption loss, can be made by depositing titanium dioxide or a sandwich on the faces of two prisms and then cementing with resin CR-39. However, since the cementing considerably reduces the reflection, both surfaces to be cemented should be coated; two cemented surfaces give about the same reflection as one uncemented surface, as quoted above. Although a single film of titanium dioxide is quite neutral in transmission and reflection, a sandwich film, reflecting most highly in the green, shows a magenta transmission. This fact is often very useful in beam-splitting devices where a color differential is desired. The color difference can be made more intense by increasing the thickness of the films. Control of film thickness can also change the maximum reflection to any desired part of the spectrum, or for any angle of incidence.

JOURNAL OF THE OPTICAL SOCIETY OF AMERICA VOLUME 37, NUMBER 9 SEPTEMBER, 1947

Three-Layered Reflection-Reducing Coatings

LUTHER B. LOCKHART, JR. AND PETER KING
Naval Research Laboratory, Washington, D. C.

(Received May 23, 1947)

An analysis of the various factors involved in several typical three-layered reflection-reducing coatings has been made from both an experimental and a theoretical standpoint. By taking into account the approximate dispersions of the materials, reasonable agreement between the experimental and calculated reflection curves has been obtained.

Interesting results were obtained on electron diffraction studies of the various coating materials. Thin films of titanium dioxide, the high index material used, were found to have crystalline patterns that varied with the coated material and that, in general, were not recognizable as titanium dioxide patterns. Thus it was considered impossible to assign any definite values to the refractive indices of such thin films without specifying the substrate.

INTRODUCTION

THE U. S. Naval Technical Mission in Europe reported that Schott and Company, Jena, Germany, had developed a method of reducing reflections from glass surfaces through the use of three superimposed layers of different refractive indices and controlled thicknesses.[1,2] An examination[3] of representative samples of this type coating showed them to be quite effective in reducing reflection over practically the entire visible spectrum. Since this type of coating proved to approach closely the desired "non-reflecting" surface over a broad region, a study was made of it considering the following points: (1) effect of coatings of different indices

[1] U. S. Naval Technical Mission in Europe, Technical Report No. 473–45 of September 1945.
[2] Swiss Patent 223344 of January 4, 1943, issued to Jena Glass Works, Schott and Genossen, Jena, Germany.
[3] H. A. Tanner, and L. B. Lockhart, J. Opt. Soc. Am. **36**, 701 (1946).

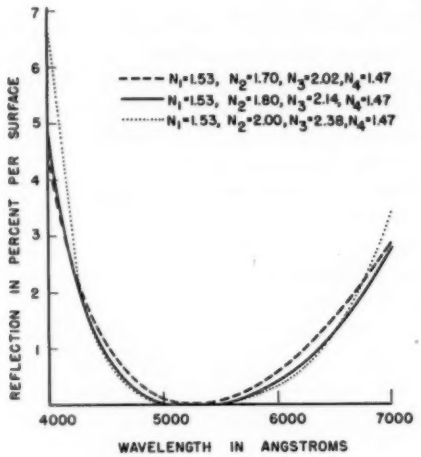

FIG. 1. Spectral reflections of coatings composed of three quarter-wave layers. Theoretical.

and thicknesses, (2) method of application, and (3) nature of deposited films.

THEORETICAL CONSIDERATIONS

The analysis of the reflection of a three-layered coating deposited on a transparent surface involves the evaluation of the sum of the reflections from four interfaces and must take into account the interaction (constructive and destructive interference) between the reflections from the several boundaries. This analysis is simplified by the use of the general theory mentioned before and applied to the case of two-layered coatings.[4] Calculation of the reflection from a system composed of three distinct layers deposited on a transparent substrate may be readily handled by the following relations. For the case where the incident light is normal to the coated surface,

$$R=|(X-1)/(X+1)|^2, \qquad (1)$$

where

$$\begin{aligned} X=&[(n_2n_3n_4-n_2^2n_4\tan\omega_2\tan\omega_3 \\ &-n_2^2n_3\tan\omega_2\tan\omega_4-n_2n_3^2\tan\omega_3\tan\omega_4)\cdots \\ &+i(n_1n_3n_4\tan\omega_2+n_1n_2n_4\tan\omega_3 \\ &+n_1n_2n_3\tan\omega_4-n_1n_3^2\tan\omega_2\tan\omega_3\tan\omega_4)]/ \\ &\cdots[(n_1n_2n_3n_4-n_1n_3^2n_4\tan\omega_2\tan\omega_3 \\ &-n_1n_3n_4^2\tan\omega_2\tan\omega_4-n_1n_2n_4^2\tan\omega_3\tan\omega_4) \\ &\cdots+i(n_2^2n_3n_4\tan\omega_2+n_2n_3^2n_4\tan\omega_3 \\ &+n_2n_3n_4^2\tan\omega_4-n_2^2n_4^2\tan\omega_2\tan\omega_3\tan\omega_4)], \end{aligned}$$

and where

$\omega_j=2\pi n_j d_j/\lambda$,
n_1 = index of refraction of coated material,
n_2 = index of refraction of bottom layer, d_2 its thickness,
n_3 = index of refraction of middle layer, d_3 its thickness,
n_4 = index of refraction of top layer, d_4 its thickness,
λ = wave-length of incident light,
$i=(-1)^{\frac{1}{2}}$.

This expression reduces to that for the two-layered system reported before when the thickness of the top layer (d_4) is set equal to zero and $n_4=1$, and to the single-layered case when both d_3 and d_4 are equal to zero and $n_3=n_4=1$.

A consideration of the general expression for the reflection from a three-layered system shows that several simple arrangements of film thicknesses will result in zero reflection for light of a particular wave-length. Two particular cases are examined here.

(a) Each film is one-quarter wave-length in thickness (optical thickness is meant in all cases).

Since under this condition

$$\tan\omega_2=\tan\omega_3=\tan\omega_4=\infty,$$

dividing by $\tan\omega_2\tan\omega_3\tan\omega_4$ gives

$$X=n_1n_3^2/n_2^2n_4^2$$

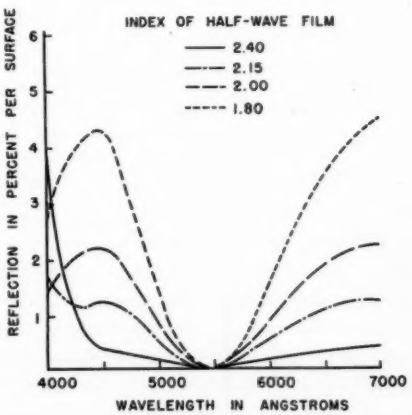

FIG. 2. Spectral reflections of three-layered coatings composed of quarter-wave bottom layers of 1.80 index, half-wave middle layers of various indices, and quarter-wave top layers of 1.47 index on glass of 1.53 index. Theoretical.

[4] P. King and L. B. Lockhart, J. Opt. Soc. Am. **36**, 513 (1946).

and

$$R=[(n_1n_3^2-n_2^2n_4^2)/(n_1n_3^2+n_2^2n_4^2)]^2.$$

Thus $R=0$ when

$$n_3=n_2n_4/n_1^{\frac{1}{2}}. \quad (2)$$

(b) The top and bottom films are each one-quarter wave-length thick and the middle film is one-half wave-length thick.

Since under this condition $\tan\omega_2=\tan\omega_4=\infty$ and $\tan\omega_3=0$, dividing by $\tan\omega_2\tan\omega_4$ and then setting $\tan\omega_3=0$ gives

$$X=n_2^2/n_1n_4^2$$

and

$$R=[(n_2^2-n_1n_4^2)/(n_2^2+n_1n_4^2)]^2.$$

Thus $R=0$ when

$$n_2^2=n_1n_4^2. \quad (3)$$

Case (b) is interesting in that the condition for zero reflection is independent of the index (n_3) of the middle layer. This is to be expected, since for a particular wave-length a film a half-wave-length in optical thickness (or multiples thereof) has the same properties as a film of zero thickness.

The spectral reflections of several systems composed of three layers of different indices which result in zero reflection at one wave-length and whose indices are governed by Eqs. (2) or (3), have been calculated. Figures 1 and 2 show the reflection characteristics to be expected from these types of coatings. Those composed of three quarter-wave films have broader reflection minima than the two-layered coatings previously reported. However, the three-layered coatings composed of films a quarter-, a half-, and a quarter-wave-length in optical thickness have the broadest reflection minima of any system so far studied.

One property of the calculated reflection curves illustrated in Fig. 2 should be mentioned. Although the combination of indices which gives zero reflection and is defined by Eq. (3) is independent of the index of the half-wave film, the over-all shape of the reflection curve is greatly influenced by its value. It is apparent that the half-wave-length film must have an index of refraction in the range 2.3–2.4 to obtain a really broad minimum. This rather high value limits the materials which can be used without introducing considerable absorption.

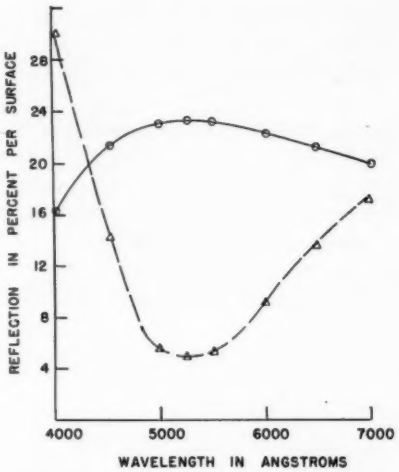

FIG. 3. Spectral reflections of coatings a quarter-wave and a half-wave-length in optical thickness. Experimental. Solid line—quarter-wave film of 2.09 index; broken line—two superimposed quarter-wave films of 2.09 index.

As in the case of the two-layered coatings, many other combinations of film thicknesses and indices can result in zero reflection for a particular wave-length. However, other combinations differing from the two cases mentioned will not be considered as the two examples chosen indicate the general characteristics of this system for reducing reflection.

EXPERIMENTAL

The component parts of three-layered systems for reducing reflection can be deposited by several different methods: evaporation in a high vacuum, vapor deposition at atmospheric pressure,[1,3] or from solutions of various types.[4,5] In this work the latter two methods were used.

The method of attack consisted of defining the experimental conditions necessary for depositing films a quarter-wave-length in optical thickness at the desired wave-length and possessing the desired refractive index. This was done by preparing a number of series of glass disks coated with single films of different compositions under varying conditions and then determining the

[5] W. Geffcken, German Patent 742,463 of January 18, 1944.

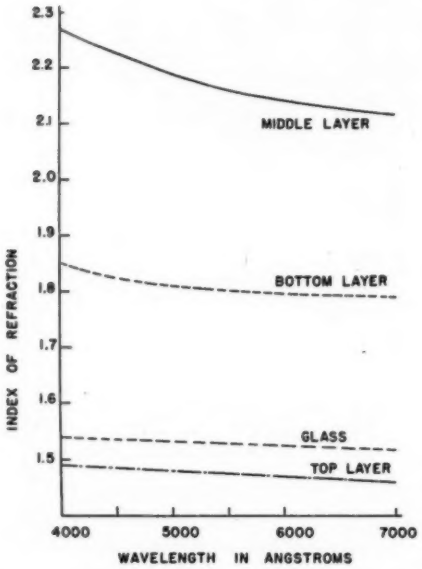

FIG. 4. Dispersion curves of component parts of three-layered solution-type coatings.

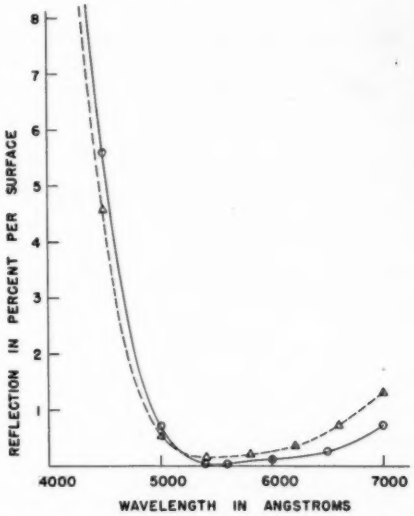

FIG. 5. Spectral reflections of coatings composed of three quarter-wave layers where $n_1=1.53$, $n_2=1.80$, $n_3=2.14$, and $n_4=1.47$. Experimental.

correct experimental conditions from the positions and values of the reflection maxima or minima. The values of the refractive indices of the films were determined from the extreme points by use of the following relation:

$$n_f=[n_g(1+R^{\frac{1}{2}})/(1-R^{\frac{1}{2}})]^{\frac{1}{2}},$$

where

n_f = index of the film,
n_g = index of the glass,
R = reflection.

The dispersions of the coatings were determined from reflection measurements of a number of coated disks having reflection minima (or maxima) at different positions in the visible spectrum. Films a half-wave-length in optical thickness and of the desired index were prepared by superimposing two quarter-wave films under identical experimental conditions. The justification for this procedure is shown in Fig. 3. Here the reflection maximum of the quarter-wave film and the minimum of the half-wave film occur at the same wave-length.

Another method of calculating dispersion curves for the high index materials gave anomalous results. In this procedure the index of the coating at various wave-lengths was taken as that required to cause coincidence of a calculated and an experimental reflection curve. The resulting values for the indices calculated for quarter-wave and half-wave films of the same material and having their maximum and minima at the same wave-length were entirely out of line with each other. For this reason the indices calculated from the maxima of a series of quarter-wave films were accepted as the most reasonable values.

Once conditions had been established, systems of any desired combinations could be made. The results obtained with the two chosen systems are discussed in the following section.

DISCUSSION OF RESULTS

The dispersion curves of solution-deposited coatings of the different coating materials are shown in Fig. 4. The values given are only approximations of the true values of the refractive indices as a result of previously discussed difficulties and to the effect of the substrate. However, it can be seen that there is considerable change in the refractive index of the high index material toward the short wave-lengths.

An attempt was made to identify positively the exact nature of the various layers. The

chemical compositions of the vapor-deposited coatings were determined and found to be TiO_2, SiO_2, and a mixture of the two, but the exact crystalline form was unknown. Electron diffraction studies on the films deposited from vapor gave interesting but discouraging results.[6] The silicon dioxide layer was found to be crystobalite, the mixed layer to be amorphous, and the titanium dioxide layer to change with each substrate. When deposited on glass, quartz, nickel, or rutile the latter was originally amorphous, but, when heated to 450°C for two hours, it developed a definite crystalline pattern different for each base material. The results on rutile were especially interesting in that the amorphous layer gave the rutile pattern after the heat treatment at 450°C.

Coatings deposited from solution were equally hard to interpret. The silicon dioxide films were crystalline when heated to 110°C for 64 hours but amorphous when heated at 450°C for two hours. The mixed coating was crystalline when heated at 400°C or 450°C but amorphous when heated at 110°C for 64 hours. This differs from the vapor deposition of the mixed layer. Titanium dioxide deposited over the mixed layer and heated at 450° for two hours gave a crystalline pattern.

The results showed that no general dispersion curve could be prepared for the high index layer. The value of the index depends on the crystalline structure which is determined by the substrate. However, the approximate dispersion curves given in Fig. 4 were determined for a particular base material and those values used in the calculations.

Two experimental curves of coatings whose indices and thicknesess approximately meet the requirements of Eq. (2) are shown in Fig. 5. They may be compared with the calculated curves of Fig. 6, for a system which does meet the above requirements. One of the calculated curves takes into account the dispersions as defined by the curves of Fig. 4. The small differences between the two calculated curves indicates the slight effect of the dispersion of the materials on coatings composed of three quarter-wave films.

Case (b), which results in the broadest minimum, was investigated more completely. Experimental and calculated curves of a typical coating

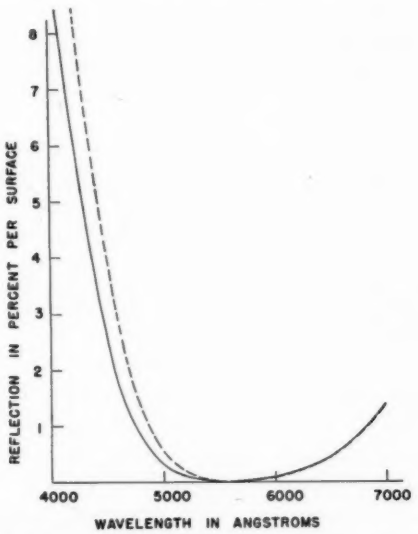

FIG. 6. Spectral reflections of coatings composed of three quarter-wave layers where $n_1 = 1.53$, $n_2 = 1.80$, $n_3 = 2.14$, and $n_4 = 1.47$. Theoretical. Solid line—assuming no dispersion; broken line—assuming dispersion according to Fig. 4.

[6] This was done by J. Karle and C. Glover of the Naval Research Laboratory; studies are being continued by them.

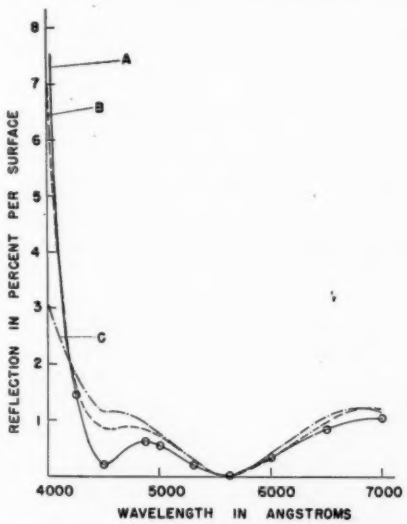

FIG. 7. Spectral reflections of three-layered coatings composed of quarter-wave, half-wave, and quarter-wave superimposed films. Curve *A*—experimental; curve *B*—calculated curve assuming dispersion according to Fig. 4; curve *C*—calculated curve assuming no dispersion.

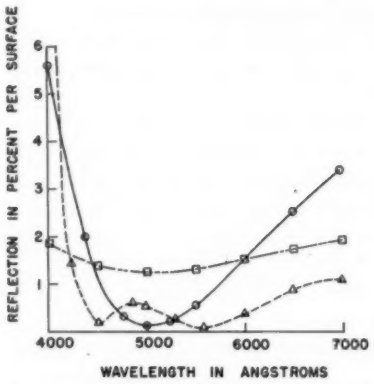

FIG. 8. Comparison of spectral reflections of typical one-, two-, and three-layered coatings. Experimental. □ MgF_2 on 1.517 index glass; ○ two-layered coating; △ three-layered coating.

conforming with Eq. (3) are shown in Fig. 7. The agreement between the two is satisfactory, considering the possible error in the dispersion curves of the component parts. If no dispersion is assumed, the values represented by curve *C* of Fig. 7 are obtained. A comparison of curves *B* and *C* shows the great effect of the dispersion in this case. In the one-layered, two-layered, and three-layered quarter-wave cases it does not contribute to any extent to the calculated reflection curves. The larger effect here is due to the fact that when $\tan\omega_3$ refers to a half-wave film, it changes much more rapidly with changes in optical thickness and wave-length than when it refers to a quarter-wave film and consequently has more effect on the reflection.

Analysis of the reflection of the component parts of the German three-layered coatings indicated the bottom layer to have an index of refraction of about 1.70 and the half-wave layer to have an index of about 2.40. Presumably the top layer had an index of about 1.45–1.47 since this coating was composed of silica. This combination of coatings does not fit that required to give zero reflection for $\lambda/4$, $\lambda/2$, and $\lambda/4$ layers, but possibly slight variations in thicknesses of the layers in conjunction with the above indices meet the requirements for zero reflection of another of the many possible solutions.

TABLE I. Luminous reflection of various coatings toward I.C.I. illuminant *C*.

Coating*	Type	Producer	Reflection Daylight	Night
3-layer	vapor deposition	Schott	0.21%	0.35%
3-layer	solution	Schott	0.56	0.37
3-layer	solution	N.R.L.	0.26	0.38
2-layer	solution	N.R.L.	0.81	0.50
1-layer	magnesium fluoride	N.G.F.**	1.43	1.31

* Coatings applied to glass of about 1.52–1.53 index.
** Naval Gun Factory, Washington, D. C.

In Fig. 8 typical reflection curves for different types of reflection-reducing coatings on glass of about 1.53 index are shown. Table I lists the luminous reflection of these coatings toward I.C.I. illuminant *C*. The response to both the daylight and night adapted eye is given. It can be seen that the three-layered systems are much more efficient than either the one- or two-layered ones considered.

From these studies, a choice may be made of the type of coating system desired for a given application. In those cases where there are many surfaces and the last bit of light is needed, the three-layered system is the most effective. However, because of the difficulty in application, it would be used sparingly.

A Table of Logarithmic Corrections to the Wien Radiation Law

ELLIOT Q. ADAMS
Lamp Development Laboratory, General Electric Company, Nela Park, Cleveland, Ohio
(Received May 16, 1947)

For many purposes the Wien radiation law is a sufficiently close approximation to the Planck equation. When it is not, the subtraction in the denominator of the Planck equation interferes with logarithmic calculation. It has been found possible to construct a table which can be entered with the negative of the exponent of the Wien equation, expressed in terms of common (Briggsian) logarithms: $c_2 \lg e/(\lambda T)$, to get the logarithmic correction to four significant figures. Moreover, the same table can be used if successive approximations are necessary.

THE Wien radiation law, in the visible spectrum and for temperatures attainable in the laboratory, is a close approximation to the Planck radiation law; but for precise work the correction needs to be made.

In the course of preparing tables[1] of the radiometric and colorimetric properties of the blackbody between 2800°K and 3800°K, a table of the logarithmic corrections as a function of $c_2 \lg e/(\lambda T)$ was prepared, giving the correction to four significant figures. Since this table does not depend upon the particular values of c_2, λ, or T, it may be of general use.

By expanding in series, and conversion to common logarithms,[2] the Planck equation takes the form:

$$\lg W_\lambda = \lg c_1 - 5\lg\lambda - \frac{c_2 \lg e}{\lambda T} + \lg e(10^{-c_2 \lg e/\lambda T} + \tfrac{1}{2}10^{-2c_2 \lg e/\lambda T} + \tfrac{1}{3}10^{-3c_2 \lg e/\lambda T} + \cdots), \quad (1)$$

where the first three terms on the right-hand side give the Wien approximation, and the logarithmic correction, $-\lg(1-10^{-c_2 \lg e/\lambda T})$, is given by the sum of the remaining terms.

For the second approximation, the logarithmic correction,

$$-\lg(1-10^{-c_2 \lg e/\lambda T}) \doteq \lg e \cdot 10^{-c_2 \lg e/\lambda T}. \quad (2)$$

Taking logarithms

$$\lg[-\lg(1-10^{-c_2 \lg e/\lambda T})] \doteq \lg \lg e - \frac{c_2 \lg e}{\lambda T}, \quad (3)$$

whence

$$\frac{c_2 \lg e}{\lambda T} \doteq \lg \lg e - \lg[-\lg(1-10^{-c_2 \lg e/\lambda T})], \quad (4)$$

since

$$n \equiv \lg 10^n \equiv -\lg 10^{-n}, \quad (5)$$

$$n + \frac{c_2 \lg e}{\lambda T} \doteq \lg \lg e - \lg[-10^n \lg(1-10^{-c_2 \lg e/\lambda T})], \quad (6)$$

that is to say, if $c_2 \lg e/(\lambda T)$ is given over a range of unity as a function of the logarithmic correction, $-\lg(1-10^{-c_2 \lg e/\lambda T})$, values of the logarithmic correction for higher values of $c_2 \lg e/(\lambda T)$ can be found by dividing the logarithm by 10 for each unit increase in $c_2 \lg e/(\lambda T)$.

Table I gives $c_2 \lg e/(\lambda T)$ as a function of $-\lg(1-10^{-c_2 \lg e/\lambda T})$ from 1 to 10. If, for example, $c_2 \lg e/(\lambda T)$ is 3 units greater than the tabulated value, the logarithmic correction will be 0.001 times the tabulated value.

From Eq. (1), further approximations may be made by entering the table with $2c_2 \lg e/(\lambda T)$, and dividing the resulting logarithmic correction by 2; entering the table with $3c_2 \lg e/(\lambda T)$, and dividing the resulting logarithmic correction by 3; etc.; until a correction is given which is negligible in the last decimal place to which $\lg W_\lambda$ is being computed.

The correction is given to 4 significant figures. For a correction less than 0.001, i.e., a 0.23 percent correction in W_λ, the table will suffice for computing W_λ to 7 significant figures. Where the correction runs to more than 4 significant figures it will probably be less work to perform the indi-

[1] E. Q. Adams and W. E. Forsythe, Denison Univ. Bulletin, J. Sci. Labs. **38**, 52 (1943).
[2] E. Q. Adams, Rev. Sci. Inst. **4**, 622 (1933).

TABLE I.

	0	1	2	3	4	5	6	7	8	9
1.0	$\bar{1}.6378$	$\bar{1}.6335-$	$\bar{1}.6292$	$\bar{1}.6249$	$\bar{1}.6208$	$\bar{1}.6166$	$\bar{1}.6125-$	$\bar{1}.6084$	$\bar{1}.6044$	$\bar{1}.6004-$
1.1	$\bar{1}.5964$	$\bar{1}.5925-$	$\bar{1}.5886$	$\bar{1}.5847$	$\bar{1}.5809$	$\bar{1}.5771$	$\bar{1}.5733$	$\bar{1}.5696$	$\bar{1}.5659$	$\bar{1}.5622$
1.2	$\bar{1}.5586$	$\bar{1}.5550-$	$\bar{1}.5514$	$\bar{1}.5479$	$\bar{1}.5444$	$\bar{1}.5409$	$\bar{1}.5374$	$\bar{1}.5340$	$\bar{1}.5306$	$\bar{1}.5272$
1.3	$\bar{1}.5238$	$\bar{1}.5205+$	$\bar{1}.5172$	$\bar{1}.5139$	$\bar{1}.5107$	$\bar{1}.5075-$	$\bar{1}.5042$	$\bar{1}.5011$	$\bar{1}.4979$	$\bar{1}.4948$
1.4	$\bar{1}.4917$	$\bar{1}.4886$	$\bar{1}.4855-$	$\bar{1}.4824$	$\bar{1}.4794$	$\bar{1}.4764$	$\bar{1}.4734$	$\bar{1}.4705-$	$\bar{1}.4675+$	$\bar{1}.4646$
1.5	$\bar{1}.4617$	$\bar{1}.4588$	$\bar{1}.4559$	$\bar{1}.4531$	$\bar{1}.4503$	$\bar{1}.4475-$	$\bar{1}.4447$	$\bar{1}.4419$	$\bar{1}.4391$	$\bar{1}.4364$
1.6	$\bar{1}.4337$	$\bar{1}.4310$	$\bar{1}.4283$	$\bar{1}.4256$	$\bar{1}.4229$	$\bar{1}.4203$	$\bar{1}.4177$	$\bar{1}.4151$	$\bar{1}.4125-$	$\bar{1}.4099$
1.7	$\bar{1}.4073$	$\bar{1}.4048$	$\bar{1}.4023$	$\bar{1}.3997$	$\bar{1}.3972$	$\bar{1}.3947$	$\bar{1}.3923$	$\bar{1}.3898$	$\bar{1}.3874$	$\bar{1}.3849$
1.8	$\bar{1}.3825+$	$\bar{1}.3801$	$\bar{1}.3777$	$\bar{1}.3753$	$\bar{1}.3730$	$\bar{1}.3706$	$\bar{1}.3683$	$\bar{1}.3659$	$\bar{1}.3636$	$\bar{1}.3613$
1.9	$\bar{1}.3590$	$\bar{1}.3568$	$\bar{1}.3545-$	$\bar{1}.3522$	$\bar{1}.3500-$	$\bar{1}.3477$	$\bar{1}.3455+$	$\bar{1}.3433$	$\bar{1}.3411$	$\bar{1}.3389$
2.0	$\bar{1}.3368$	$\bar{1}.3346$	$\bar{1}.3324$	$\bar{1}.3303$	$\bar{1}.3282$	$\bar{1}.3260$	$\bar{1}.3239$	$\bar{1}.3218$	$\bar{1}.3197$	$\bar{1}.3176$
2.1	$\bar{1}.3156$	$\bar{1}.3135+$	$\bar{1}.3114$	$\bar{1}.3094$	$\bar{1}.3074$	$\bar{1}.3053$	$\bar{1}.3033$	$\bar{1}.3013$	$\bar{1}.2993$	$\bar{1}.2973$
2.2	$\bar{1}.2954$	$\bar{1}.2934$	$\bar{1}.2914$	$\bar{1}.2895-$	$\bar{1}.2875+$	$\bar{1}.2856$	$\bar{1}.2837$	$\bar{1}.2818$	$\bar{1}.2798$	$\bar{1}.2779$
2.3	$\bar{1}.2761$	$\bar{1}.2742$	$\bar{1}.2723$	$\bar{1}.2704$	$\bar{1}.2686$	$\bar{1}.2667$	$\bar{1}.2649$	$\bar{1}.2630$	$\bar{1}.2612$	$\bar{1}.2594$
2.4	$\bar{1}.2576$	$\bar{1}.2558$	$\bar{1}.2540$	$\bar{1}.2522$	$\bar{1}.2504$	$\bar{1}.2486$	$\bar{1}.2468$	$\bar{1}.2451$	$\bar{1}.2433$	$\bar{1}.2416$
2.5	$\bar{1}.2398$	$\bar{1}.2381$	$\bar{1}.2364$	$\bar{1}.2347$	$\bar{1}.2330$	$\bar{1}.2312$	$\bar{1}.2295+$	$\bar{1}.2279$	$\bar{1}.2262$	$\bar{1}.2245-$
2.6	$\bar{1}.2228$	$\bar{1}.2211$	$\bar{1}.2195-$	$\bar{1}.2178$	$\bar{1}.2162$	$\bar{1}.2145+$	$\bar{1}.2129$	$\bar{1}.2113$	$\bar{1}.2096$	$\bar{1}.2080$
2.7	$\bar{1}.2064$	$\bar{1}.2048$	$\bar{1}.2032$	$\bar{1}.2016$	$\bar{1}.2000$	$\bar{1}.1985-$	$\bar{1}.1969$	$\bar{1}.1953$	$\bar{1}.1937$	$\bar{1}.1922$
2.8	$\bar{1}.1906$	$\bar{1}.1891$	$\bar{1}.1875+$	$\bar{1}.1860$	$\bar{1}.1845-$	$\bar{1}.1829$	$\bar{1}.1814$	$\bar{1}.1799$	$\bar{1}.1784$	$\bar{1}.1769$
2.9	$\bar{1}.1754$	$\bar{1}.1739$	$\bar{1}.1724$	$\bar{1}.1709$	$\bar{1}.1694$	$\bar{1}.1680$	$\bar{1}.1665-$	$\bar{1}.1650+$	$\bar{1}.1636$	$\bar{1}.1621$
3.0	$\bar{1}.1607$	$\bar{1}.1592$	$\bar{1}.1578$	$\bar{1}.1563$	$\bar{1}.1549$	$\bar{1}.1535-$	$\bar{1}.1521$	$\bar{1}.1506$	$\bar{1}.1492$	$\bar{1}.1478$
3.1	$\bar{1}.1464$	$\bar{1}.1450+$	$\bar{1}.1436$	$\bar{1}.1422$	$\bar{1}.1409$	$\bar{1}.1395-$	$\bar{1}.1381$	$\bar{1}.1367$	$\bar{1}.1354$	$\bar{1}.1340$
3.2	$\bar{1}.1326$	$\bar{1}.1313$	$\bar{1}.1299$	$\bar{1}.1286$	$\bar{1}.1272$	$\bar{1}.1259$	$\bar{1}.1246$	$\bar{1}.1232$	$\bar{1}.1219$	$\bar{1}.1206$
3.3	$\bar{1}.1193$	$\bar{1}.1180$	$\bar{1}.1166$	$\bar{1}.1153$	$\bar{1}.1140$	$\bar{1}.1127$	$\bar{1}.1114$	$\bar{1}.1102$	$\bar{1}.1089$	$\bar{1}.1076$
3.4	$\bar{1}.1063$	$\bar{1}.1050+$	$\bar{1}.1038$	$\bar{1}.1025-$	$\bar{1}.1012$	$\bar{1}.1000$	$\bar{1}.0987$	$\bar{1}.0975-$	$\bar{1}.0962$	$\bar{1}.0950-$
3.5	$\bar{1}.0937$	$\bar{1}.0925-$	$\bar{1}.0912$	$\bar{1}.0900$	$\bar{1}.0888$	$\bar{1}.0876$	$\bar{1}.0863$	$\bar{1}.0851$	$\bar{1}.0839$	$\bar{1}.0827$
3.6	$\bar{1}.0815-$	$\bar{1}.0803$	$\bar{1}.0791$	$\bar{1}.0779$	$\bar{1}.0767$	$\bar{1}.0755-$	$\bar{1}.0743$	$\bar{1}.0731$	$\bar{1}.0719$	$\bar{1}.0708$
3.7	$\bar{1}.0696$	$\bar{1}.0684$	$\bar{1}.0672$	$\bar{1}.0661$	$\bar{1}.0649$	$\bar{1}.0638$	$\bar{1}.0626$	$\bar{1}.0614$	$\bar{1}.0603$	$\bar{1}.0591$
3.8	$\bar{1}.0580$	$\bar{1}.0569$	$\bar{1}.0557$	$\bar{1}.0546$	$\bar{1}.0535-$	$\bar{1}.0523$	$\bar{1}.0512$	$\bar{1}.0501$	$\bar{1}.0490$	$\bar{1}.0478$
3.9	$\bar{1}.0467$	$\bar{1}.0456$	$\bar{1}.0445-$	$\bar{1}.0434$	$\bar{1}.0423$	$\bar{1}.0412$	$\bar{1}.0401$	$\bar{1}.0390$	$\bar{1}.0379$	$\bar{1}.0368$
4.0	$\bar{1}.0357$	$\bar{1}.0346$	$\bar{1}.0336$	$\bar{1}.0325-$	$\bar{1}.0314$	$\bar{1}.0303$	$\bar{1}.0293$	$\bar{1}.0282$	$\bar{1}.0271$	$\bar{1}.0261$
4.1	$\bar{1}.0250+$	$\bar{1}.0239$	$\bar{1}.0229$	$\bar{1}.0218$	$\bar{1}.0208$	$\bar{1}.0197$	$\bar{1}.0187$	$\bar{1}.0176$	$\bar{1}.0166$	$\bar{1}.0156$
4.2	$\bar{1}.0145+$	$\bar{1}.0135+$	$\bar{1}.0125-$	$\bar{1}.0114$	$\bar{1}.0104$	$\bar{1}.0094$	$\bar{1}.0084$	$\bar{1}.0074$	$\bar{1}.0063$	$\bar{1}.0053$
4.3	$\bar{1}.0043$	$\bar{1}.0033$	$\bar{1}.0023$	$\bar{1}.0013$	$\bar{1}.0003$	$\bar{2}.9993$	$\bar{2}.9983$	$\bar{2}.9973$	$\bar{2}.9963$	$\bar{2}.9953$
4.4	$\bar{2}.9943$	$\bar{2}.9933$	$\bar{2}.9924$	$\bar{2}.9914$	$\bar{2}.9904$	$\bar{2}.9894$	$\bar{2}.9884$	$\bar{2}.9875-$	$\bar{2}.9865+$	$\bar{2}.9855+$
4.5	$\bar{2}.9846$	$\bar{2}.9836$	$\bar{2}.9826$	$\bar{2}.9817$	$\bar{2}.9807$	$\bar{2}.9798$	$\bar{2}.9788$	$\bar{2}.9778$	$\bar{2}.9769$	$\bar{2}.9760$
4.6	$\bar{2}.9750+$	$\bar{2}.9741$	$\bar{2}.9731$	$\bar{2}.9722$	$\bar{2}.9713$	$\bar{2}.9703$	$\bar{2}.9694$	$\bar{2}.9685-$	$\bar{2}.9675+$	$\bar{2}.9666$
4.7	$\bar{2}.9657$	$\bar{2}.9648$	$\bar{2}.9638$	$\bar{2}.9629$	$\bar{2}.9620$	$\bar{2}.9611$	$\bar{2}.9602$	$\bar{2}.9593$	$\bar{2}.9584$	$\bar{2}.9574$
4.8	$\bar{2}.9565+$	$\bar{2}.9556$	$\bar{2}.9547$	$\bar{2}.9538$	$\bar{2}.9529$	$\bar{2}.9520$	$\bar{2}.9511$	$\bar{2}.9503$	$\bar{2}.9494$	$\bar{2}.9485-$
4.9	$\bar{2}.9476$	$\bar{2}.9467$	$\bar{2}.9458$	$\bar{2}.9449$	$\bar{2}.9441$	$\bar{2}.9432$	$\bar{2}.9423$	$\bar{2}.9414$	$\bar{2}.9406$	$\bar{2}.9397$
5.0	$\bar{2}.9388$	$\bar{2}.9379$	$\bar{2}.9371$	$\bar{2}.9362$	$\bar{2}.9354$	$\bar{2}.9345-$	$\bar{2}.9336$	$\bar{2}.9328$	$\bar{2}.9319$	$\bar{2}.9311$
5.1	$\bar{2}.9302$	$\bar{2}.9294$	$\bar{2}.9285+$	$\bar{2}.9277$	$\bar{2}.9268$	$\bar{2}.9260$	$\bar{2}.9251$	$\bar{2}.9243$	$\bar{2}.9235-$	$\bar{2}.9226$
5.2	$\bar{2}.9218$	$\bar{2}.9209$	$\bar{2}.9201$	$\bar{2}.9193$	$\bar{2}.9185-$	$\bar{2}.9176$	$\bar{2}.9168$	$\bar{2}.9160$	$\bar{2}.9152$	$\bar{2}.9143$
5.3	$\bar{2}.9135+$	$\bar{2}.9127$	$\bar{2}.9119$	$\bar{2}.9111$	$\bar{2}.9102$	$\bar{2}.9094$	$\bar{2}.9086$	$\bar{2}.9078$	$\bar{2}.9070$	$\bar{2}.9062$
5.4	$\bar{2}.9054$	$\bar{2}.9046$	$\bar{2}.9038$	$\bar{2}.9030$	$\bar{2}.9022$	$\bar{2}.9014$	$\bar{2}.9006$	$\bar{2}.8998$	$\bar{2}.8990$	$\bar{2}.8982$
5.5	$\bar{2}.8974$	$\bar{2}.8966$	$\bar{2}.8958$	$\bar{2}.8951$	$\bar{2}.8943$	$\bar{2}.8935-$	$\bar{2}.8927$	$\bar{2}.8919$	$\bar{2}.8912$	$\bar{2}.8904$
5.6	$\bar{2}.8896$	$\bar{2}.8888$	$\bar{2}.8880$	$\bar{2}.8873$	$\bar{2}.8865+$	$\bar{2}.8857$	$\bar{2}.8850-$	$\bar{2}.8842$	$\bar{2}.8834$	$\bar{2}.8827$
5.7	$\bar{2}.8819$	$\bar{2}.8811$	$\bar{2}.8804$	$\bar{2}.8796$	$\bar{2}.8789$	$\bar{2}.8781$	$\bar{2}.8774$	$\bar{2}.8766$	$\bar{2}.8759$	$\bar{2}.8751$
5.8	$\bar{2}.8744$	$\bar{2}.8736$	$\bar{2}.8729$	$\bar{2}.8721$	$\bar{2}.8714$	$\bar{2}.8706$	$\bar{2}.8699$	$\bar{2}.8691$	$\bar{2}.8684$	$\bar{2}.8677$
5.9	$\bar{2}.8669$	$\bar{2}.8662$	$\bar{2}.8655-$	$\bar{2}.8647$	$\bar{2}.8640$	$\bar{2}.8633$	$\bar{2}.8625+$	$\bar{2}.8618$	$\bar{2}.8611$	$\bar{2}.8604$

TABLE I.—*Continued.*

	0	1	2	3	4	5	6	7	8	9
6.0	$\bar{2}.8596$	$\bar{2}.8589$	$\bar{2}.8582$	$\bar{2}.8575-$	$\bar{2}.8567$	$\bar{2}.8560$	$\bar{2}.8553$	$\bar{2}.8546$	$\bar{2}.8539$	$\bar{2}.8532$
6.1	$\bar{2}.8525-$	$\bar{2}.8517$	$\bar{2}.8510$	$\bar{2}.8503$	$\bar{2}.8496$	$\bar{2}.8489$	$\bar{2}.8482$	$\bar{2}.8475-$	$\bar{2}.8468$	$\bar{2}.8461$
6.2	$\bar{2}.8454$	$\bar{2}.8447$	$\bar{2}.8440$	$\bar{2}.8433$	$\bar{2}.8426$	$\bar{2}.8419$	$\bar{2}.8412$	$\bar{2}.8405+$	$\bar{2}.8398$	$\bar{2}.8391$
6.3	$\bar{2}.8384$	$\bar{2}.8378$	$\bar{2}.8371$	$\bar{2}.8364$	$\bar{2}.8357$	$\bar{2}.8350+$	$\bar{2}.8343$	$\bar{2}.8336$	$\bar{2}.8330$	$\bar{2}.8323$
6.4	$\bar{2}.8316$	$\bar{2}.8309$	$\bar{2}.8302$	$\bar{2}.8296$	$\bar{2}.8289$	$\bar{2}.8282$	$\bar{2}.8276$	$\bar{2}.8269$	$\bar{2}.8262$	$\bar{2}.8255+$
6.5	$\bar{2}.8249$	$\bar{2}.8242$	$\bar{2}.8235+$	$\bar{2}.8229$	$\bar{2}.8222$	$\bar{2}.8215+$	$\bar{2}.8209$	$\bar{2}.8202$	$\bar{2}.8196$	$\bar{2}.8189$
6.6	$\bar{2}.8182$	$\bar{2}.8176$	$\bar{2}.8169$	$\bar{2}.8163$	$\bar{2}.8156$	$\bar{2}.8150-$	$\bar{2}.8143$	$\bar{2}.8137$	$\bar{2}.8130$	$\bar{2}.8124$
6.7	$\bar{2}.8117$	$\bar{2}.8111$	$\bar{2}.8104$	$\bar{2}.8098$	$\bar{2}.8091$	$\bar{2}.8085-$	$\bar{2}.8078$	$\bar{2}.8072$	$\bar{2}.8066$	$\bar{2}.8059$
6.8	$\bar{2}.8053$	$\bar{2}.8046$	$\bar{2}.8040$	$\bar{2}.8034$	$\bar{2}.8027$	$\bar{2}.8021$	$\bar{2}.8015-$	$\bar{2}.8008$	$\bar{2}.8002$	$\bar{2}.7996$
6.9	$\bar{2}.7989$	$\bar{2}.7983$	$\bar{2}.7977$	$\bar{2}.7971$	$\bar{2}.7964$	$\bar{2}.7958$	$\bar{2}.7952$	$\bar{2}.7946$	$\bar{2}.7939$	$\bar{2}.7933$
7.0	$\bar{2}.7927$	$\bar{2}.7921$	$\bar{2}.7914$	$\bar{2}.7908$	$\bar{2}.7902$	$\bar{2}.7896$	$\bar{2}.7890$	$\bar{2}.7884$	$\bar{2}.7878$	$\bar{2}.7871$
7.1	$\bar{2}.7865+$	$\bar{2}.7859$	$\bar{2}.7853$	$\bar{2}.7847$	$\bar{2}.7841$	$\bar{2}.7835-$	$\bar{2}.7829$	$\bar{2}.7823$	$\bar{2}.7817$	$\bar{2}.7811$
7.2	$\bar{2}.7805-$	$\bar{2}.7798$	$\bar{2}.7792$	$\bar{2}.7786$	$\bar{2}.7780$	$\bar{2}.7774$	$\bar{2}.7768$	$\bar{2}.7762$	$\bar{2}.7757$	$\bar{2}.7751$
7.3	$\bar{2}.7745-$	$\bar{2}.7739$	$\bar{2}.7733$	$\bar{2}.7727$	$\bar{2}.7721$	$\bar{2}.7715-$	$\bar{2}.7709$	$\bar{2}.7703$	$\bar{2}.7697$	$\bar{2}.7691$
7.4	$\bar{2}.7686$	$\bar{2}.7680$	$\bar{2}.7674$	$\bar{2}.7668$	$\bar{2}.7662$	$\bar{2}.7656$	$\bar{2}.7650+$	$\bar{2}.7645-$	$\bar{2}.7639$	$\bar{2}.7633$
7.5	$\bar{2}.7627$	$\bar{2}.7621$	$\bar{2}.7616$	$\bar{2}.7610$	$\bar{2}.7604$	$\bar{2}.7598$	$\bar{2}.7593$	$\bar{2}.7587$	$\bar{2}.7581$	$\bar{2}.7575+$
7.6	$\bar{2}.7570$	$\bar{2}.7564$	$\bar{2}.7558$	$\bar{2}.7553$	$\bar{2}.7547$	$\bar{2}.7541$	$\bar{2}.7536$	$\bar{2}.7530$	$\bar{2}.7524$	$\bar{2}.7519$
7.7	$\bar{2}.7513$	$\bar{2}.7507$	$\bar{2}.7502$	$\bar{2}.7496$	$\bar{2}.7490$	$\bar{2}.7485-$	$\bar{2}.7479$	$\bar{2}.7474$	$\bar{2}.7468$	$\bar{2}.7462$
7.8	$\bar{2}.7457$	$\bar{2}.7451$	$\bar{2}.7446$	$\bar{2}.7440$	$\bar{2}.7435-$	$\bar{2}.7429$	$\bar{2}.7424$	$\bar{2}.7418$	$\bar{2}.7413$	$\bar{2}.7407$
7.9	$\bar{2}.7402$	$\bar{2}.7396$	$\bar{2}.7391$	$\bar{2}.7385+$	$\bar{2}.7380$	$\bar{2}.7374$	$\bar{2}.7369$	$\bar{2}.7363$	$\bar{2}.7358$	$\bar{2}.7352$
8.0	$\bar{2}.7347$	$\bar{2}.7342$	$\bar{2}.7336$	$\bar{2}.7331$	$\bar{2}.7325+$	$\bar{2}.7320$	$\bar{2}.7314$	$\bar{2}.7309$	$\bar{2}.7304$	$\bar{2}.7298$
8.1	$\bar{2}.7293$	$\bar{2}.7288$	$\bar{2}.7282$	$\bar{2}.7277$	$\bar{2}.7272$	$\bar{2}.7266$	$\bar{2}.7261$	$\bar{2}.7256$	$\bar{2}.7250+$	$\bar{2}.7245+$
8.2	$\bar{2}.7240$	$\bar{2}.7234$	$\bar{2}.7229$	$\bar{2}.7224$	$\bar{2}.7219$	$\bar{2}.7213$	$\bar{2}.7208$	$\bar{2}.7203$	$\bar{2}.7198$	$\bar{2}.7192$
8.3	$\bar{2}.7187$	$\bar{2}.7182$	$\bar{2}.7177$	$\bar{2}.7171$	$\bar{2}.7166$	$\bar{2}.7161$	$\bar{2}.7156$	$\bar{2}.7151$	$\bar{2}.7145+$	$\bar{2}.7140$
8.4	$\bar{2}.7135+$	$\bar{2}.7130$	$\bar{2}.7125-$	$\bar{2}.7120$	$\bar{2}.7114$	$\bar{2}.7109$	$\bar{2}.7104$	$\bar{2}.7099$	$\bar{2}.7094$	$\bar{2}.7089$
8.5	$\bar{2}.7084$	$\bar{2}.7079$	$\bar{2}.7073$	$\bar{2}.7068$	$\bar{2}.7063$	$\bar{2}.7058$	$\bar{2}.7053$	$\bar{2}.7048$	$\bar{2}.7043$	$\bar{2}.7038$
8.6	$\bar{2}.7033$	$\bar{2}.7028$	$\bar{2}.7023$	$\bar{2}.7018$	$\bar{2}.7013$	$\bar{2}.7008$	$\bar{2}.7003$	$\bar{2}.6998$	$\bar{2}.6993$	$\bar{2}.6988$
8.7	$\bar{2}.6983$	$\bar{2}.6978$	$\bar{2}.6973$	$\bar{2}.6968$	$\bar{2}.6963$	$\bar{2}.6958$	$\bar{2}.6953$	$\bar{2}.6948$	$\bar{2}.6943$	$\bar{2}.6938$
8.8	$\bar{2}.6933$	$\bar{2}.6928$	$\bar{2}.6923$	$\bar{2}.6918$	$\bar{2}.6913$	$\bar{2}.6908$	$\bar{2}.6904$	$\bar{2}.6899$	$\bar{2}.6894$	$\bar{2}.6889$
8.9	$\bar{2}.6884$	$\bar{2}.6879$	$\bar{2}.6874$	$\bar{2}.6869$	$\bar{2}.6864$	$\bar{2}.6860$	$\bar{2}.6855-$	$\bar{2}.6850-$	$\bar{2}.6845+$	$\bar{2}.6840$
9.0	$\bar{2}.6935+$	$\bar{2}.6831$	$\bar{2}.6826$	$\bar{2}.6821$	$\bar{2}.6816$	$\bar{2}.6811$	$\bar{2}.6807$	$\bar{2}.6802$	$\bar{2}.6797$	$\bar{2}.6792$
9.1	$\bar{2}.6787$	$\bar{2}.6783$	$\bar{2}.6778$	$\bar{2}.6773$	$\bar{2}.6768$	$\bar{2}.6764$	$\bar{2}.6759$	$\bar{2}.6754$	$\bar{2}.6749$	$\bar{2}.6745-$
9.2	$\bar{2}.6740$	$\bar{2}.6735+$	$\bar{2}.6731$	$\bar{2}.6726$	$\bar{2}.6721$	$\bar{2}.6716$	$\bar{2}.6712$	$\bar{2}.6707$	$\bar{2}.6702$	$\bar{2}.6698$
9.3	$\bar{2}.6693$	$\bar{2}.6688$	$\bar{2}.6684$	$\bar{2}.6679$	$\bar{2}.6674$	$\bar{2}.6670$	$\bar{2}.6665+$	$\bar{2}.6660$	$\bar{2}.6656$	$\bar{2}.6651$
9.4	$\bar{2}.6647$	$\bar{2}.6642$	$\bar{2}.6637$	$\bar{2}.6633$	$\bar{2}.6628$	$\bar{2}.6624$	$\bar{2}.6619$	$\bar{2}.6614$	$\bar{2}.6610$	$\bar{2}.6605+$
9.5	$\bar{2}.6601$	$\bar{2}.6596$	$\bar{2}.6591$	$\bar{2}.6587$	$\bar{2}.6582$	$\bar{2}.6578$	$\bar{2}.6573$	$\bar{2}.6569$	$\bar{2}.6564$	$\bar{2}.6560$
9.6	$\bar{2}.6555+$	$\bar{2}.6551$	$\bar{2}.6546$	$\bar{2}.6542$	$\bar{2}.6537$	$\bar{2}.6533$	$\bar{2}.6528$	$\bar{2}.6524$	$\bar{2}.6519$	$\bar{2}.6515-$
9.7	$\bar{2}.6510$	$\bar{2}.6506$	$\bar{2}.6501$	$\bar{2}.6497$	$\bar{2}.6492$	$\bar{2}.6488$	$\bar{2}.6483$	$\bar{2}.6479$	$\bar{2}.6474$	$\bar{2}.6470$
9.8	$\bar{2}.6466$	$\bar{2}.6461$	$\bar{2}.6457$	$\bar{2}.6452$	$\bar{2}.6448$	$\bar{2}.6443$	$\bar{2}.6439$	$\bar{2}.6435-$	$\bar{2}.6430$	$\bar{2}.6426$
9.9	$\bar{2}.6421$	$\bar{2}.6417$	$\bar{2}.6413$	$\bar{2}.6408$	$\bar{2}.6404$	$\bar{2}.6400$	$\bar{2}.6395+$	$\bar{2}.6391$	$\bar{2}.6387$	$\bar{2}.6382$

cated subtraction in the denominator of the Planck equation.

For other properties of the blackbody than the spectral radiant flux density (spectral radiancy) W_λ, the appropriate value of c_1 should be substituted.

Chromaticities of Lovibond Glasses

GERALDINE WALKER HAUPT AND FLORENCE LESCH DOUGLAS
National Bureau of Standards, Washington, D. C.

This paper reports by means of a series of graphs the chromaticity coordinates of certain Lovibond unit glasses and of pairs of such glasses in combination with an illuminant of color temperature 2842°K (Illuminant *A*). The chromaticities were computed according to the 1931 I.C.I. standard observer and coordinate system. The points graphically representing the x and y values have been labelled according to the Lovibond numbers and have been connected by lines to form a network. A similar graph is included for a few Lovibond glasses in combination with Illuminant *C*. The Lovibond glasses are those from the NBS set designated as "BS9940," and the spectrophotometric data on which the colorimetric computations are based are those published by Gibson and Harris.

CONTENTS

I. Purpose 698
II. Lovibond Glasses 698
1. General Description 698
2. National Bureau of Standards Set 700
3. Permanence 700
4. Effect of Temperature on Color 701
III. Discussion of the Graphs 701
IV. Summary 706

I. PURPOSE

THESE graphs were prepared to supply additional colorimetric data about the set of Lovibond glasses, BS9940, in possession of this Bureau and, insofar as these data are representative of all sets of Lovibond glasses, to describe further the Lovibond color system.

Single Lovibond glasses or combinations of glasses may be used to match the chromaticities of a large number of luminous and transparent substances. While it is important that glasses be available to make such chromaticity matches, it is equally important that the chromaticities so obtained be described in fundamental terms. Graphs of this type make this fundamental description possible for they afford a rapid method for converting "Lovibond number" to trichromatic coordinates, and *vice versa*.

II. LOVIBOND GLASSES

1. General Description

Sets of Lovibond glasses were first made available as color standards sometime after 1896, when the company, The Tintometer, Ltd., was organized. A complete set of Lovibond glasses consists of a set each of red, yellow, and blue glass slides which absorb selectively chiefly in the green, violet, and orange regions, respectively, of the visible spectrum. Each set of colored glasses is graded by a series of numbers which are intended to be proportional to the amount of the colorant flashed onto the slides. Thus a combination of any two glasses of the same nominal hue is approximately equivalent to a single glass whose series number is equal to the sum of the series numbers of the two component glasses; for example, two Lovibond glasses numbered 5 red and 3 red are intended to be equivalent in chromaticity to a glass numbered 8 red. In addition to the nominal additivity of the glasses of each of the three hues, the amounts of colorants used in the respective series are such that the combination of a red, a yellow, and a blue glass of the same number gives a chromaticity (with daylight illuminant) that is approximately achromatic.

The glasses normally available in the three sets of colors have nominal values ranging as follows: 0.01, 0.02···0.20, 0.22···0.90, 0.95···2.0, 2.1···5.0, 5.2···11.0, 11.5···20.0. Each glass slide is approximately 5 cm long and 1.7 cm wide; the thicknesses of the glasses vary from 1 to 3 mm. A more detailed description of the Lovibond system may be found in NBS Scientific Paper 547[1] which contains the spectrophotometric analysis of the Lovibond unit glasses, i.e., 1.0, 2.0···20.0, contained in the set designated as "BS9940"; these spectrophotometric data are the basis for the computations reported in the present paper.

[1] K. S. Gibson and F. K. Harris, Sci. Pap. Bur. Stand. 22, 1 (1927), S 547.

Earlier colorimetric studies[2] have shown that red glasses from different sets are frequently quite different even though they are numbered alike. Further studies on the inconsistencies between red glasses from different Lovibond sets[3] resulted in the development of a method for regrading the red glasses so that their new numbers are consistently additive when used in combination with Lovibond 35 yellow.[4] This method was based on colorimetric data derived from the spectrophotometric measurements on the red unit glasses in set BS9940. Furthermore, these spectrophotometric data provided a means of determining the extent to which the series numbers ascribed to the glasses in any one set fail to be proportional to the logarithms of the spectral transmittances. These inconsistencies within and between sets explain why the Optical Society of America Committee on Colorimetry considered it more appropriate to discuss the Lovibond system as a subtractive colorimeter, that is, the tintometer, rather than as a system of color standards.[5]

Although the inconsistencies in the grading of the Lovibond glasses are often considerably greater than the least perceptible difference associated with a particular color, the glasses, nevertheless, furnish a practical set of color standards which has become increasingly useful in a wide variety of industrial applications. They may be used to match the chromaticities of a large number of transparent and luminous substances, the comparisons being made between the light transmitted by the Lovibond glasses and the light transmitted or emitted by the substance of unknown chromaticity. While the range of chromaticities obtainable with Lovibond glasses does not extend to those of highest purity, it nevertheless covers a larger area on the I.C.I. chromaticity diagram than is covered by any other set of material color standards for which comparable data are available. The use of these glasses not only enables many chromaticity matches to be made, but also enables such matches to be made conveniently in rather small hue steps.

In recent years the demand for calibrations of red glasses has decreased sharply largely because of the fact that the need for such standards in the vegetable oil industry has already largely been met. On the other hand, while fewer in number, these recent requests for standardization of Lovibond red glasses represent a diverse group of industries. In the Bureau's work, typical uses of the Lovibond glasses are (1) colorimetric measurements required for obtaining duplicates of the red and yellow lantern glasses for certification as railroad signal standards, (2) determinations of the colors of neon lights and luminous flares, (3) check of the locations of the hue-name boundaries on the I.C.I. diagram according to the ISCC–NBS system,[6] and determination of chromaticity limits for the signal color designated as identification lunar-white, which were suggested and later adopted as Amendment-1 to the Army-Navy Specification Colors, AN-C-56.

By means of the graphs described below, we have thus extended our use of the Lovibond glasses to obtain approximate chromaticity coordinates (x, y) of any unknown color within the Lovibond range. The method is to compare the unknown color (of a transparent filter, or of a light source, such as a pyrotechnic, or a phosphorescent or fluorescent material) with various combinations of Lovibond glasses with Illuminant *A* until a satisfactory match is obtained or until by interpolation the Lovibond notation of the unknown is found. Then the chromaticity coordinates of the unknown are read from the graph. To the extent that the Lovibond numerals are reliable, these graphs can serve the same purpose for combinations of Lovibond glasses possessed by other investigators.

We have also used these graphs to facilitate our use of combinations of Lovibond glasses as chromaticity standards in our measurements of chromaticity coordinates (x, y) by means of the chromaticity-difference colorimeter.[7] In this application the graph aids in the choice of the chromaticity standard agreeing most closely with

[2] Irwin G. Priest, *Report of Proceedings of the Fourth Annual Meeting of the Society of Cotton Products Analysts*, pp. 6–14 (June 1913); The Cotton Oil Press (1921).

[3] Deane B. Judd and Geraldine K. Walker, Oil and Fat Industries **5**, 16 (1928); Geraldine K. Walker, Bur. Stand. J. Research **12**, 269 (1934).

[4] Kasson S. Gibson and Geraldine Walker Haupt, Bur. Stand. J. Research **13**, 433 (1934).

[5] "Colorimeters and Color Standards" (Chapter VIII of the report of the Committee on Colorimetry of the Optical Society of America), J. Opt. Soc. Am. **35**, 1 (1945).

[6] Kenneth L. Kelly, J. Opt. Soc. Am. **33**, 627 (1943).

[7] Deane B. Judd, Textile Research **9**, 253 (1939).

TABLE I. Comparisons of chromaticity coordinates and luminous transmittances obtained from 3 sets of measurements on 4 Lovibond red glasses in combination with Illuminant *A*.

Glass number	Date of measurements	Chromaticity coordinates x	y	Luminous transmittance
12 red	1923	0.566_1	0.345_6	0.363
	1930	$.565_1$	$.345_9$	.363
	1938	$.565_6$	$.344_6$	.359
13 red	1923	$.571_2$	$.343_5$	.347
	1930	$.570_4$	$.344_2$	.348
	1938	$.570_6$	$.343_2$	.345
17 red	1923	$.596_8$	$.336_9$	.270
	1930	$.595_2$	$.337_3$	.270
	1938	$.595_4$	$.336_6$	.267
20 red	1923	$.605_0$	$.332_0$	.257
	1930	$.604_6$	$.332_2$	.256
	1938	$.605_6$	$.330_5$	.250

that of the unknown, and the graph also serves as a convenient source of the chromaticity coordinates of the standard chosen.

2. National Bureau of Standards Set

In 1913 the Society of Cotton Products Analysts, now American Oil Chemists' Society, agreed that the National Bureau of Standards set of Lovibond glasses, set BS9940, be adopted as the standard and that all their glasses be compared with glasses of this standard set to eliminate the inconsistencies found in the grading of edible oils. Spectral-transmittance measurements were accordingly made on the twenty red unit glasses in order to supply the fundamental data required for their standardization. While similar measurements were made at the same time on the twenty unit blue and yellow glasses, only the red glasses, needed by the oil industry, were standardized. These red glasses have been used at this Bureau in calibrating more than three thousand[8] of the Lovibond red glasses for use in the grading of vegetable and cottonseed oils alone.[9]

Further importance is attached to this set since the spectrophotometric data on these sixty glasses have been used as the basis for conversion charts published by The Tintometer, Ltd.[10] Their graphs are to be used for converting the tintometer instrumental readings to I.C.I. chromaticity coordinates for certain Lovibond glasses, singly and in paired combinations, with Illuminants *B* and *C*, respectively. According to Dr. R. K. Schofield,[11] the chromaticities shown on the graphs "were computed from three spectrophotometric curves which are now the ultimate standards to which the glasses approximate very closely," and these curves are defined[12] by the spectrophotometric data published by this Bureau.[13]

3. Permanence of Lovibond Glasses

The spectrophotometric data used in making the computations for the present paper were made in 1923. The spectral transmittances of thirteen glasses of set BS9940, including the unit red glasses, 12.0, 13.0, 17.0, and 20.0, were remeasured in 1930 and again in 1938. The maximum difference in the x or y values of these 4 unit glasses for the three sets of measurements is 0.001_7, as shown in Table I of the following section. These discrepancies are to be attributed to

[8] Geraldine Walker Haupt, Oil and Soap **15**, 282 (1938).

[9] The colors of vegetable oils vary in general from pale yellow to deep reddish orange. The Lovibond red glasses by themselves are purplish red and do not match the oil colors unless combined with Lovibond yellow glasses. Over a considerable range the vegetable oil colors are adequately matched by a combination of Lovibond 35 yellow and variable red, and all of the Lovibond red glasses recalibrated for the vegetable oil industry have been standardized on this basis. A comparison of vegetable oil colors and Lovibond yellow plus red colors is given in a paper by H. J. McNicholas, "Color and spectral transmittance of vegetable oils," J. Research Nat. Bur. Stand. **15**, 99 (1935), RP815, and Oil and Soap **12**, 167 (1935).

[10] R. K. Schofield, J. Sci. Inst. **16**, 74 (1939); "Colorimetry: Part 1, Lovibond System, Part 2, Lovibond-Schofield System." (Pamphlet published by the Tintometer, Ltd.)

[11] G. S. Fawcett, Proc. Phys. Soc. **86**, 8 (1944); see page 20 of "Discussion" following this paper.

[12] A letter from Mr. G. S. Fawcett, Managing Director, The Tintometer, Ltd., dated November 7, 1944, states that "the data published in B.S. Sci. Paper No. 547 formed the basis for computing the nomographs for standard Illuminants *B* and *C* which we have published. Irregularities in the curves were smoothed out, and the data on certain glasses which show marked irregularities, or were noted as being defective by the undersigned when he visited the Bureau in 1931, was entirely ignored in averaging for the true values. These defective glasses are 3.0, 4.0, 7.0, 20.0 red, and 17.0, 20.0 blue. Apart from these glasses, which undoubtedly are not up to present day standards, we feel any other slight irregularities in the curves can well be due to the smallness of the area tests—particularly as they are flashed glasses and very small striae or other defects would have a relatively big effect on such a small area, and that your tests were made about the geometrical centre of the glass and our tests only take into account the lower third of the glass."

[13] The set BS9940 consists of 470 glasses. This paper contains data for only sixty of them. These are the ones numbered 1.0, 2.0···20.0 in the three colors. Extensive measurements have been made on several of the tenths and hundredths glasses of this set, but these data have not been published.

improved methods of measuring spectral transmittances rather than to any change in chromaticity with time. This is considered further below.

4. Effect of Temperature on the Colors of Lovibond Glasses

The effect of a temperature increase of 25°C on the chromaticities of Lovibond glasses $35\,Y$, $7.2R$, and $35\,Y$ plus $7.2R$ has been reported[14] as being approximately the same as adding 0.2 Lovibond red units. No comparable study has been made for the blue glasses, but unpublished spectral-transmission data[15] for a cobalt blue glass, approximately equivalent in chromaticity to a Lovibond blue glass of 18 value, show that the x and y coordinates change by amounts equal to $+0.000_7$ and $+0.001_0$, respectively, when the temperature of the glass is raised from 25°C to 50°C. It is probable, therefore, that the temperature changes which Lovibond glasses undergo during normal conditions of usage cause only negligible changes in their chromaticities.

III. DISCUSSION OF THE GRAPHS

Figure 1 shows the chromaticity coordinates, according to the 1931 I.C.I. standard observer and coordinate system,[16] of the twenty unit

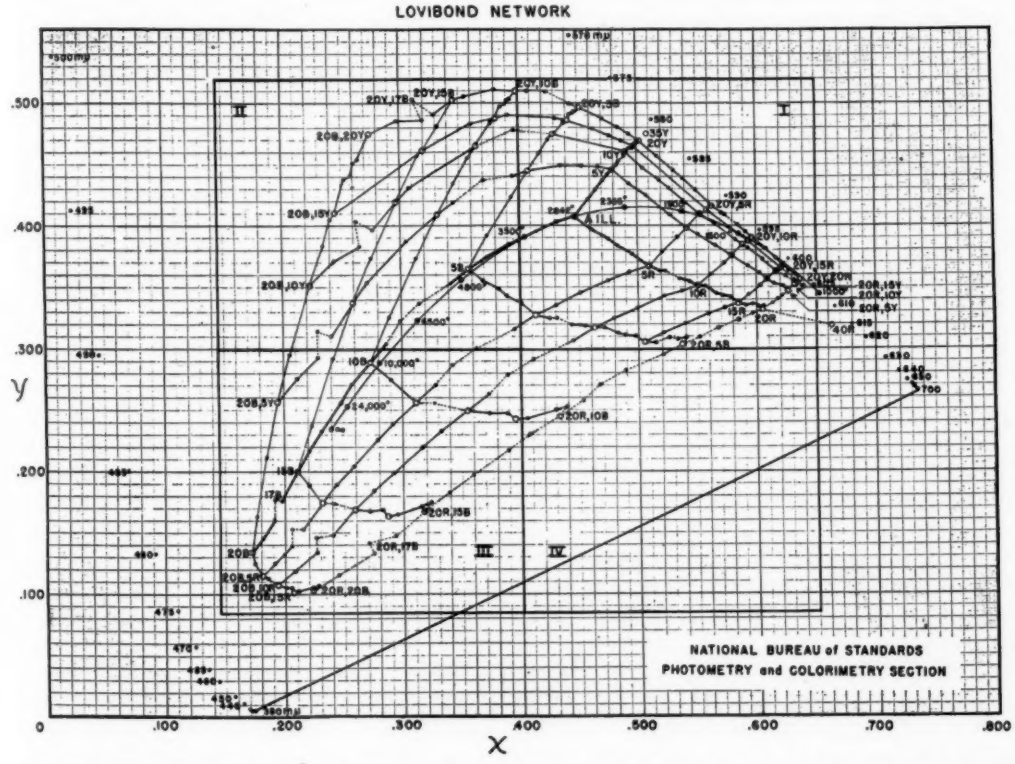

FIG. 1. Chromaticities (x, y), in terms of the 1931 International Commission on Illumination (I.C.I.) standard observer and coordinate system, of Lovibond red, yellow, and blue glasses, singly and in pairs (yellow, red; blue, yellow; red, blue) as indicated, when combined with I.C.I. illuminant A (2842°K, representative of incandescent light). The four sections of this diagram are reproduced to larger scale in Figs. 3, 4, 5, and 6, wherein the chromaticities of many additional pairs of glasses are also shown.

[14] Deane B. Judd, Bur. Stand. J. Research **1**, 859 (1928).
[15] Data obtained by Lois A. Peterson on a cobalt blue glass, 3.00 mm in thickness, designated as "Corning G55Aα^{19}." This glass is one of the spectrophotometric standards in possession of the National Bureau of Standards.
[16] Deane B. Judd, J. Opt. Soc. Am. **23**, 259 (1933).

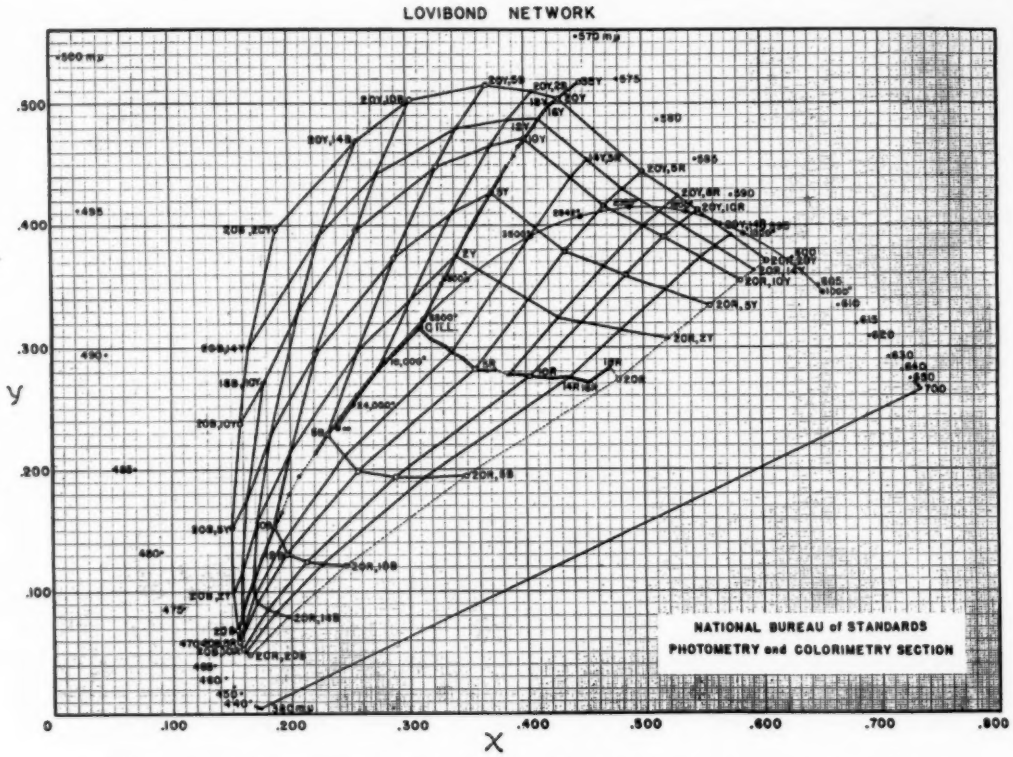

FIG. 2. Same as Fig. 1, except that the illuminant is I.C.I. Illuminant *C* (approximately 6500°K, representative of average daylight).

glasses in each of the red, yellow, and blue series, each glass in combination with I.C.I. standard illuminant *A* (color temperature 2842°K), and, for the same illuminant, the chromaticity coordinates of various combinations of the unit glasses, each combination consisting of two unit glasses of different colors. This figure orients the Lovibond network with respect to the spectrum and Planckian loci on the I.C.I. diagram and shows the four divisions of the network, which have been drawn to a larger scale in Figs. 3 to 6, inclusive. Data similar to those in Fig. 1 are shown in Fig. 2 except that I.C.I. standard Illuminant *C* (representative of average daylight) is used instead of Illuminant *A*, and fewer points are shown. This graph should be useful for comparisons with the similar graph of smoothed data which has been prepared by Dr. R. K. Schofield of The Tintometer, Ltd. Figures 3, 4, 5, and 6 are sections of Fig. 1 drawn to a larger scale as warranted by the accuracy of the data. These sections, moreover, show the chromaticities of many more combinations of the Lovibond glasses than are shown in the orientation chart of Fig. 1.

The chromaticity loci for the red, yellow, and blue series extend radially from the points representing Illuminants *A* or *C* and form boundaries between the areas wherein are plotted the chromaticities of the combinations. The combinations red-yellow, yellow-blue, and blue-red yield chromaticities comprising a network within the yellow-red, green, and purple areas, respectively, on the mixture diagrams.[16] The points representing the chromaticities of the glasses or combinations of glasses have been connected by straight lines since these data represent exactly only the unit Lovibond glasses from set BS9940. It will be seen that such chromaticity loci might be drawn fairly well as smoothed curves, thereby masking most of the irregularities found in the

actual glasses. Smoothed curves, based on data from particular glasses of a particular set, however, do not satisfy the additivity condition[4] exactly and, on this account, are less useful than are curves based on an "ideal" Lovibond system wherein the chromaticities of the glasses and their combinations are consistent with the Lovibond numbering.

In Fig. 1, it will be noted that along the chromaticity locus for the Lovibond reds, the glasses numbered 7, 17, and 20 seem certainly irregular; similarly, 7 and 8 blue are slightly inconsistent, 17 blue is strikingly irregular, and 8 yellow is probably the most irregular yellow glass.

These deviations from the regular trend of the chromaticities apply only to these particular glasses of the BS9940 set; they are not to be thought of as characteristic of like numbered Lovibond glasses in general. Consequently the straight lines leading from any of these deviate points are dashed. Other lines considered to be a fairly safe guide to the chromaticities characteristic of the Lovibond system as a whole are indicated by solid lines.[17]

Furthermore, lines based on 17 blue and 20 red

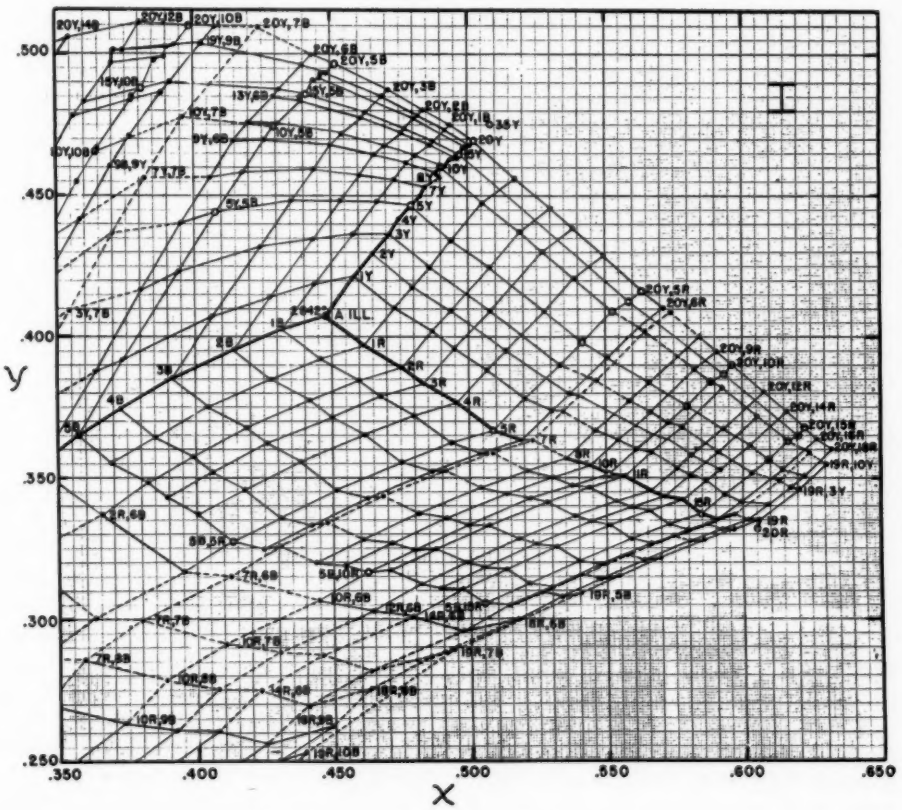

FIG. 3. Enlarged graph of section I of Fig. 1.

[17] The conversion charts published by The Tintometer, Ltd. contain curves in which the irregularities have been smoothed out, and the data for certain notably irregular glasses have not been used. Computations are in progress at this Bureau for determining the spectral transmittances of ideal Lovibond No. 1.00 glasses for each of the red, yellow, and blue series. These idealized spectral transmittances are derived by weighted averages from the measured spectral transmittances of the twenty unit glasses in each of the three colors and will provide the basis for computing "ideal" Lovibond networks typical of all the Lovibond glasses manufactured with set BS9940 as the standard.

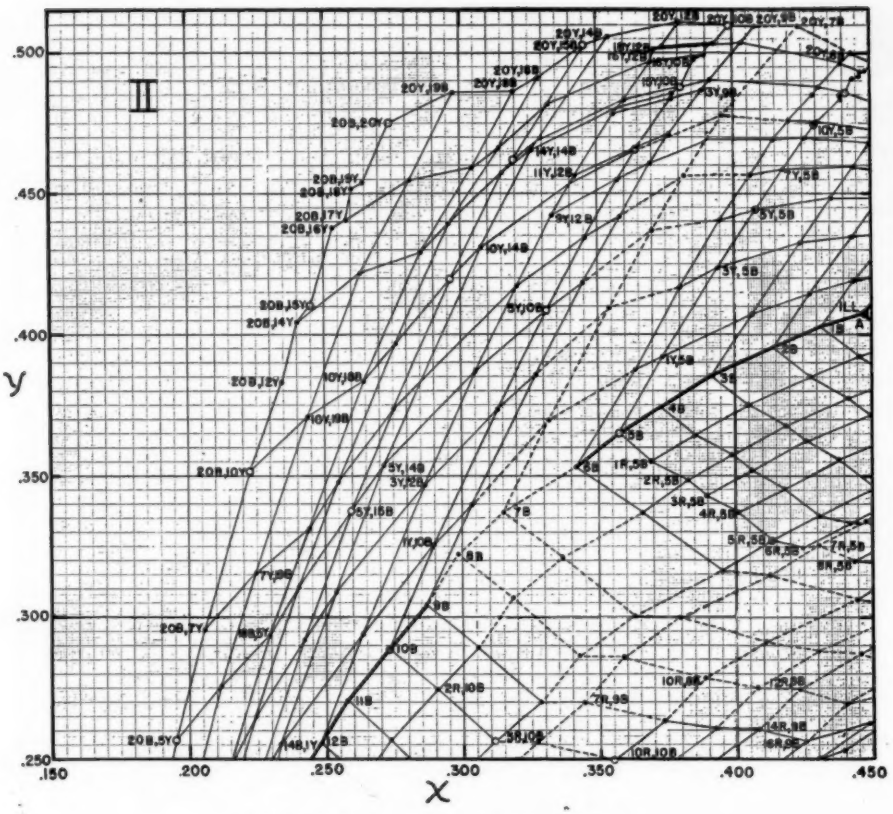

FIG. 4. Enlarged graph of section II of Fig. 1.

are omitted from the enlarged sectional drawings of Figs. 3, 4, 5, and 6 since they are obviously the least "ideal" of the glasses and their inclusion would, at best, complicate interpolations being made from the graphs, and, at worst, introduce errors which may not be typical of all similarly numbered glasses. Dashed lines are used in the large-scale drawings to join all points involving the four glasses, 7 and 17 red, and 7 and 8 blue, as a reminder that the straight lines, joining glasses consecutively numbered to these irregular ones, cannot be used in interpolating for intermediate points with the same degree of accuracy as elsewhere on the charts.

The irregularities in the graphs led to a reconsideration of the spectrophotometric measurements that had been made for certain red glasses and to additional measurements for certain blue glasses. The chromaticities of the red and blue glasses, to a greater extent than those of the yellow glasses, might be affected by impermanence of the glasses or by improved techniques of measurement.

The original spectrophotometric measurements were made in 1923 on the Koenig-Martens spectrophotometer without using rotating sectors in those wave-length regions where the transmittances were very low.[18] In 1930 and again in

[18] For very low transmittances the analyzing Nicol must be turned close to the extinction points for photometric match. In these positions stray unpolarized light in the field becomes relatively important, and the Nicol has to be turned significantly farther towards the extinction points than would be true if the unpolarized light were not present. This results in erroneously low values of transmittance being obtained. Accuracy is restored by the use of rapidly rotating sectors of known aperture in the blank beam, the angle of photometric match being thus returned to a part of the scale known to give reliable results.

1938, the transmittances of many of the glasses of set BS9940 were remeasured on the Koenig-Martens using the ten percent and one percent sector disks at the low transmittances. These remeasured glasses include four of the red unit glasses, 12.0, 13.0, 17.0, and 20.0; values for their chromaticity coordinates and luminous transmittances are summarized in Table I. With the improved technique in 1930, higher spectral-transmittance values were obtained in the region from 500 to 550 mμ, and these higher values tended to yield chromaticities of slightly lower purity. The 1938 measurements were further improved by the elimination of certain possible errors in wave-length calibrations. The maximum variation in x and y values in all the sets of measurements was only 0.001_7, however, and this is not considered of enough importance, for the purposes of the present paper, to substitute later measurements for the 1923 data.

TABLE II. Comparisons of values obtained for 2 Lovibond blue glasses, in combination with Illuminant A, from measurements made without and with rotating sectors.

Glass number	Sector used for trans. less than 10%	Chromaticity coordinates x	y	Luminous transmittance
18 blue	No	0.190_9	0.160_2	0.050
	Yes	$.193_9$	$.163_8$	.052
20 blue	No	$.172_2$	$.134_0$	.036
	Yes	$.175_4$	$.137_7$	.038

Spectral transmittances of the 18 and 20 blue glasses were remeasured in 1945 using the rotating sectors at all wave-lengths where the values reported in S547 and measured in 1923 were less than ten percent. These new measurements were substituted for the corresponding measurements made in 1923, and the computations for the x and y values were revised accordingly. The results of these computations are shown in Table II.

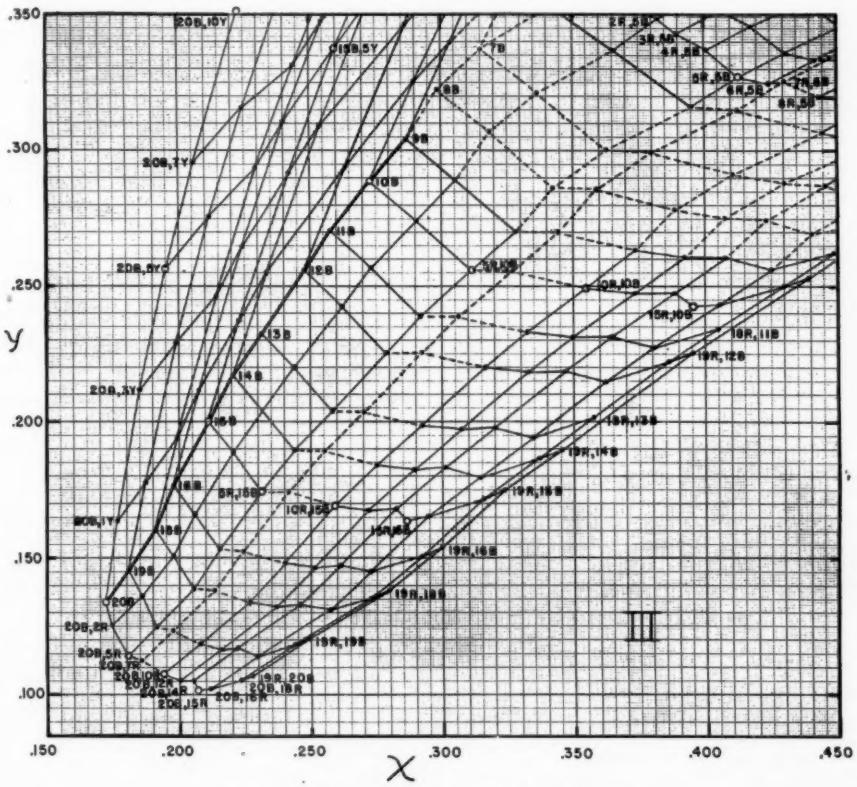

FIG. 5. Enlarged graph of section III of Fig. 1.

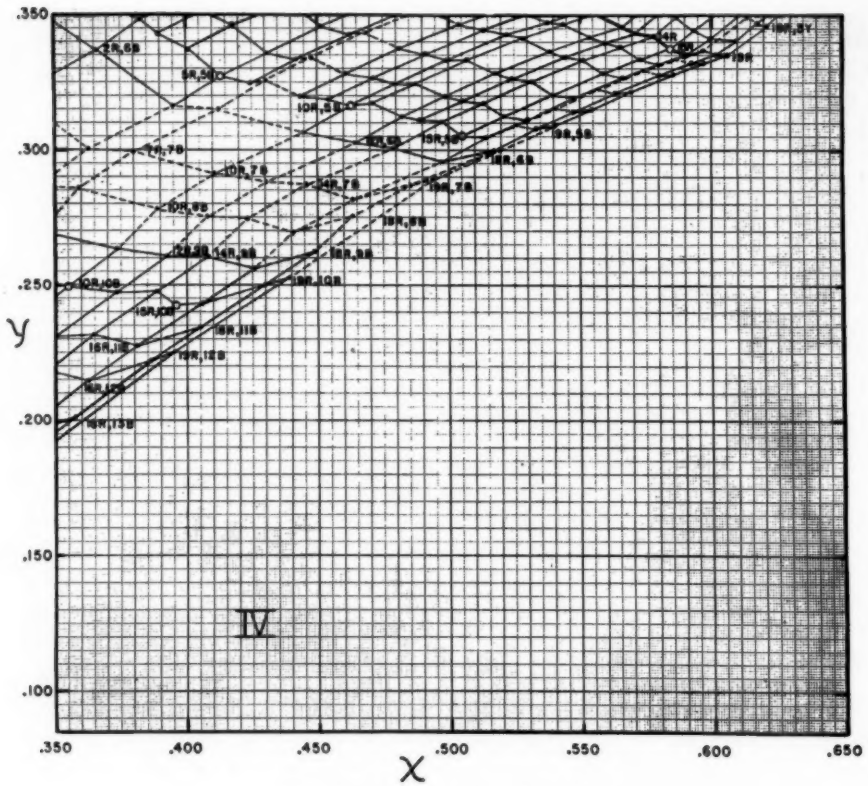

FIG. 6. Enlarged graph of section IV of Fig. 1.

IV. SUMMARY

This paper presents a series of graphs showing the chromaticities, computed according to the 1931 I.C.I. standard observer and coordinate system, of certain Lovibond unit glasses from set "BS9940" and of pairs of such glasses. There are five graphs (one general, four large-scale sections) for Illuminant *A* (representative of gas-filled incandescent lamps), and one general graph for Illuminant *C* (representative of average daylight).

JOURNAL OF THE OPTICAL SOCIETY OF AMERICA VOLUME 37, NUMBER 9 SEPTEMBER, 1947

Direct-Reading Spectrometer for Ferrous Analysis

R. O'B. CARPENTER, E. DUBOIS, AND J. STERNER
Baird Associates, Inc., Cambridge, Massachusetts

(Received June 2, 1947)

The direct-reading spectrometer, previously described by Saunderson, Caldecourt, and Peterson of the Dow Chemical Company, has been adapted for ferrous analysis. Data is given on reproducibility of analytical results obtained for Ni, Cr, Si, Mn, Cu, Mo, Al, and Sn in steel. The inherent accuracy of the instrument is discussed with respect to both the electronic and photometric systems employed. Errors introduced are shown to be small compared with spectrochemical uncertainties inherent in the source.

INTRODUCTION

A DIRECT-READING spectrometer of the type described by Saunderson, Caldecourt, and Peterson,[1] and which is used by the Dow Chemical Company for analysis of magnesium alloys, has been modified for application to ferrous analysis. The instrument is analogous to a spectrograph in which the photographic plate is replaced by photo-tubes and a direct-reading electronic measuring system. It provides an accurate quantitative spectrochemical analysis in less than one minute. The very simple and highly accurate electronic system of the earlier instrument has been followed very closely. It is, therefore, the purpose of this paper to treat in detail only the necessary modifications for ferrous analysis and to report data on the analytical precision obtained.

DESCRIPTION OF THE SPECTROMETER

A. Optical System

The complexity of the iron spectrum necessitates the use of a high dispersion instrument. The fifteen thousand lines-per-inch, three-meter focal length grating used is in a modified Paschen mounting, and is so arranged that a fixed spectral region of 2800 to 4400A in the second order is available with a dispersion of 2.8A per mm. On this portion of the Rowland circle, fixed exit slits are placed so as to select sensitive lines of the elements to be analyzed.

The greatest problem in such a system is one of physical alignment. For this reason precaution has been taken to make the system rigid, and devices are introduced to minimize the analytical error resulting from mechanical stress or vibration. The entrance slit, the exit slits, and the grating are rigidly fixed on a heavy steel assembly which is mounted independently of the rest of the instrument on a three-point kinematic and shockproof support. The apparatus is automatically temperature controlled to $90° \pm 2°$F. An eyepiece and cross-hair unit sighted on a visible portion of the spectrum permits a check on optical alignment at any time. Correction is provided for by a virtual shift of the entrance slit position, which is accomplished by the micrometer adjustment of a 45° mirror located between the entrance slit and the grating. The entrance slit is 100 microns in width. Exit slits of 200 microns are used in order to render ineffective those shifts which are too small to be noticed in the eyepiece. Where closely spaced lines must be used, exit slits of 50 microns are substituted. In the first case a shift of 50 microns, and in the second case a shift of 25 microns is permissible before there is any decrease in energy at the light receiver. Since a shift of about fifteen microns can be discerned in the eyepiece, the entire system can be adequately controlled. The instrument has

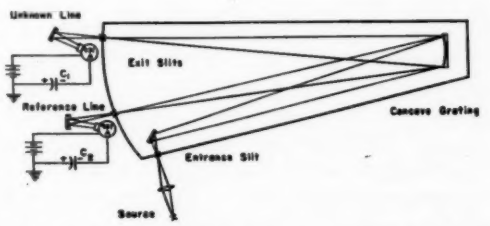

FIG. 1. Schematic of spectrometer electronic circuit during exposure. Only one unknown element is indicated here.

[1] Saunderson, Caldecourt, and Peterson, J. Opt. Soc. Am. **35**, 681 (1945).

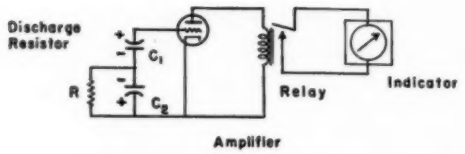

FIG. 2. Basic electronic circuit during measurement.

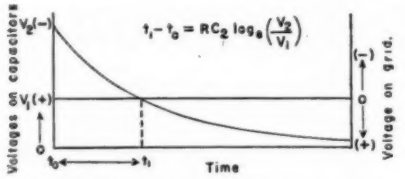

FIG. 3. Voltage *vs.* time relations during the measurement period.

performed satisfactorily under severe conditions of vibration and outside temperature variation.

After the selected spectrum line has passed through the exit slit, the radiation falls on a concave, cylindrical mirror which focuses it a short distance in front of the window of a photomultiplier tube. Because the cathode surface of this type of tube is not uniformly sensitive, it is preferable that the light be dispersed over the entire cathode surface. This is accomplished by ground glass diffusing windows placed 8 mm in front of the photo-tubes. The optical material of the windows is chosen to filter out radiation arising from overlapping orders. Also incorporated in the optical system is a background correction shutter which will be discussed later.

B. Electronic Measuring System

The measuring system can best be described by reference to Figs. 1, 2, and 3. Figure 1 is a simplified schematic diagram of the instrument showing the circuit employed during the exposure period. The exit slits illustrated select one unknown line and an internal standard line, in this case of iron. During the exposure period, the capacitors are charged to voltages proportional to the time integral of the light intensities. For the measurement period the circuits are switched to the arrangement of Fig. 2. The function of the amplifier and relays is to measure the ratio V_1/V_2 of the unknown and reference-capacitor voltages, and hence the ratio of the integrated light collected by the unknown and reference lines. The trigger point of the amplifier-relay system has been previously adjusted to occur when the algebraic sum of V_1 and V_2 is zero. During measurement C_1 and C_2 are arranged in opposition, and if $|V_1| < |V_2|$, the initial value of the input voltage is negative. This negative voltage triggers the relay, starting the corresponding time indicator. The voltage on C_2 then decays exponentially because of the discharge resistor R. At the time when $|V_2| = |V_1|$, the trigger point is reached, the relay opens, and the indicator stops. The time recorded (see Fig. 3) is then:

$$t = RC_2 \log(V_2/V_1) = RC_2 \log(I_2/I_1) + K.$$

These diagrams are simplified to show only one unknown line. In practice, as many as eight condensers charged from eight unknown lines are connected simultaneously in opposition to the same standard condenser and discharge resistor, one amplifier being required for each unknown.

The logarithmic result has several advantages. First, it gives the concentration ratio directly and is independent of the total light intensity. Second, it permits coverage of a wide range of concentrations and can be read with the same relative accuracy at any concentration. Furthermore, any change in sensitivity in the light collecting and measuring system of one element will change K only, and the calibration will be merely trans-

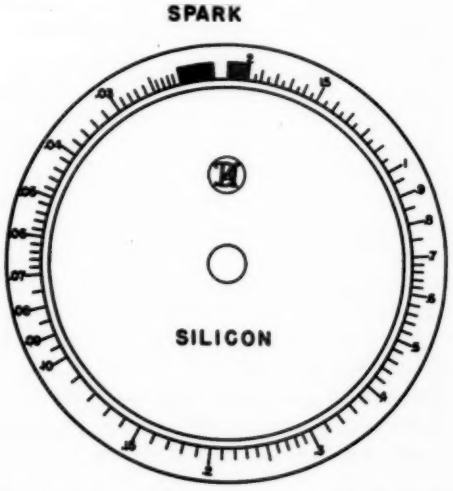

FIG. 4. Silicon calibration plotted on indicator dial.

lated in time, the shape of the curve remaining the same.

ANALYTICAL CALIBRATION

The time indicators have a single hand with a ten-second sweep. The calibration curves are plotted directly in percent concentration on the indicator dial. By rotating the dial, correction can be made for zero drift. Since the shape of the working curve is invariant, this standardization may be made by running a single standard sample. Figure 4 shows a typical indicator dial calibrated for the spark analysis of silicon.

The shape of the working curve depends on the time constant of the discharge resistor, the relation between concentration and light intensity, and the "background" light. Referring to a semi-logarithmic plot of time *versus* concentration, Fig. 5, it may be observed that there is a straight line portion of the spark curve between 0.1 and 1 percent molybdenum. In general, there will be a straight line portion of approximately the same slope in similar calibration curves of the other elements. At lower concentrations the curve falls off because of the effect of background light in the spectrum. At high concentrations this effect is negligible, but at low concentrations, where the sensitive line of the element is weak, a greater proportion of the light passed through a slit to the photo-multiplier is due to background. The resulting loss of working curve slope can be partially remedied by the introduction of an automatic background correction, or by the substitution of an arc source, which reduces the background-to-line spectrum intensity ratio. There is also a slight loss of working curve slope at high concentrations of some elements due both to self reversal and to the reduction of iron concentration as the concentration of alloying elements increases.

In dealing with low intensity spectral lines, especially with spark excitation, the background light becomes an important factor. If the background is strong, there is little difference between the total light passed to a photo-cell for a weak line and for no line at all. The result is a loss of "contrast" in the working curve. Reference can again be made to Fig. 5, which shows calibration curves for molybdenum: for arc, in which case the

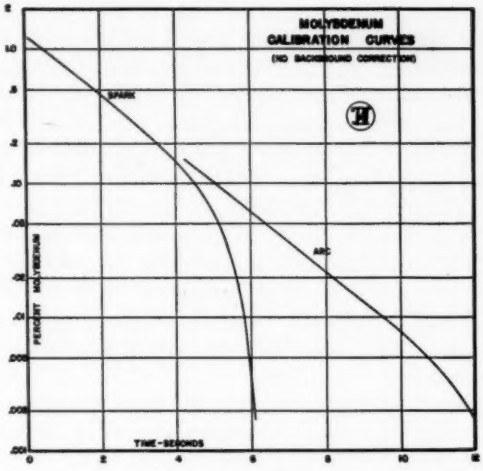

FIG. 5. Working curves for molybdenum in a ferrous alloy, using spark and arc excitation, showing difference in background light.

background is weak; and for spark, where it is strong and causes a dropping off of the spark calibration curve. The method of background correction described by Saunderson has been incorporated in this instrument. In brief, a photo-tube receives, alternately, light from the spectral line of the unknown element, and light from an adjacent blank portion of the spectrum, each for a period of one second. This cycling, accomplished by a shutter in front of the tubes, continues during the entire exposure period. In synchronism with the movement of the shutter, the condensers which have been charged by the photo-tubes are reversed in the circuit. Hence the condenser is charged for one second by a current proportional to the spectral line plus background, and then is discharged for one second by a current proportional to background alone. Thus the background is cancelled out, with the net effect of straightening the working curve.

It might be thought that a 100 percent background correction, accomplished in the manner described above, would be desirable. This, however, would result in very low voltages across the condensers for low concentrations, and would make it possible for an occasional net negative charge to result from intensity fluctuations. This would lead to an infinite discharge time and an indeterminate measurement. For this reason only

a partial background correction is used, this being accomplished by masking off part of the background slit. Figure 6 shows a nickel calibration curve without background correction, and above it one with a partial background correction. The maximum spread and the reproducibility of an analysis on the knee of the curve are given for both conditions. This example shows no improvement resulting from the background correction. This can be attributed to the fact that the light involved in the background correction is not collected simultaneously with that arising from the spectral lines. Variations in total light intensity throughout the exposure may, therefore, show up as errors in the measurement. However, the background correction does eliminate three errors: crowding the circular scale, with consequent increase of reading error; effect of background variations from sample to sample, especially where widely different alloys are measured from a single calibration scale; and any effect of phototube dark current, since its fluctuation is small compared to source fluctuation.

ACCURACY

The possible sources of inaccuracy are best discussed under two topics: instrumental accuracy, concerning errors which would have their origin in the electronic system; and spectrochemical accuracy, which is a function chiefly of the source. Throughout the discussion all results will be expressed in terms of "standard deviation," which is defined as the root mean square of the deviation from the average of a series of reproducibility measurements.

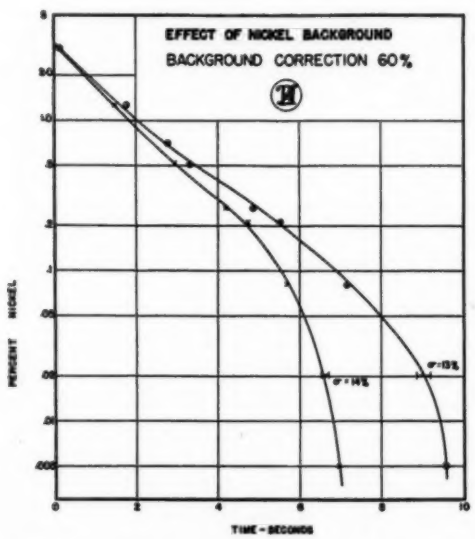

FIG. 6. Working curves for nickel with and without background correction; standard deviations are shown for the same sample under both conditions.

A. Instrumental Accuracy

Omitting for the moment effects involving the photo-multiplier light receivers, the accuracy of determining the ratio of two voltages impressed on a pair of condensers will be considered. The pertinent factors are: condenser absorption and leakage; amplifier-relay stability; relay-time indicator reaction time; and scale reading error.

By using condensers with a polystyrene dielectric (residual charge, 0.02 percent), possible error from absorption is rendered negligible. The leakage error is the ratio of the time consumed in exposure and measurement, 30 seconds, to the leakage time constant of one of the condensers. The leakage resistance is kept above 50,000 megohms, and the smallest condenser used is 0.1 microfarad, so the leakage error is less than 0.6 percent.

The stability error is expressed as $(\Delta V/V) \times 100$, where ΔV is the change in trigger point occasioned by a drift of amplifier or relay characteristics, and V is the voltage to be measured. The amplifier, as designed by Saunderson and his associates, has a high gain during measurement and a degenerative self-stabilizing feature during standby such that the drift during measurement is less than three millivolts. In practice, the lowest voltage measured is 0.5 volt, so the stability error is always less than 0.6 percent.

The reaction time, that is the interval between the time when the grid reaches the triggering voltage and the indicator stops, is of the order of 0.01 second. Any variation in this from run to run is insignificant.

The reading error is best evaluated by reference to Fig. 4. The circular scale of the indicator dial is 9.5 inches in circumference. The discharge time is arranged to give a range of approximately 2 logarithmic cycles of concentration. This makes the reading accuracy 1 percent, which is the

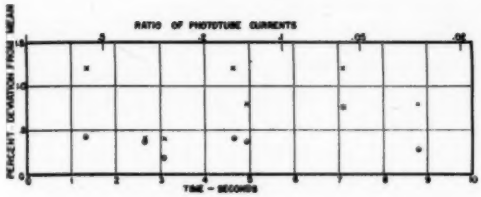

FIG. 7. Standard deviation in measuring the ratio of photo-currents produced by a mercury arc light source placed at the position of the grating. ⊙—standard deviation in 20 determinations; ×—maximum single deviation in 20 determinations.

largest source of instrumental error, but is less than the spectrochemical error, as is demonstrated below.

It has been experimentally verified, by charging the condensers from batteries, that the reproducibility in measuring the ratio of the two voltages is less than 0.5 percent over the range of 0 to 10 seconds. (This test was made with a more accurate time indicator to eliminate the reading error.)

So far the discussion of instrument reproducibility has not taken into consideration the effect of the light receivers, which can be studied by means of a constant light test. In this test, a controlled mercury lamp is placed at the position of the grating so that constant energy passes through the exit slits and falls on the photo-tubes. Otherwise the instrument is operated exactly as it is in making spectrochemical determinations. Twenty runs were made using this method, and indicator readings were recorded. From the known rate of discharge (time constant) of the standard condenser, the deviations in reading were converted into deviations in the energy falling on the photo-tubes. These results are plotted in Fig. 7. Circles represent standard deviations for twenty runs; crosses represent the maximum single deviation. Each pair of points represents measurements on a different exit slit and photo-tube, all of which are compared with the same reference slit and photo-tube. It can be seen that the standard deviation is less than 0.5 percent in every case, and that the greatest single deviation in a total of 140 determinations is 1.2 percent.

The results of this test, which are typical, are a measure of the over-all reproducibility of the instrument, and include all factors except those introduced by the analytical light source itself. It can be concluded that the main problem in obtaining good reproducibility is not a function of the direct reading spectrometer, but of the spectrochemical source itself.

B. Spectrochemical Accuracy

The spectrochemical accuracy of this instrument is dependent on the light source. The source used is a condensed spark obtained through the use of a 25,000 volt, 3 KVA transformer, 0.0025 mf of capacity, and 2 microhenries of inductance. The current is interrupted by an air blast[2] which blows across a 1.5-mm auxiliary gap. Although the instrument can be arranged to analyze flat samples on a Petrey stand, most of the work done

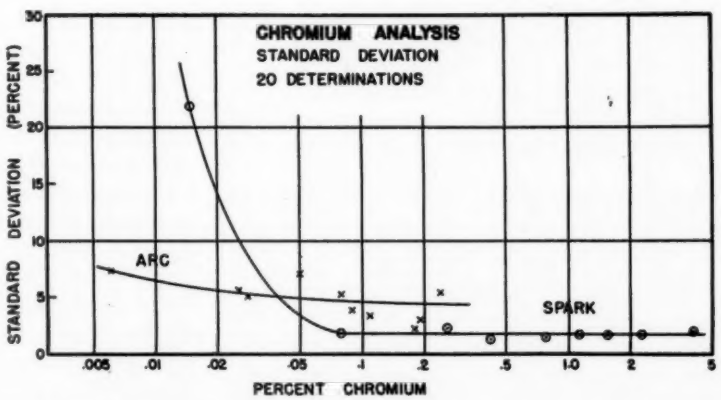

FIG. 8. Analytical error in percent of amount present plotted against the concentration of the sample; each point represents the standard deviation in 20 analyses of the same sample; reproducibility with arc and with spark excitation are shown.

[2] R. G. Fowler and R. A. Wolfe, J. Opt. Soc. Am. **35**, 170 (1945).

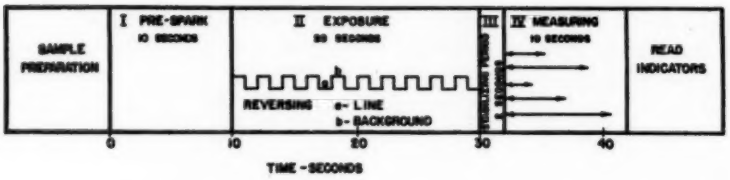

FIG. 9. Time cycle for the quantitative analysis of eight elements in one sample.

so far, and all of the results reported in this paper, concern pin samples. When using pin samples, which are usually $\frac{7}{32}$-inch cylindrical rods, the specimens are ground to a 135-degree conical point, and then clamped so that they are separated by a 2-mm gap.

The instrument is also provided with an arc source, which is useful in the analysis for low concentrations. This is an a.c. arc, energized by a 2200 volt transformer which is operated with a secondary current of between 2 and 3 amperes. The arc is stabilized by a current-limiting ballast resistor. A high frequency spark source is coupled into the arc source by an air transformer in order to provide a means for starting the arc. The spark exposure used is 20 seconds, with a 10 second preburn. The arc exposures are 10 seconds, with 5 second preburns.

Even though great care is taken in the design of a source and in the technique of making analyses, source instability cannot be completely eliminated. However, its seriousness can be minimized. Since each analytical result is dependent on the ratio of the intensities of an unknown line and a standard line, a small variation in total light intensity is not important. Furthermore, the fact that the light is integrated over an exposure period averages out the short-period variations in relative line intensity.

There can now be discussed a series of reproducibility runs, all of which were made during the same week. Several steel samples that covered a wide composition range were selected; their chemical analyses had been found to be reliable. Each of these was sparked twenty times, the sample being reground after each analytical run. Reproducibility runs were also made using the a.c. arc. Standard deviation, i.e., root mean square deviation from the average of twenty runs, was then plotted as percent of amount of each "unknown" element in the sample.

Figure 8 shows a typical plot for chromium. Note that the standard deviation for most samples is of the order of 2 percent. As the background becomes appreciable at low concentrations, there is a loss in accuracy. The advantage of using the arc for very low concentrations is well demonstrated by this plot.

Table I gives a summary of the results obtained for the eight elements studied. The third column shows the concentration range over which spark excitation provides analysis of satisfactory accuracy. The fourth column gives the order of magnitude in percentage units of the standard deviation obtained for this range. The fifth and sixth columns similarly describe the useful ranges of the arc source. The last column indicates the lower limit of concentration which can be measured with better than 25 percent standard deviation.

TABLE I. Summary of analytical results iron line 3719.9.

Element	Wave-length	Spark range	Std. dev.	Arc range	Std. dev.	Conc. at 25% std. dev.
Ni	3414	.05–5.0	2.0	.01 –.2	7	.004
Cr	4254	.05–5.0	1.5	.005–.2	5	.001
Si	2881	.07–5.0	2.5	.02 –.5	6	.007
Mn	2933	.05–5.0	3.0	.02 –.2	9	.01
Cu	3274	.01–1.0	2.0			
Mo	3864	.04–5.0	2.5	.002–.2	6	.001
Al	3944	.04–5.0	2.5	.005–.1	5	.002
Sn	3175			.01 –.5	7	.005

ANALYTICAL SPEED

Figure 9 illustrates the speed with which analytical data can be obtained with this instrument. Note that the time scale is in seconds, and that the entire cycle from the beginning of the prespark to the reading of the analytical data consumes approximately 45 seconds. The speed of sample preparation and of reading the indicators depends on the experience of the operator. In the course of obtaining data for this paper two operators made forty complete runs, each involving analysis of eight elements in the space of fifty minutes, a rate of less than 10 seconds per element determination. For a single operator the rate is about fifteen seconds per determination.

CONCLUSION

In conclusion, it may be stated that the direct-reading spectrometer described here introduces no inaccuracies in ferrous analysis which are comparable in magnitude to those inherent in the source itself. It has been demonstrated that the instrument performs with analytical accuracy comparable with ordinary spectrographic methods, and that it does so with considerable saving in labor and time. It should be noted that this has been achieved at the expense of flexibility; the instrument cannot be as easily shifted from one type and range of analysis to another as can conventional spectrographs. However, in industrial control, the field for which this instrument was developed, flexibility can usually be sacrificed for marked gain in speed and simplicity of operation.

JOURNAL OF THE OPTICAL SOCIETY OF AMERICA VOLUME 37, NUMBER 9 SEPTEMBER, 1947

Gratings as Broad Band Filters for the Infra-Red

JOHN U. WHITE
The Perkin-Elmer Corporation, Glenbrook, Connecticut
(Received June 18, 1947)

An effective means of removing the short wave-length light from a beam containing infra-red radiation of all wave-lengths, uses an echelette grating as a simple mirror. Light of wave-lengths short compared to the grating space, is diffracted out of the beam into the dispersed spectra. Light of wave-lengths long compared to the grating space, can only go into the undispersed zero-order spectrum, which falls in the direction of normal reflection if the grating were a mirror. By the use of echelette gratings with high intensities in the dispersed spectra, large reductions in the amount of short wave-length light in the central image can be effected. The wave-length at which most of the light changes from normal reflection into the beam to diffraction out of it, may be quite sharp, so that the effective filtering action may vary by a factor as large as four in a two-micron interval. When such a grating is substituted for a plane mirror in the illuminating system of an infra-red spectrometer, the scattered light in the monochromator is reduced by a factor of ten.

INTRODUCTION

THE general use of infra-red absorption spectra in chemical analysis requires instruments capable of separating narrow wave-length bands of infra-red light, and measuring their intensities accurately. One of the worst problems is the elimination of photometric errors caused by stray light of undesired wave-lengths. Even with the best optical parts obtainable, scattered light becomes noticeable in most infra-red monochromators at wave-lengths longer than about six microns. Beyond about ten microns, it may interfere seriously with intensity measurements and analytical results based on them.

A number of methods have been used to reduce the effects of scattered light. The most successful and the best is the double monochromator. This would be the ideal solution if its expense and complexity were not so great that they have prohibited its general use. Another method is the use of scattering filters to remove short wave-length light from a beam and transmit the light

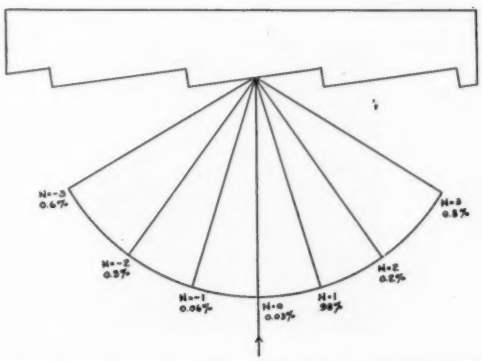

FIG. 1. Energy distribution from grating: normal incidence wave-length 4.78μ, grating space 16.933μ, groove angle 8° 12′.

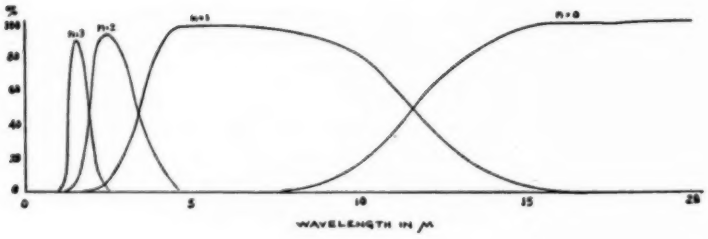

FIG. 2. Schematic variation with wave-length of light distribution among the most intense spectra of a grating: normal incidence groove angle 8° 12′, spacing 16.933μ.

of longer wave-lengths. Magnesium oxide powder deposited on salt plates has been used for this purpose. The fog that develops on salt plates in a damp atmosphere may also be used, with the advantage that its transmission is reduced by Reststrahlen bands only at very long wave-lengths. The effects of stray light may also be reduced without actually removing it from the light beam, by using a selective shutter that transmits the scattered light but not light of the desired wave-length. The scattered light is then present when both the zero point of no light intensity and the desired spectrum are being measured, and its effects are canceled out. Glass and LiF shutters are most commonly used for this purpose. Selective reflections from crystals are also effective in removing extraneous radiation in restricted wave-length intervals.

A more general method of filtering shorter wave-length radiation from that of longer wave-lengths is by scattering. Strong[1] has shown that the short wave-length radiation in a light beam may be reduced by roughing the surface of a mirror from which it is reflected. Better selectivity and sharper cut-offs may be obtained by the use of diffraction gratings as broad band filters. When white light falls on a grating, some of it is deflected out of its normal direction into the diffracted spectra. The distribution of the different colors has been calculated on the assumption that each ruling on the grating is a small prism set to emit light at a given angle.

Calculations by Stamm[2] from an equation by Rowland,[3] give the light distribution from echelette gratings. Figure 1 illustrates one of the results obtained by Stamm.[4] It shows an enlarged section of a grating illuminated from below at normal incidence. 98 percent of the light is, in this case, diffracted into the first-order spectrum on the right-hand side, with only 0.03 percent going into the specularly reflected direction at normal emergence. Calculations for other wave-lengths always give similar distributions, with most of the light going into whichever order spectrum lies closest to the blaze angle. As long

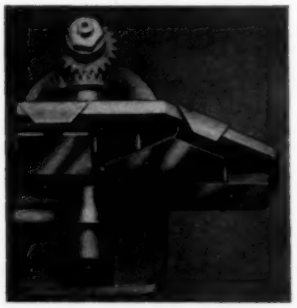

FIG. 3. Interchangeable mount for gratings and mirrors.

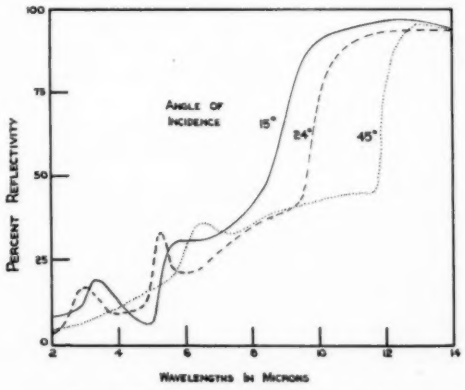

FIG. 4. Reflectivity of 3610-line grating.

[1] John Strong, Phys. Rev. **38**, 1818 (1931).

[2] R. F. Stamm and J. J. Whalen, J. Opt. Soc. Am. **36**, 2 (1946).

[3] H. A. Rowland, Phil. Mag. **35**, 397 (1893).

[4] The data in this figure are taken from Stamm's paper with his permission.

as a diffracted spectrum lies close to the blaze angle, little light is specularly reflected. When such data are plotted for a number of wave-lengths, the order of the most intense spectrum is seen to increase as the wave-length decreases. Figure 2 shows schematically how light of wave-lengths longer than a critical value appears in the zero order, undiffracted spectrum, and light of progressively shorter wave-lengths is concentrated in the spectra of progressively higher orders. Light with wave-lengths between the critical value and about half this value is divided between the zero- and first-order spectra. The first-, second-, and higher order spectra are spread out over wide angular ranges, giving the high dispersion commonly obtained from diffraction gratings. The zero-order spectrum contains all the light that is specularly reflected (or transmitted) by the grating surface. If such a grating is put into a light beam, either as a reflecting or transmitting element, it diffracts out of the beam the light of higher orders and effectively acts as a filter with a transmission curve similar to the intensity distribution shown in Fig. 2 for the zero-order spectrum.

This effect can be used as a filter in an infra-red spectrometer by removing one of the plane mirrors in the optical system and substituting for it a suitable reflecting grating. The long wave-length light is then specularly reflected by the grating into the same image that would be formed by a mirror, but the short wave-length radiation is diffracted off to one side and lost from the light beam. A photograph of a convenient arrangement for quickly changing from a mirror to a grating is shown in Fig. 3. This device consists of a mirror and two gratings of different spacings mounted on a shaft that can be readily rotated to place any one of the three in the same orientation in the light beam. The gratings shown, with 3610 and 7500 lines per inch, are suitable for use at wave-lengths longer than 12 and 6 microns, respectively.

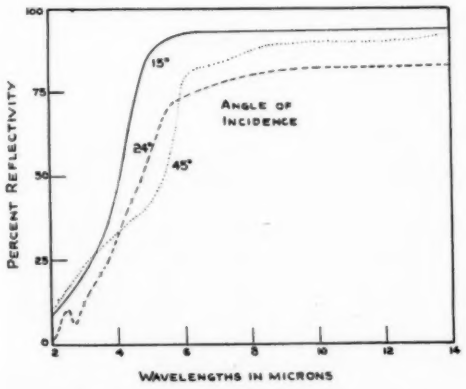

FIG. 5. Reflectivity of 7500-line grating.

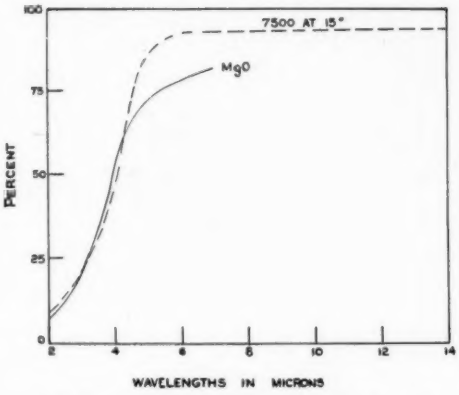

FIG. 6. Comparison of MgO filter and grating.

APPARATUS

The reflectivities of several gratings were measured with a Perkin-Elmer Model 12B infra-red spectrometer[5] equipped with a General Motors breaker-type amplifier[6] and a Brown strip chart recorder. A special illuminating system including several plane mirrors was set up in front of the

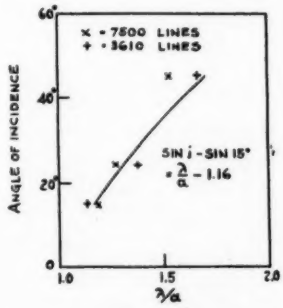

FIG. 7. Angular variation in cut-off wave-length plotted as angle for 50 percent reflection against ratio of wave-length to grating space.

[5] R. B. Barnes, R. S. McDonald, V. Z. Williams, and R. F. Kinnaird, J. App. Phys. **16**, 77 (1945).

[6] M. D. Liston, C. E. Quinn, W. E. Sargeant, and G. G. Scott, Rev. Sci. Inst. **17**, 194 (1946).

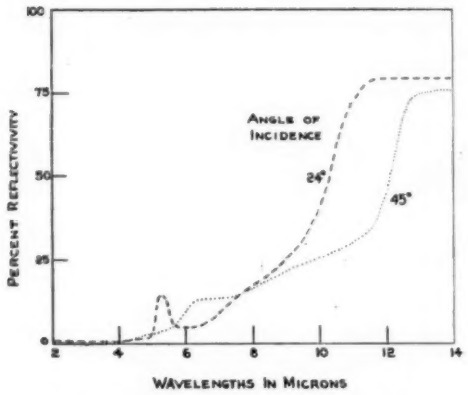

FIG. 8. Reflectivity of two 3610-line gratings.

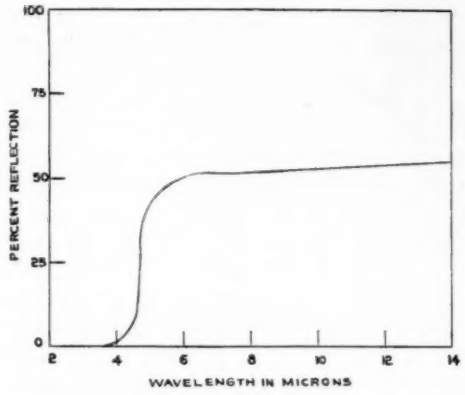

FIG. 10. Reflection from four 7500-line gratings at 45° incidence.

entrance slit of the monochromator. Measurements were made by recording the energy entering the monochromator with mirrors mounted in the collimating system (*Io*) and the energy entering it when one or more gratings were substituted for the mirrors (*I*). The reflectivity was taken as *I*/*Io*. As the substitution involves refocusing of the collimating system each time, the energy obtained depended on reproducing the exact focal conditions.

RESULTS

The energy distributions in the specularly reflected images from two replica gratings with spacings of 3610 and 7500 lines per inch were each measured at angles of incidence of 15, 24, and 45 degrees. These reflectivities are shown in Figs. 4 and 5, respectively. The fluctuation at the long wave-length ends of these curves are probably due to the presence of scattered light and to inexact alignment of the collimating system. For comparison with these curves, Fig. 6 shows the transmission of an MgO powder filter.

In Fig. 7, the variation in cut-off wave-length with angle of incidence is compared with the variation calculated on the assumption that the intensity of the diffracted spectrum always approaches zero at about the same angle of diffraction. This predicts that the cut-off wave-length should vary approximately as the sine of the angle of incidence. In estimating the sharpness of cut-off obtainable from gratings with available groove forms, the 13° convergence of the light beam used in these experiments must be con-

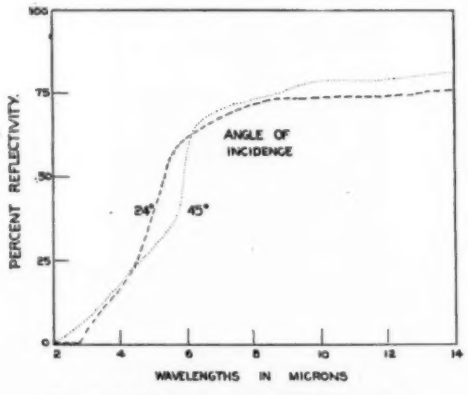

FIG. 9. Reflectivity of two 7500-line gratings.

TABLE I. Reduction of scattered light by use of 3610-line grating at 15° angle of incidence, expressed as 100× the ratio of light transmitted by LiF shutter to light absorbed by opaque shutter.

Wave-length by micron	Without grating	With grating	Improvement factor	Without grating	With grating	Improvement factor
15.1	25	3.5	7	150	14	10
14.6	17	2	8	—	6.6	—
14.0	12	1.5	8	55	5.1	11
13.5	10	1	10	45	3.3	13
12.9	8	1	8	31	2.2	14
12.3	7	1	7	22	1.5	14
11.6	5	0.5	10	17	1.1	15
10.9	4	0.5	8	13	0.8	11
10.2	4	0.5	8	11		
9.3	2	0.5	4	10		
8.5	2	0		5		

sidered. The difference attributable to this effect between the two edges of the beam can be seen from Fig. 7 to be about one micron for each position of the 3610-line grating, and about half a micron for the 7500-line grating. This is interpreted to mean that if measurements were made with parallel light, the sloping parts of the curves would have been shorter and steeper.

Figures 8 and 9 show the reflectivity of pairs of the gratings used together. The optical densities of the two gratings do not appear to be completely additive at points near the break of the curve. At shorter wave-lengths, where better concentration of the light into specific orders is possible, the optical densities appear to be additive.

A further sharpening of the cut-off and improvement of the filtering characteristics can be obtained by using still more reflections. Figure 10 shows the transmission of a filter composed of four gratings set at 45°. The gratings were so arranged that the light beam emerging from them was traveling in the same direction along the same line as the incident beam. In this case, the cut-off wave-length was varied by rotating the gratings about an axis perpendicular to their surface, the curve shown being measured with the rulings inclined at 45° to the horizontal.

The effectiveness of the gratings in reducing scattered light was tested in a normal rocksalt monochromator and in one with a prism so foggy that it could not ordinarily be used. Table I gives the scattered light at 14.5μ with and without the use of a 3610-line grating at 15° incidence. Scattered light was measured as the difference in deflection observed with an opaque shutter and an LiF shutter in the light beam. It shows that the scattered light was in each case reduced by a factor of about 10 throughout the range where the filter is applicable. In the second case, the scattered light was about five times that which is normally present, and the figures on its reduction

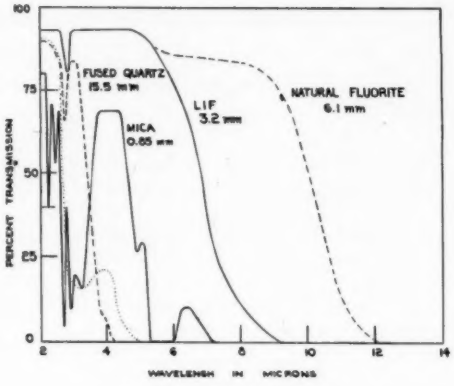

FIG. 11. Transmission curves.

are probably more accurate, as they do not involve measurements of such small quantities. The observed decrease in scattered light reduction at the longest wave-lengths is probably caused by failure of the LiF shutter to indicate all of the scattered light that was present.

These gratings may be used in combination with other filters to isolate broad bands of infrared radiation. Some of the useful materials for combination with them are, fluorite, lithium fluoride, mica, quartz, and glass. Typical transmission curves for these materials are given in Fig. 11. As the cut-off point of these materials varies with thickness and the cut-off point of the grating varies with angle of incidence, it is possible to make a combination of the two that has its maximum transmission at almost any wave-length. For example, to get the maximum transmission at 11 microns, the 3610-line grating might be used at 24° angle of incidence in conjunction with a fluorite filter 1 mm thick. The decrease in intensity of the blackbody-radiation curve may also be used as the long wave-length cut-off, and the sharpness of cut-off may be improved by combining these filters with selective gas or solid absorption filters, or by Reststrahlen.

Modulation of the Resonance Lines in a Cesium Arc*

J. M. Frank, W. S. Huxford, and W. R. Wilson
Department of Physics, Northwestern University, Evanston, Illinois

(Received June 16, 1947)

A detailed study has been made of the electrical characteristics and light-modulation properties of a 90-watt cesium vapor arc having a three-inch column. The range of frequencies used extend from 100 to 10^6 c.p.s. When operated on a d.c. biasing current of 5 amp., the arc has a positive resistance; below 20,000 c.p.s. its reactance is inductive, while above this frequency the reactance is chiefly capacitative. The modulation ratio for the resonance lines at 8521A and 8944A has a nearly constant value of 0.85 below 2000 c.p.s., and for higher frequencies varies inversely with the square root of the frequency.

I. THE CESIUM ARC

THE arc lamps used in this study were developed for use in infra-red communication systems as a wartime project by the Westinghouse Lamp Division. A detailed description of lamp structure and manufacturing techniques has recently been published.[1] Figure 1 is a photograph of two lamp models used for military purposes. In these lamps the inner Pyrex bulb contains the cesium metal and is filled with argon to a pressure of about 20 cm of mercury. This arcing chamber is mounted in an evacuated outer envelope so that during operation of the arc its temperature is sufficiently high to maintain a cesium vapor pressure of about 2 mm of mercury. The electrodes are coiled tungsten filaments which are used to preheat the inner bulb and vaporize the cesium, and to anchor the discharge along the tube axis. The larger model of lamp, type CL-2, having a three-inch arc column, was used in the present studies.

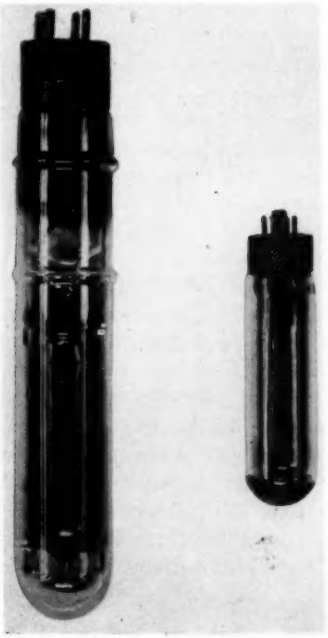

FIG. 1. The large lamp, type CL-2, has a 3" electrode spacing. The small lamp is a 50-watt model, having 2½" distance between electrodes.

The discharge is a wall-stabilized form of low voltage arc requiring a copious supply of electrons from the cathode. For this purpose the filament used as cathode is coated with a barium-strontium oxide mixture. In starting the discharge the filaments are preheated for about two minutes, after which a one-ampere arc may be set up using a two- or three-hundred volt a.c. source and ballast, and the arc switched over to the d.c. source when sufficient metal has been vaporized; or the arc may be initiated after preheating of the inner bulb by attaching the d.c. supply and using a high frequency electrodeless discharge to effect ionization of the argon. Temperature equilibrium is established in the lamp six or eight minutes after the arc discharge is set up.

Figure 2 shows the static characteristics of one of the CL-2 lamps obtained by first increasing the arc current, and then decreasing it. If the arc current is allowed to flow for two or three minutes

* Presented at the Washington Meeting of the American Physical Society, May 1, 1947. This work was sponsored by the U. S. Navy, Bureau of Ships.

[1] N. C. Beese, J. Opt. Soc. Am. 36, 555 (1946).

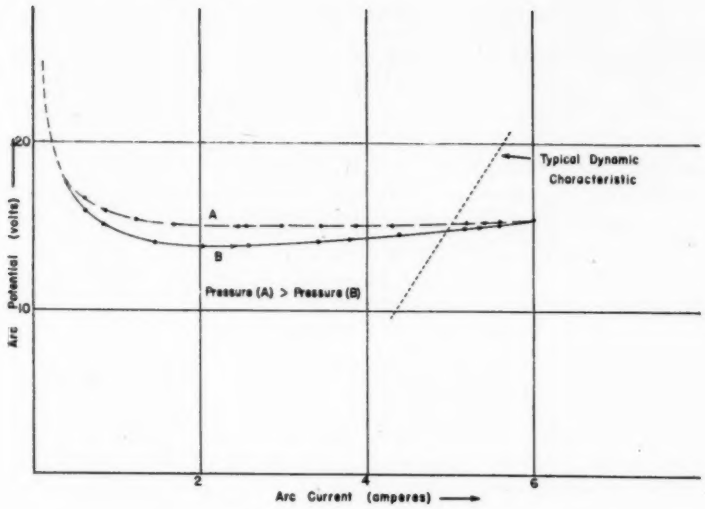

FIG. 2. Potential-current curve for the d.c. cesium arc and typical dynamic characteristic.

between readings a single curve is obtained. A typical dynamic characteristic is also shown.

The high infra-red efficiency of this lamp is due chiefly to the energy radiated in the two resonance lines of cesium at 8521A and 8944A. For laboratory studies this radiation is satisfactorily isolated by using a Wratten No. 87 filter and a Cs-Ag-O photo-cathode receiver. Measurements show that approximately 22 percent of the total power supplied to the arc is emitted as resonance radiation. For a new lamp containing an excess of cesium the intensities of the two resonance lines are nearly equal.

This source has proved of great value for infra-red communication purposes because of its high conversion efficiency and its excellent modulation characteristics. For both practical and theoretical reasons it is important to have complete and detailed information concerning the dynamic properties of the arc over the entire range of frequencies for which a useful component of modulated radiation can be obtained and for which accurate measurements can be carried out. The present study was undertaken to secure this information.

II. EXPERIMENTAL PROCEDURE

When the cesium arc is used as a source of modulated radiation the discharge is maintained by means of a biasing direct current, and this current is modulated by impressing an a.c. potential across the arc electrodes. The biasing current in the present work was supplied by a 120-volt bank of large storage cells. Three types of generators were used as alternating current sources. The first was an audio oscillator driving a power amplifier and having a frequency range from 100 c.p.s. to 30,000 c.p.s. The second source was a long wave power oscillator (25 kc/sec. to 300 kc/sec.) especially designed and constructed in this laboratory for use in exciting gaseous discharges. The third generator was a Navy type TDE transmitter having an average power output of 150 watts and capable of supplying currents ranging in frequency from 300 to 18,000 kc/sec. It was possible with these generators to supply alternating currents of good sine-wave form to the arc sufficient to secure at least 75 percent current modulation over the entire range of frequencies from 100 c.p.s. to 10^6 c.p.s.

When applying a.c. modulating potentials to the arc, provision was made for varying the depth of current modulation and making impedance matching adjustments. The alternating current was supplied to the arc through a coupling capacitor the size of which depended upon the lowest frequency at which measurements were taken. At audiofrequencies the dynamic impedance of the arc is of the order of two ohms, so that an 800-μfd electrolytic capacitor was employed for the lower modulation frequencies. Above 50 kc/sec. an 8-μfd capacitor was used.

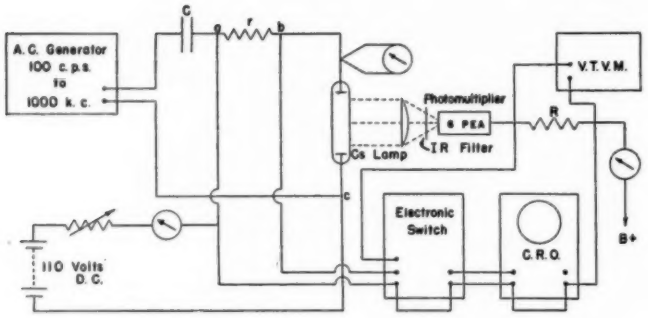

FIG. 3. Block diagram showing all components of the measuring circuit.

Method of Measuring Current Modulation

At one of the lamp terminals a calibrated thermocouple was inserted in the circuit so that both the d.c. and a.c. currents passed through it. The total current recorded by the thermocouple meter is referred to as I_t and the reading of the d.c. meter in the circuit is designated I_0. The r.m.s. value of a.c. current through the arc is given by

$$I_L = (I_t^2 - I_0^2)^{\frac{1}{2}}.$$

The degree of current modulation is conveniently expressed in terms of the peak value of a.c. through the arc and the d.c. operating current. Thus, the percent current modulation is given by the relation,

$$M_I = (\sqrt{2} I_L / I_0) \cdot 100 \text{ percent.} \qquad (1)$$

Method of Measuring Light Modulation

The apparatus for determining the degree of modulation of the resonance radiation consisted of a condensing lens, a Wratten No. 87 infra-red filter, photo-tube multiplier, vacuum-tube voltmeter, and d.c. microammeter (see Fig. 3). The Wratten No. 87 filter was used because it passes both of the resonance lines of cesium and excludes all wave-lengths below about 7500A. The photo-tube multiplier was a Farnsworth-type 6PEA with Cs-Ag-O cathode having its maximum sensitivity at 8300A and threshold at about 13,000A. For frequencies below 100 kc/sec. a 5000-ohm load resistor was used in the final multiplier stage, and at higher frequencies a 1000-ohm resistor (R, Fig. 3). When the multiplier is used in this manner the a.c. current through the load resistor is accurately proportional to the flux received by the photo-cathode at all frequencies.

The unmodulated component of light flux produces a current i_0 in the d.c. output meter of the multiplier. The modulated component produces an a.c. potential across the photo-multiplier load resistor, R, equal to e_L r.m.s. volts. e_L was measured with a vacuum-tube voltmeter. The percent light modulation equals the ratio of the peak value of the alternating component of photo-current to the average d.c. value, or

$$M_L = (\sqrt{2} e_L / R i_0) \cdot 100 \text{ percent.} \qquad (2)$$

The ratio of the percent modulation of resonance radiation to the percent current modulation has been designated the "radiation-current modulation ratio." Its value at any frequency was calculated from (1) and (2); thus, the modulation ratio M is given by

$$M = M_L / M_I. \qquad (3)$$

Studies of wave form of the current and light waves, and measurements of the current-potential and light-current phase angles were made by means of a cathode-ray oscilloscope and an electronic switch. For this work a DuMont Model 248 oscilloscope was used, and an electronic switch of special design. The latter consisted of a Hewlett-Packard square-wave generator used to deliver a 60-cycle, 50-volt negative maximum square wave to the plates of two triode vacuum tubes, driving them alternately to cut-off plate current. An a.c. potential drop proportional to the arc current was applied to the grid of one tube and the a.c. component of the arc potential, or a.c. output of the multiplier photo-tube, to the grid of the second tube. The cathode-follower

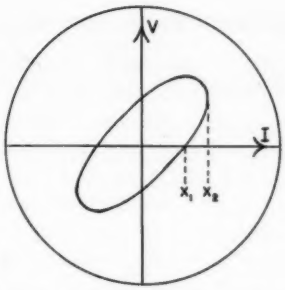

FIG. 4. $\sin\theta = x_1/x_2$, θ = angle between current and potential waves.

output of the two tubes was then applied to the vertical amplifier of the oscilloscope. In this way the current and light waves could be viewed simultaneously on the oscilloscope screen, and wave shapes and phase shifts accurately measured at all frequencies up to one megacycle.

The determinations of percent modulation of current and of radiation were checked at several frequencies by measurements of the amplitudes of these waves as viewed on the oscilloscope screen. By means of the electronic switch the zero-current deflection was indicated simultaneously on the screen along with the current waves. In all cases satisfactory agreement was found between scope measurements and those obtained by the use of the thermocouple ammeter and d.c. current measurements, and by the corresponding measurements for the light wave as indicated by the output current of the photo-tube multiplier.

III. ELECTRICAL CHARACTERISTICS

The electrical properties of the modulated arc are complicated functions of the d.c. biasing current, the frequency and depth of modulation, the cesium vapor pressure, the size of discharge tube, and length of the arc column and its position in the earth's gravitational field. For the present experiments the arc was operated in a horizontal position and on a d.c. current of 5 amperes. In the case of the electrical measurements all data refer to fifty percent current modulation at all frequencies used.

Potential-Current Phase Angle

The oscilloscope was used to measure the phase angle between arc potential and arc current as a function of frequency. A special non-inductive resistor having a resistance of 0.25 ohm was inserted in the circuit so that both the d.c. and a.c. components of arc current flowed through it. (r, Fig. 3.) The a.c. component of voltage developed across this resistor, which is proportional to the a.c. component of lamp current, was applied to one set of deflecting plates. Very good ellipses were formed on the oscilloscope screen for depths of current modulation not exceeding fifty percent. The phase angle was measured as indicated in Fig. 4. The accuracy of the method is about $\pm 1°$ for small angles and $\pm 5°$ for angles in the vicinity of $\pm 90°$.

Figure 5 gives the results of phase-angle

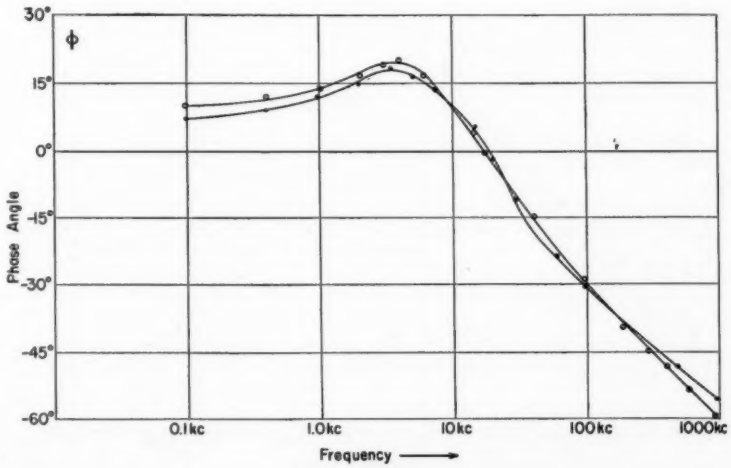

FIG. 5. Measured angle of lag of current behind potential plotted as a function of the modulation frequency.

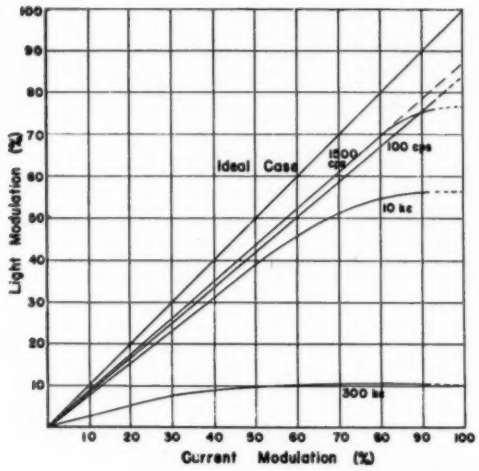

FIG. 6. Variation of observed percent light modulation with depth of current modulation at several frequencies.

measurements for two arcs. The potential wave leads the current wave by progressively increasing angles from 100 c.p.s. to about 3000 c.p.s. Beyond this point the angle decreases and passes through zero phase shift at 20 kc/sec. For frequencies above 20,000 c.p.s. the angle is negative and the a.c. arc current leads the potential by increasing amounts up to a value of $\theta = -55°$ at one megacycle.

Equivalent Reactance of the Arc

The results of potential-current phase-angle measurements indicate that the cesium arc may be thought of as a parallel combination of inductance, capacitance, and resistance which is resonant at 20.0 kilocycles. At frequencies below 20 kc/sec. it can be resolved into an equivalent electrical circuit consisting of a resistance in series with an inductance. When a variable resistor was placed in series with the modulated arc, it was found impossible at any frequency to obtain a 90° phase shift which would be produced if the arc resistance at any point were negative. Bridge measurements carried out in the audio-frequency range resulted in a mean value of resistance of the 5-amp. arc of $+1.5$ ohms, and an equivalent inductance of approximately $70 \cdot 10^{-6}$ henries. Such bridge measurements are not satisfactory, however, since the small amplitude a.c. currents used in the arms of the bridge produce negligible modulation in the arc, and hence do not reveal dynamic impedances characteristic of normal operation of the arc. The nature of the arc reactance at a modulating frequency of 1000 c.p.s. was indicated by shunting the arc with a condenser of capacitance equal to one micro farad. This caused the eccentricity of the ellipse to increase, showing that the discharge behaves inductively in this frequency region.

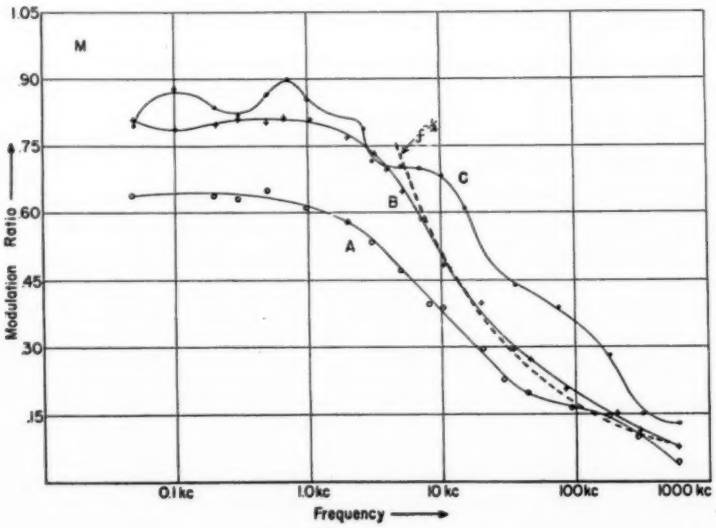

FIG. 7. Radiation-current modulation ratios for three lamps. The dashed curve in the case of lamp *B* shows how the ratio would vary if it is assumed that it is inversely proportional to the square root of the frequency.

IV. CHARACTERISTICS OF THE MODULATED RADIATION

Radiation-Current Modulation Ratio

Figure 6 shows measured values of percent modulation of the cesium resonance radiation plotted as a function of the depth of current modulation. The line having an inclination of 45° represents the ideal case for which the ratio M_L/M_I is unity. The parameter for these plots is the modulation frequency. For any frequency less than 10 kc/sec. the modulation ratio is constant for current modulations up to nearly 85 percent. As the modulation frequency is increased, however, the modulation ratios are constant over smaller and smaller ranges of values of percent current modulation.

Modulation ratios as defined in Eq. (3) were determined for a number of CL-2 lamps using a constant current depth of 50 percent. The results of these measurements are shown in Fig. 7. The irregular curve is typical of lamps which have been used for a hundred hours or more and in which most of the cesium has been lost through chemical reaction, probably at the bulb walls. In such lamps the glass walls became partially opaque and assumed a brownish color. The smooth curves are typical of normal lamps with clear bulbs in which an excess of cesium metal is always visible on the cooler portions of the inner tube.

The maximum modulation ratio for normal lamps is approximately 0.85, the curves being nearly constant at this value over the frequency range from 100 c.p.s. to 2 kc/sec. Beyond this region the light-modulation ratio decreases, varying approximately inversely as the square root of the frequency. This relation has also been found to hold at higher modulation frequencies for the high pressure mercury arcs studied by Mangold.[2] Mangold also found empirically that the frequency beyond which the modulation ratio was not constant was a function of the arc length, the "turnover point" occurring at lower frequencies for arcs having greater electrode distances.

Current-Radiation Phase Angle

An attempt was made to measure the phase angle between the a.c. component of the current in the modulated arc and the a.c. current output of the photo-tube multiplier, using the method described above for determining the potential-current phase angle. Figure 8 indicates typical oscillograms using this procedure. The traces are distorted ellipses from which no accurate calculations could be made. They indicate that the angle of lag of the light wave behind the current wave

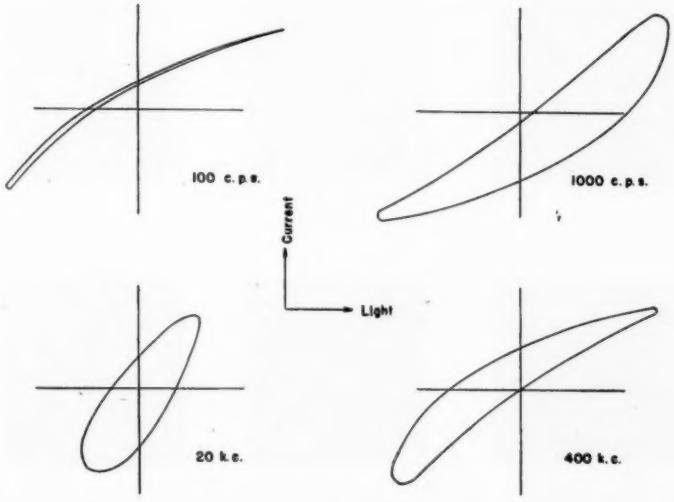

FIG. 8. Typical oscillograms obtained when the current and light waves are applied to the vertical and horizontal sweeps of the oscilloscope.

[2] H. Mangold, E. N. T. **17**, 57 (1940).

increases with frequency up to about 20 kc/sec. and then decreases for higher modulation frequencies.

The use of the electronic switch previously described to secure two separate signal traces on the oscilloscope screen, one representing current and the other representing the radiation as measured by the photo-tube current, is illustrated in the circuit arrangement shown in Fig. 3. By comparing the displacement of corresponding points on each trace to the length of the complete cycle, the phase shift is obtained directly.

Oscilloscope traces obtained at several frequencies are shown in Fig. 9. In general it was found that the phase displacement of the positive peaks of the two sine curves differed from the phase displacement of the negative peaks. Accordingly, the phase angle was recorded for both the positive and negative halves of the two waves representing current and light.

The measured phase angles are plotted in Fig. 10 as a function of the modulation frequency. These results refer to observations made at current modulations of 50 percent. At 100 c.p.s. the phase difference between light and current waves was zero for both peaks. Between 500 and 1000 c.p.s. the positive current peaks lead the positive light peaks by angles which vary from 1° to 9°, while there is a shift in the opposite direction of several degrees for the negative peaks. At frequencies from 2 to 5 kc/sec. both halves of the light wave show the same lag angle of about 20°. In the region between 5 kc/sec. and 600 kc/sec. both halves of the light wave lag behind the corresponding portions of the current wave, the positive peaks always by a greater angle than the negative peaks. Maximum angles of lag of 98° and 90° occur at a frequency of 30 kc/sec., and from there on both lag angles decrease with increase of modulation frequency.

DISCUSSION

In all of the arcs studied it was observed that at approximately 5 kc/sec. an unstable shifting of the luminosity of the arc column occurred, such as might have been produced if a standing sound wave were present. Again at about twice this frequency a bowing up and shifting of the arc column appeared. It is believed that oscillations of the arc plasma may have been excited in this frequency region, and that anomalous changes in the shape of the light wave due to this complication may explain the peculiar shift of the wave peaks and merging of the positive and negative phase angles observed between 2 kilocycles and 10 kilocycles (Fig. 10).

Weizel, Rompe, and Schulz[3] predict an increase in phase angle between current and temperature

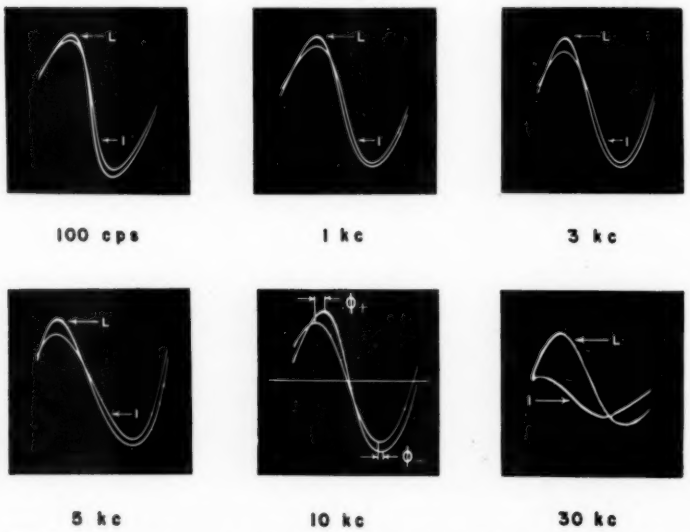

FIG. 9. Photographs of oscilloscope traces of superimposed current and light waves for several modulation frequencies.

[3] W. Weizel, R. Rompe, and P. Shulz, Zeits. f. Physik **117**, 545 (1941); **119**, 237 (1942).

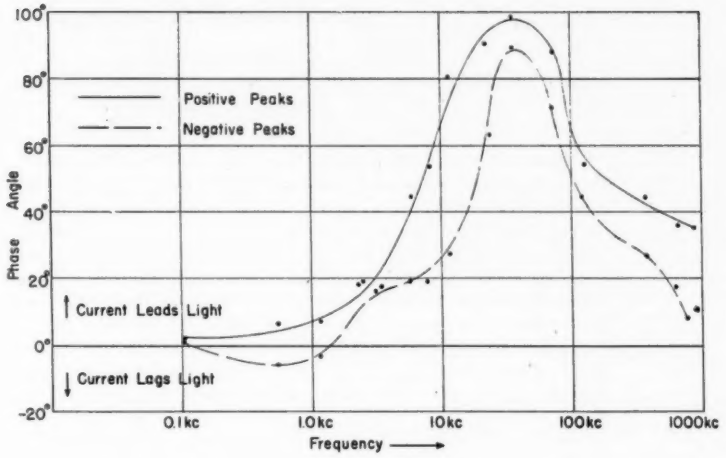

FIG. 10. Variation of the phase angle between current and light waves for both positive and negative peaks.

waves with increasing frequency, the shift approaching $\pi/2$ at high frequencies. Mangold[2] observed phase shifts between current and light waves in the case of a convection stabilized mercury arc discharge and found that the lag angle increased to a value of about $\pi/2$ at $f=10^5$ c.p.s., the highest frequency used. No decrease in angle with frequency was noted, and no separation was made of the shifts corresponding to positive and negative wave peaks. If, as should be the case at the lower frequencies, thermal excitation of radiation is the predominant mechanism, increase of phase lag with frequency is to be expected. Also, because of thermal hysteresis effects, the lag should be greater for the positive half of the cycle than for the negative half, and the light wave should be distorted, the maxima somewhat pointed and the minima (or negative halves of the wave) flattened. Indications of such distortions are clearly evident in the radiation-wave forms of Fig. 9.

Above a certain frequency the amplitude of the cyclic temperature variations becomes very small and the production of modulated radiation depends chiefly on excitation by the impressed high frequency field. For this method of excitation the phase angle between current and radiation waves will now depend on a lag which is determined by collision processes between electrons and atoms in an alternating field. A theoretical study of the excitation processes in the modulated arc is contemplated.

The Polanret Microscope*

HAROLD OSTERBERG
Research Division, American Optical Company, Scientific Instrument Division, Buffalo, New York
(Received June 12, 1947)

Variable contrast in the image of non-uniform objects is obtained by polarizing orthogonally the deviated and undeviated bundles of light due to diffraction by the object. Advantage is taken of this orthogonality of polarization to effect variable phase difference between, and variable amplitude ratio of the deviated and undeviated bundles. These modified, interfering bundles produce the image and permit continuously variable contrast.

Of many possible polanret systems two are described. In the preferred system, the phase difference between the deviated and undeviated bundles is varied throughout one wave-length by rotation of the polarizer, and the amplitude ratio is varied practically in all proportions by rotation of the analyzer. The light is plane polarized either before or after passage through the object, passes through a uniform quarter-wave plate, through the zonal polarizer, and finally through the analyzer. The zonal polarizer consists of two thin, adjoining, plane-polarizing elements oriented at right angles. One element covers the image of the condenser diaphragm as formed by the intervening lenses of the condenser and objective, the other, the remaining area of the clear aperture. The principal axes of the quarter-wave plate bisect the transmission directions of the zonal polarizer.

Wide range in contrast has been obtained with experimental polanret systems with microscope objectives of long focal length.

I. INTRODUCTION

THE polanret microscope is a modification of the recently developed phase microscope. Its purpose is to provide a more flexible instrument for accomplishing the results attained with the phase microscope. In the phase microscope the amplitude ratio of, and the phase difference between the deviated and undeviated bundles of light which are formed by diffraction at the object are varied discontinuously by interchanging diffraction plates. The polanret system permits continuous variation of the above-mentioned amplitude ratio and phase difference. Continuous variations in the contrast of the image are therefore made possible.

The following considerations of the optical system of the phase microscope shown in Fig. 1 lead in a simple manner to the principles of the polanret microscope. The condenser diaphragm is focused upon the plane of the diffraction plate by the intervening lenses of the substage condenser and of the objective. The opening in the condenser diaphragm, whatever its shape, will therefore be imaged upon some portion of the diffraction plate. This important area of the diffraction plate is conjugate to the opening in the condenser diaphragm and is therefore called the *conjugate area*. The remaining portion of the diffraction plate is called the *complementary area*. The physical significance of the conjugate area is that all of the light which is transmitted through the condenser diaphragm, and which subsequently obeys the laws of geometrical optics, will in the absence of aberrations pass through the conjugate area. The effect of placing a non-uniform object upon the slide is to introduce diffraction at the object. Practically all of the deviated part of the diffracted light passes through the complementary area provided that the conjugate area is suitably small. The deviated and undeviated bundles of light which leave the object may, therefore, be said to be separated at the complementary and conjugate areas of the diffraction plate.

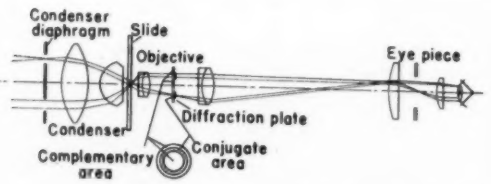

FIG. 1. Optical system of the phase microscope. The microscope lamp, which is not shown, is focused for Kohler illumination.

* Presented at the meeting of the Optical Society of America in New York, New York, 1946.

The contrast and to some extent the shape of the image are determined by the interference phenomena which take place between the deviated and undeviated bundles when these are brought together at the focal plane of the eyepiece. Consequently, the contrast of the image may be modified by introducing phase differences between and by changing the amplitude ratio of the deviated and undeviated bundles. In phase microscopy, changes in the phase difference and amplitude ratio of the deviated and undeviated bundles are affected by the direct procedure of interposing a diffraction plate at the real image of the condenser diaphragm. The conjugate and complementary areas of this plate are differently coated with a combination of refracting and light absorbing materials. Experience has shown that in order to obtain the desired contrast in the image of several objects, and sometimes for a single specimen, a limited series of diffraction plates is often required. The polanret microscope was devised as a possible means of providing an infinite series.

The point of departure of the polanret microscope consists of polarizing the conjugate and complementary areas differently and preferably at right angles. This can be accomplished by replacing the diffraction plate by two zonal polarizers of high optical quality. One of these covers the conjugate area, the other, the complementary area. The deviated and undeviated bundles now remain physically separated until they are subsequently brought into a common direction of vibration by passage through an analyzer. Consequently, the phase differences between, and the amplitude ratio of the deviated and undeviated bundles can be modified by the interaction of polarizers and birefringent elements which do not have to be located at the zonal polarizers.

II. A DIRECT POLANRET SYSTEM

Actually, a large number of polanret systems are possible. The simple and more direct system of Fig. 2 was originated in collaboration with A. H. Bennett. The conjugate area is shown as a disk located on the optical axis. For purposes of illustration the plane conjugate to the condenser diaphragm is shown as falling outside of the objective. This generally occurs with the longer

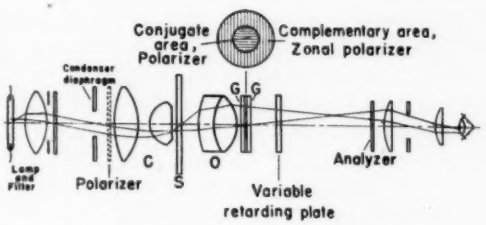

FIG. 2. A direct polanret system. *C* is the substage condenser; *S*, the object slide; *O*, the objective; *G* are glass plates which are cemented to the orthogonal zonal polarizers. The variable retarding plate may be a Berek or a uniform field Babinet compensator. Analyzer and polarizer are rotatable.

focus objectives. After passage through the zonal polarizers, the deviated and undeviated bundles traverse the birefringent plate which introduces a phase difference between these two bundles. Let it be assumed henceforth that the transmission directions of the two zonal polarizers are orthogonal. The slow or fast axis of the birefringent plate is then oriented parallel to the transmission direction of the conjugate area, according as the undeviated bundle is to be retarded or advanced in phase with respect to the deviated bundle. To secure variable phase differences the birefringent plate may consist of one of the following: a uniform field Babinet compensator; a Berek compensator; a device in which the birefringence is altered by varying the mechanical stress; or a crystal such as ammonium dihydrogen phosphate in which the birefringence is varied electro-optically. A non-variable retarder such as a plate of mica may be used where a single phase advance or retardation suffices. The subsequent passage of the deviated and undeviated bundles through the analyzer serves two purposes: their electrical vibrations are brought to a common direction of vibration; the transmitted components of the two bundles and hence their amplitude ratio are governed by rotation of the analyzer.

The above optical system is operated as follows. The system is first aligned by focusing and centering the aperture of the condenser diaphragm upon the conjugate area of the zonal polarizers. In doing so, the eyepiece is replaced by a short focus telescope for viewing the zonal polarizers, and the condenser diaphragm is adjusted. When the eyepiece has been returned and the usual precautions have been taken for aligning

a standard microscope for Kohler illumination, the specimen is brought into focus. Contrast in the image is then varied by rotating the analyzer and adjusting the phase retarder, that is, the elements of variable birefringence, alternately. To reverse the sign of the phase difference which is introduced by the phase retarder, this retarder is rotated as a whole through 90°.

Experiment has shown that the contrast variations are markedly improved by the addition of a rotatable polarizer, Fig. 2. For obtaining the best results both analyzer and polarizer are rotatable, but the analyzer may be fixed. Rotation of the polarizer governs the amplitude ratio of the deviated and undeviated bundles, because polarized light is incident upon the orthogonal zonal polarizers. Whenever it is undesirable to pass polarized light through the system, a polarizer of high optical quality is placed between the specimen and the zonal polarizers. The preferred position is that adjacent to the zonal polarizers, but this position is usually inconvenient for mechanical reasons.

When polarized light is incident upon the zonal polarizers, the elements of the zonal polarizer may be constructed of other than polarizing materials. For example, one element may consist of left-handed quartz and the other of right-handed quartz, both of which rotate the plane of polarization through 45°. Again, the two elements may consist of two properly oriented half-wave plates. Such elements introduce additional optical difficulties which render them unsuitable except, perhaps, for specialized applications.

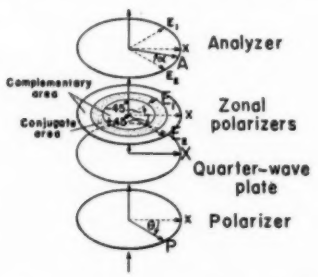

FIG. 3. The essential elements and parameters of a preferred polanret system. A and P are the transmission directions of the uniform analyzer and polarizer, E_1 and E_2, of the zonal polarizers which cover the conjugate and complementary areas, respectively. X is the direction of vibration of the slow ray in the quarter-wave plate and is selected as the direction of reference. The zonal polarizers and quarter-wave plate are fixed; the analyzer and polarizer, rotatable. The indicated θ-direction is positive, namely, that in which rotation of the polarizer increases the optical path of the conjugate area with respect to that of the complementary area.

III. THE PREFERRED POLANRET SYSTEM

The principles of a system which is preferred from the standpoints of its effectiveness, operational convenience, and mechanical simplicity are illustrated with the aid of Fig. 3. The light passes successively through a rotatable polarizer, a quarter-wave plate, the zonal polarizers, and a rotatable analyzer. The transmission directions E_1 and E_2 of the zonal polarizers are fixed in the indicated $\pm 45°$ orientation with respect to X where X is parallel to the electric vector of the slow ray of the quarter-wave plate. It can be shown[1] that if the polarizer is rotated through the angle θ, the phase difference so introduced between the transmitted electrical vectors E_1 and E_2 is equal to 2θ. This phase difference can be varied from $-180°$ to $+180°$ by rotating the polarizer from $\theta = -90°$ to $\theta = +90°$. Furthermore, the amplitudes of E_1 and E_2 remain equal and are not altered by rotating the polarizer. The effect of rotating the transmission direction, A, of the analyzer throughout the quadrant between E_1 and E_2 is to vary the transmitted ratio of E_1 to E_2 from zero to infinity, provided that the polarizing elements give complete polarization. If then, E_1 is associated with the conjugate area and E_2 with the complementary area, rotation of the analyzer varies in a continuous manner the amplitude ratio of the undeviated and deviated bundles and rotation of the polarizer varies in a continuous manner the phase difference between these two bundles. These two variations are independent of each other and are known quantitatively from the positions of the analyzer and polarizer.

The manner of applying the above principles to a microscope is shown in Fig. 4 in which the conjugate area is illustrated as annular. The diffraction plate of the phase microscope is replaced by a combination which will be called a *micoid disk*. It consists of the zonal polarizers and the quarter-wave plate which have the relative orientation shown in Fig. 3. These elements are cemented (not shown) between thin, glass plates

[1] H. Osterberg, J. Opt. Soc. Am. 36, 473–474 (1946).

of high optical quality. The annular opening of the condenser diaphragm is focused and centered upon the annular zone of the micoid disk. If it is desired that the object shall be illuminated by unpolarized light, the polarizer is placed between the object and the micoid disk and may in some instances be used as the cover glass.

The mode of operation of this system is similar to that described for the system of Fig. 2, except that contrast variations in the image are produced by rotating the analyzer or polarizer or both. The phase retarder now consists of the combination of polarizer and micoid disk.

Monochromatic light for which the quarter-wave plate has been designed is preferred as the illuminant, but an unfiltered tungsten lamp serves moderately well in conjunction with a quarter-wave plate designed for 5500 angstroms.

IV. CORRELATION OF THE PHASE AND AMPLITUDE SETTINGS OF THE POLANRET MICROSCOPE WITH THOSE OF THE PHASE MICROSCOPE

A nomenclature for designating the four types of diffraction plates which can arise in phase microscopy has been described.[2] Readings of the phase and amplitude settings of the polanret microscope may be translated into this nomenclature in the following manner.

Since the phase difference, d, and the amplitude ratio, r, are determined by the dial readings of the polarizer and analyzer, respectively, these dial readings may be calibrated to give direct readings of the phase difference and of the amplitude ratio. In the final setting of the analyzer, its transmission direction should fall in the *neutral quadrant*,[3] marked on the dial, since rotation of the analyzer out of its neutral quadrant has the effect of introducing an abrupt phase difference of 180° or one-half wave-length between the undeviated and deviated bundles. The energy transmission ratio, T, of the conjugate to complementary area is related to r by the equation.

$$T=r^2. \tag{1}$$

Let these T-values be designated on the dial of the analyzer and let the phase difference, d, be expressed in wave-lengths. According as T is less than or greater than unity, the polanret readings correspond to an A- or B-type diffraction plate, and the readings are recorded in the form $TA+d$ or $TB+d$ in which T and d are the numerical values of the dial readings. If, for example, in a given setting $T=0.15$ and $d=-0.25\lambda$, the setting is recorded as $0.15A-0.25\lambda$, since the phase difference is numerically negative.

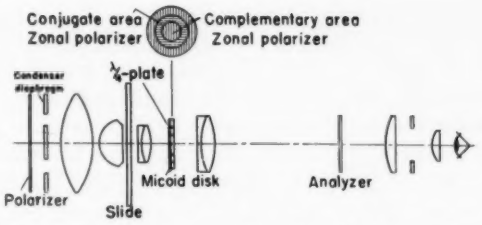

FIG. 4. The optical system of a preferred polanret system. The microscope lamp is not shown. In the experimental system the quarter-wave plate and zonal polarizers were cemented to one another and between glass plates.

If the dial of the polarizer is calibrated in degrees, measured from the zero position,

$$d=\frac{2\theta}{360}=\frac{\theta}{180}\ \text{wave-lengths}. \tag{2}$$

If the analyzer is marked in degrees and its zero position is oriented so as to block the completely polarized light from the conjugate area,

$$T=r^2=\tan^2\alpha, \tag{3}$$

in which α is the number of degrees rotation of the analyzer from its zero position. This zero position is easily checked by removing the eyepiece and adjusting the analyzer until the conjugate area appears darkest. As indicated in Fig. 3 the direction X bisects the neutral quadrant. Opposite quadrants are equivalent. It is suggested that in order to avoid confusion the objective and micoid disk assembly be oriented so that the X direction, marked on the objective, always runs from left to right with respect to the observer.

If facilities are not available for locating the X-direction precisely, the zero position of the polarizer can be found from observations upon the diffraction patterns produced by pin holes in a silvered slide.[4] The positive θ-direction of rotation of the polarizer can be found by viewing a

[2] Bennett, Jupnik, Osterberg, and Richards, Trans. Am. Micro. Soc. **65**, 105–106 (1946).

[3] H. Osterberg, J. Opt. Soc. Am. **36**, 474 (1946).

[4] H. Osterberg, J. Opt. Soc. Am. **36**, 475–476 (1946).

small, but resolvable, transparent particle in the polanret microscope. If this particle is immersed in a medium whose refractive index is slightly below that of the particle, the particle will appear bright with the polanret equivalent[5] of a $TA+0.25\lambda$ diffraction plate, that is with θ set near $+45°$. The corresponding value of T is ordinarily less than 0.20 so that α is less than 24°. The analyzer is set in the neutral quadrant.

V. EXPERIMENTAL RESULTS

Both the direct and preferred polanret systems of Figs. 2 and 4, respectively, have been constructed and studied with a 16-mm focus (N.A. 0.25) and with an 8-mm focus (N.A. 0.45) objective. Annular conjugate areas were used in both systems. The quarter-wave plate of the micoid disk was selected for 5461A and, correspondingly, a filtered *H*-4 lamp was used as illuminant. Good to excellent results were obtained with both systems. Wide and continuous contrast variations were produced in the images of many objects. One of these was the Salivary Chromosome of Drosophila. Its bands were rendered with maximum darkness against the background. It was possible to distinguish the unstained chromomeres in these bands even with the 16-mm focus objective, although their size fell at the Airy Limit of resolution of this objective. White light was used with fair success. The method was much more difficult to apply to objectives of shorter focal length than 8 mm without impairing definition. On the other hand, the method should provide immediate advantages in optical systems of long focal lengths such as may be employed in modified schlieren apparatus.

These investigations of the polanret microscope were made in connection with a broad research program in the field of phase microscopy. The polanret microscope is in the research stage and is not commercially available.

The writer is indebted to G. E. Pride, who constructed the polanret systems and assisted in the various tests. Pertinent comments and tests with biological specimens were made by Dr. O. W. Richards.

[5] Bennett, Jupnik, Osterberg, and Richards, Trans. Am. Micro. Soc. 65, 124–125 (1946).

JOURNAL OF THE OPTICAL SOCIETY OF AMERICA VOLUME 37, NUMBER 9 SEPTEMBER, 1947

Letter to the Editor

On the Influence of Accommodation on Spherical Aberration in the Human Eye, an Attempt to Interpret Night Myopia

A. IVANOFF
Museum National d'Histoire Naturelle, Paris, France
(April 21, 1947)

BY using Maxwellian view (after Professor Yves Le Grand's suggestion) I have measured[1] spherical aberration in the human eye—in its horizontal meridian—for several states of accommodation.[2] Figure 1 shows the mean of the results found in 10 eyes. The abscissae represent values of the aberration in diopters, which is either positive when marginal rays are more strongly converging than central rays, or negative in the opposite case. The ordinates represent the distances from the axis in mm. Near each curve is written the state of accommodation in diopters.

When accommodating, the eye changes from under-correction to over-correction: the surfaces of the lens flatten down (Tscherning, Fincham), and over-correction by the lens becomes little by little more important than under-correction by the cornea. For an accommodation of

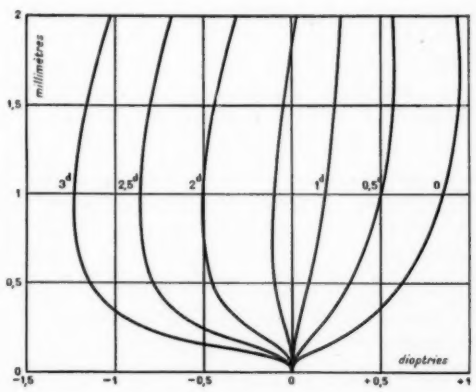

FIG. 1.

about 1.5 diopters, they counterbalance one another, and the total spherical aberration is nearly suppressed.

Calculations by Professor Yves Le Grand[3] have shown that, owing to spherical aberration in unaccommodated eye, the retinal image of a distant monochromatic luminous point source is marred with a spurious ring, which may become troublesome in a weak light on account of the lessened differential sensitivity of the retina. Therefore, I think[4] it likely that night vision may be improved by suppressing spherical aberration in the eye, *viz.* by an accommodation of 1.5 diopters, as was explained before. But in order that the eye may accommodate without any modification in focusing, we must use divergent glasses.

To a slight extent, less than 0.5 diopter, night myopia is due to the Purkinje shift joined to chromatic aberration of the eye. But I think that this phenomenon is scarcely at all one of real myopia: the image remains sharp on the retina and may be improved only by allowing the eye to accommodate, by providing it with diverging glasses.

A detailed paper on chromatic and spherical aberrations in the eye, and the part they play in night vision, has just been printed at the Revue d'Optique (Paris). It includes the results obtained by J. M. Otero, A. Duran, J. Palacios, and J. C. Gomez (1942–1945), on night "myopia," which conclusions agree with my thesis.[5]

[1] C. R. Acad. Sci. Paris **223**, 170 (1946).
[2] C. R. Acad. Sci. Paris **223**, 1027 (1946).
[3] Lectures delivered at the Institut d'Optique in Paris.
[4] C. R. Acad. Sci. Paris **223**, 1185 (1946).
[5] Revue d'Optique (Paris) **26**, 145 (1947).

JOURNAL OF THE OPTICAL SOCIETY OF AMERICA VOLUME 37, NUMBER 9 SEPTEMBER, 1947

Book Reviews

Photoelectric Cells

A. Sommer. Pp. 104+viii, Figs. 27. The Chemical Publishing Company, Inc., New York, 1947. Price $2.75.

Most American readers will misjudge the subject matter of A. Sommer's book from the title since it is customary for us to use the name "photo-tube" to describe photosensitive devices that involve the liberation of electrons from solid substances under the influence of light. The word "photo-cell" is used to refer to barrier-layer and photoconducting cells that do not depend on the complete release of electrons for their operation.

Sommer deals exclusively with photo-tubes, and does so from such an outdated point of view, in an attempt to simplify the presentation, that the book falls far short of satisfying the needs of an intelligent reader wishing to broaden his understanding of a subject in which he has an interest, but no desire to become an expert. The first two chapters present theories that reflect little or none of the advances in the understanding of the photoelectric effect that have rewarded the past twenty years of research in this field.

The third, and probably most interesting chapter sketches in broad outline steps in the manufacture of the two most useful photo-cathodes. These cathodes are the "silver-oxygen-cesium" type and the "antimony-cesium" cathode.

The remaining chapters describe some of the practical characteristics and properties of vacuum and gas-filled photo-tubes and multiplier types. Applications are mentioned very briefly; appropriate bibliography and an index are included.

Wayne B. Nottingham
Massachusetts Institute of Technology

Researches on Normal and Defective Colour Vision

W. D. Wright. Pp. 383+xvi, Figs. 233, 25 cm. C. V. Mosby, St. Louis, 1947. Price $10.00.

Strikingly reminiscent of Abney's *Researches in Colour Vision*, Wright's book reveals the great progress of the past three decades, not only in precision of methods and wealth of data, but most significantly in unity of treatment of the many formerly unconnected topics of color vision.

Wright's description of his book describes equally well the most fruitful source of progress in all recent studies of color vision: "first and foremost . . . a record of experimental data, with theoretical discussion and speculation occupying a very secondary position." Wright's original papers have been admirable examples of clarity and completeness, but the wealth of informative detail, comments, and discussions of possible alternatives included in his book is a revelation, not only of the thoroughness of the author's researches, but also of the inevitable limitations of publication in scientific periodicals. Among the instruments accorded such thorough description is a new model of Wright's trichromatic colorimeter, which uses spectrum primaries, and accessories making it suitable for determinations of luminosity curves with a great variety of adaptation levels, retinal locations, and field sizes, for studies of color discrimination and for binocular-matching measurements of the effects of adaptation. Wright's redetermination of the trichromatic coefficients and mixture curves of the spectrum, which, together with Guild's concordant results, were the basis of international standardization of the colorimetric characteristics of a normal observer, are

also described more completely and informatively than in the original publication.

Although primarily an account of results obtained at the Imperial College of Science and Technology during the past two decades, Wright's *Researches on Normal and Defective Colour Vision* describes work done in many other places and is a remarkably complete and balanced summary of the present knowledge of color vision. The style is clear, and the book is pleasantly informal and readable. Although the essential results of recent mathematical analyses of color discrimination are competently summarized, the text is not burdened with superfluous mathematics. The principal topics are the luminosity curve, color mixture, discrimination, adaptation, defective color vision, and the fundamental response curves. The unification mentioned above is a consequence of consistent use of chromaticity diagrams for representation of results in all of the chapters concerned with chromatic vision and consistent interpretation of the phenomena of color vision in terms of a three-receptor system. Wright may be considered to express the attitude of most modern colorimetrists when he states "although I have no serious doubts about the fundamental correctness of a three-response theory along the lines proposed by Young and Helmholtz, I would prefer at the present time to be somewhat lukewarm and tentative about my espousal of one theory or another . . . more experiments rather than more theories are the primary need. . . . There is not even the excuse that a research programme is difficult to lay out without a theory to serve as a guide, for the number of experiments awaiting experimenters is very great."

Wright's book clearly indicates "some of the more profitable lines to be followed" and will undoubtedly serve as "a stimulus to get on with the job."

DAVID L. MACADAM
Eastman Kodak Company

Monographs on the Progress of Research in Holland; Achievements in Optics

A. BOUWERS. Pp. 136, Figs. 64. Elsevier Publishing Company, Inc., New York, Amsterdam.

The appearance of this attractively printed booklet shows the important progress made in the field of optics by Dutch scientists during the war. There are four chapters: new optical systems, new optical instruments, geometrical optics, and physical optics.

In the first chapter formulas are derived for the spherical aberrations and other errors of different types of mirrors, their correction with the help of the Schmidt camera, and with the help of an additional spherical lens, which, in turn, is later replaced by a lens with surfaces concentric to the spherical mirror. In Chapter 7 a correcting plate is added to the concentric system. Third-order aberrations are discussed, as well as chromatic errors. The second chapter intends to apply the experience gained from the Schmidt camera to other optical systems. A microscope objective of about 0.3 numerical aperture is constructed and the author claims that with special eyepieces an apparent field of 70 degrees is obtained. The construction of microscopes with still higher aperture is still in an experimental stage.

A Cassegrain telescope and field glasses of the Gregory type with mirror-lens combination, as well as an x-ray camera, f:0.9, have been constructed. All these optical systems are protected by Dutch patents of the author, who claims priority over the work done in a similar direction by Maksutov.[1]

The third chapter gives a summary of the thesis of J. Korringa, and unpublished work by W. G. Stephan, which was done under the direction of A. C. S. van Heel at the University of Delft. The papers deal with higher order image-error theory, carrying out in detail some of the beautiful ideas of T. Smith with respect to the dependence of the errors from the position of object and stop. A thesis of B. R. A. Nijboer is characterized by the use of polar coordinates in the aperture plane. Instead of using the powers of $\cos\phi$, the author applies the linearly connected functions $\cos m\phi$, $\sin m\phi$, and classifies aberrations according to those variables. An article by A. C. S. van Heel studies the light distribution in the axial image. An ingenious little gadget (a bicylindrical lens in V-shaped form) demonstrates for points on the axis of an optical system the degree of resolution by stretching the Airy disk into the two bars of a V.

The fourth chapter starts with the discussion of diffraction problems by Zernike and Nijboer. Characteristic for their treatment is the replacement of the approximation by power series by an approximation using Legendre polynomials.

A short but comprehensive survey of Zernike on the phase-contrast method developed by him to make visible in microscopic objects small differences in refractive index, and a comparison of the results thus achieved with central dark-field-illumination, oblique dark field as well as Toepler's Schlieren method, end the interesting little volume.

M. HERZBERGER
Eastman Kodak Company

[1] J. Opt. Soc. Am. **34**, 270 (1944).

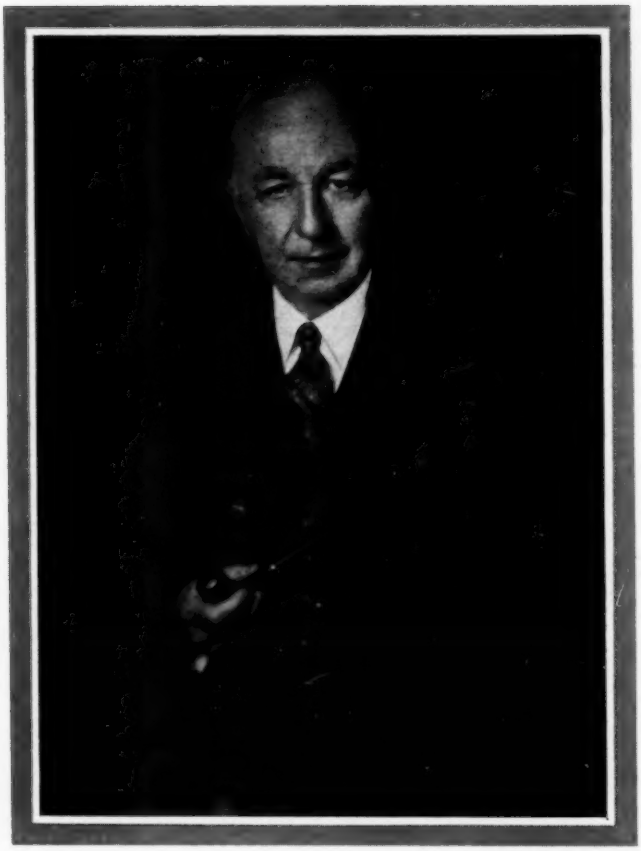

AUGUST HERMAN PFUND

Professor of Physics in the Johns Hopkins University

This issue of the Journal is made up of articles written by his former students and his colleagues to honor Professor Pfund on his retirement from active teaching.

The collection of manuscripts was in the hands of a special committee consisting of Shirleigh Silverman, *Chairman;* W. G. Fastie, J. D. Hardy, C. E. Leberknight, H. M. O'Bryan, and J. A. Sanderson.

—The Editors